

博士論文

Studies on the roles of vacuolar invertase genes in sugar
metabolism of rice and sorghum

(イネおよびソルガムの糖代謝における
液胞型インベルターゼ遺伝子の役割に関する研究)

モレ シャミタ ラオ
Morey Shamitha Rao

Copyright 2018

By

Morey Shamitha Rao

Dedicated to my dearest parents

“In the realm of ideas everything depends on enthusiasm, in the real world all rests on perseverance.”

- Johann Wolfgang von Goethe

TABLE OF CONTENTS

	Page number
LIST OF TABLES.....	i
LIST OF FIGURES.....	ii
ABBREVIATIONS.....	vi
CHAPTERS	
1. GENERAL INTRODUCTION.....	1-5
Background.....	1
Objectives of the study undertaken.....	4
2. MUTANT ANALYSIS OF TWO VACUOLAR INVERTASE GENES, <i>OsINV2</i> AND <i>OsINV3</i> IN RICE.....	6-60
Introduction.....	6
Materials and methods.....	8
Results.....	16
Discussion.....	24
3. ROLE OF <i>OsINV3</i> IN COLD STRESS RECOVERY DURING THE SEEDLING STAGE IN RICE.....	61-78
Introduction.....	61
Materials and methods.....	63
Results.....	65
Discussion.....	68
4. ROLES OF VACUOLAR INVERTASE GENES, <i>SbINV1</i> AND <i>SbINV2</i> IN SUGAR ACCUMULATION IN SORGHUM STEMS.....	79-99
Introduction.....	79
Materials and methods.....	81
Results.....	84
Discussion.....	86
5. GENERAL DISCUSSION.....	100-104
6. SUMMARY.....	105-107
ACKNOWLEDGEMENTS.....	108
REFERENCES.....	109-118

LIST OF TABLES

Table 2-1A: List of primer sequences used for the study with *OsINV2*.

Table 2-1B: List of primer sequences used for the study with *OsINV3*.

Table 2-2.1: Two-way ANOVA test for tissue dry weights per panicle for *OsINV2* WT and mutants (KO) grown in 2015 and 2016 from panicle initiation to harvest.

Table 2-2.2: Two-way ANOVA test for tissue dry weights per panicle for *OsINV3* WT and mutants (KO) grown in 2015 and 2016 from panicle initiation to harvest.

Table 2-3.1: Yield and its components for *OsINV2* WT and mutants (KO) for the years 2015 and 2016.

Table 2-3.2: Yield and its components for *OsINV3* WT and mutants (KO) for the years 2015 and 2016.

Table 4-1: List of primer sequences used for studies on sorghum.

Table 4-2.1: Morphological characteristics with sucrose content and total sugars for varieties grown in 2015.

Table 4-2.2: Morphological characteristics with sucrose content and total sugars for varieties grown in 2016.

Table 4-2.3: Correlation coefficients (R) for relationship of morphological characteristics with sucrose content and total sugars for varieties grown in 2015 and 2016.

LIST OF FIGURES

Fig. 1-1: Phylogeny of functional acid invertases across major crop species comprising Arabidopsis and major crop species namely rice, wheat, maize, barley, sorghum and sugarcane, using the Neighbor-Joining method.

Fig. 2-1: Gene constructs used for the study and verification of mutants.

Fig 2-2 (A-F): Growth analysis of the *OsINV2* and *OsINV3* WT and mutants from seedling to harvest stages.

Fig. 2-2 (G-H): SPAD at 26 days before heading (DBH) and heading, and Leaf area index (LAI), for *OsINV2* and *OsINV3* WT and mutants (KO).

Fig. 2-3 (A-B): Seedling total fresh weight, shoot and root fresh weights for WT and mutants (KO) of *OsINV2* and *OsINV3*.

Fig. 2-3 (C-F): Tissue-wise dry weight partitioning expressed in grams per panicle for *OsINV2* and *OsINV3* WT and mutants (KO) at panicle initiation, heading, 20 DAH and 40 DAH (harvest) in 2015.

Fig. 2-3 (G-L): Tissue-wise dry weight partitioning expressed in grams per panicle for *OsINV2* and *OsINV3* WT and mutants (KO) at vegetative stage, panicle initiation, heading, 10 DAH, 20 DAH and 40 DAH (harvest) in 2016.

Fig. 2-3 (M-R): Dry weight partitioning differences and photosynthesis rates in *OsINV3* WT and the mutants (KO).

Fig. 2-4 (A-B): Panicle analysis for field grown *OsINV3* mutants (KO).

Fig. 2-4 (C-F): Grain size analysis for field grown *OsINV3* mutants (KO).

Fig. 2-5.1 (A-B): Expression of *OsINV2* using *promoter::GUS* lines at harvest.

Fig. 2-5.1 C: Spatio-temporal expression of *OsINV2* in the young panicles from stages of panicle length less than 1cm to the FL stage.

Fig. 2-5.2 (A-M): Spatio-temporal expression of *OsINV3* in the panicle from initiation to 1 day before heading (DBH), and the developing endosperm using *promoter::GUS* lines.

Fig. 2-5.2 (N-R): *OsINV3 promoter::GUS* expression in the young panicles (smaller than 1cm) at the beginning of panicle initiation stage, spikelet at progressing developmental stages from 3 DBH to 15 DAF, and anthers and the lodicules at flowering and 2 DAF, magnified images of the stained anther and the pollen, and the construct used for generating *OsINV3*-GUS lines.

Fig. 2-6.1 (A-I): NSC profile of panicles of the *OsINV3* WT and the mutant (KO) during growth stages from panicle initiation to harvest.

Fig. 2-6.1 (J-M): Vacuolar invertase activity, Neutral invertase activity, Cell wall invertase activity and mRNA abundance of *OsINV2* (%RUBIQ), in young panicles (~ 4-5 cm in length) of *OsINV3* WT and mutant (KO).

Fig. 2-6.2 (A-H): NSC profile of *OsINV2* WT and KO at heading and harvest in LB, LS and C.

Fig. 2-6.2 (I-P): NSC profile of *OsINV3* WT and KO at heading and harvest in LB, LS and C.

Fig. 2-6.2 (Q-R): Total NSC in *OsINV2* and *OsINV3* WT and KO at heading and harvest.

Fig. 2-6.2 (S-V): Vacuolar invertase activity in LB, LS and C for *OsINV2* WT and KO, and *OsINV3* WT and KO.

Fig. 2-7 (A-J): *OsINV2* complementation using monocult growth conditions.

Fig. 2-7 (K-O): *OsINV2* complementation under greenhouse conditions.

Fig. 2-8 (A-G): *OsINV3* complementation, with panicle, and grain size and weight analyses.

Fig. 2-8 (H-I): Semi-quantitative PCR gel images for confirming the presence of an aberrant transcript in the *OsINV3* mutants.

Fig. 2-8 (J-N): Complementation test for *OsINV3* by determination of spikelet cell number and size analysis using Scanning Electron Microscopy (SEM).

Fig. 2-8 (O-P): Complementation test for *OsINV3* in the seedling stage.

Fig. 3-1: Experimental set up showing the treatment conditions, sampling points and type of treatment in *Experiment 2*.

Fig. 3-2: Percentage of rescued plants, visual differences in shoot density, and shoot and root dry weights for *OsINV3* WT, KO and C4 lines after recovery in *Experiment 1*.

Fig. 3-3: Shoot and root dry weights at 5 DAT for control, 12°C treated and 4°C treated seedlings and after recovery for the 12°C treated plants.

Fig. 3-4 (A-B): mRNA abundance of *OsINV2* and *OsINV3* in the shoots of *OsINV3* WT under control, 12°C treated and the 4°C treated plants at 1 DAT, 5 DAT and 15 DAT in *Experiment 2*.

Fig. 3-4 (C-E): Total soluble sugars in the shoots of *OsINV3* WT under control, 12°C treated and the 4°C treated plants at 1 DAT, 5 DAT and 15 DAT in *Experiment 2*.

Fig. 3-5: Response of *OsINV2* and *OsINV3*, to ABA at T0 (0 μM), T1 (0.5 μM) and T2 (5 μM) conditions at 0.5, 1.5, 3, 6, 24 and 48 hours after treatment.

Fig. 3-6: Response of *OsINV2* and *OsINV3* to sucrose, glucose and mannitol at T0 (0%), T1 (0.1%) and T2 (3%) concentrations at 0.5, 1.5, 3, 6, 24 and 48 hours after treatment.

Fig. 3-7: Schematic representation of the mechanism of acclimatization with regulation of *OsINV3* by ABA and glucose.

Fig. 4-1: Sorghum field in 2015 and 2016.

Fig. 4-2: NSC content in the lowermost internodes of sorghum stems, showing total soluble sugar content for 9 varieties in 2015, and 20 varieties in 2016.

Fig. 4-3: Pattern of sugar accumulation expressed in terms of brix along various growth stages after flowering in 2015, and along the whole length of the stem for varieties grown in 2016.

Fig. 4-4: Correlation of brix with sucrose content and juiciness, and the maximum theoretical ethanol yield for varieties grown in 2016.

Fig. 4-5 (A-D): mRNA abundance of *SbINV1* and *SbINV2*, and corresponding sucrose content for varieties grown in 2015 and 2016, in their lowermost internodes.

Fig. 4-5 (E-I): Correlation of sucrose content with *SbINV1* and *SbINV2* for varieties grown in 2015 and 2016.

ABBREVIATIONS

ABA – Abscissic acid

C – Culm

CO₂ – Carbon dioxide

CWIN – Cell wall invertase

DAF – Days after flowering

DAH – Days after heading

DAS – Days after sowing

DATr – Days after transplant

DAT – Days after treatment

DBH – Days before heading

EDTA – Ethylenediaminetetraacetic acid

EF1-a – Elongation factor 1-alpha

FL – Flag leaf

GUS – Beta-glucuronidase

HAT – Hours after treatment

HEPES - 4-(2-hydroxyethyl)-1-piperazineethanesulfonic acid

KCl – Potassium chloride

KO – Knockout

LB – Leaf blade

LS – Leaf sheath

MTEY – Maximum theoretical ethanol yield

NaOH – Sodium hydroxide

NIN – Neutral invertase

NSC – Non-structural carbohydrates

NSC – Non-structural carbohydrates

ORF – Open reading frame

P – Panicle

PCR – Polymerase chain reaction

RT – Room temperature

RUBIQ – Rice Ubiquitin

SDW – Sterile distilled water

SE – Standard error of the mean
SE/CC – Sieve element/Companion cell complex
SEM – Scanning electron microscopy
SNP – Single nucleotide polymorphism
SUT – Sucrose transporter
Tris-HCl – Tris(hydroxymethyl)aminomethane
TST – Tonoplast sugar transporter
UDP-glucose – Uridine diphosphate glucose
VIN – Vacuolar invertase
WT – Wild-type

CHAPTER 1

GENERAL INTRODUCTION

Background

The carbohydrates essential for growth and development of plants are rendered by assimilation of CO₂ in source leaves through photosynthesis. The assimilates synthesized are then allocated to various tissues of the plant, that are termed sinks. The source tissues are thus, net-exporters of assimilates, while the sinks are net-importers of assimilates. During the early developmental phase, rapidly growing tissues such as meristems, expanding leaves and roots serve as major sinks, while in the reproductive phase, seeds, fruits and tubers constitute as major sinks (Wardlaw, 1990). In crops, grain, that feeds the human population is considered the major sink. With an agronomic perspective, where the key intent is to increase the grain yield, this could be achieved by increasing the carbon allocation to grain.

Cleavage of sucrose, the major photoassimilate in plants is believed to play an important role in carbon allocation, not only by osmotically controlling the flux, but also by generating hexose-based signals to regulate genes involved in carbon metabolism in the sink organs (Herbers and Sonnewald, 1998; Smeekens, 2000; Koch, 2004). The enzymes that thus, catalyze sucrose cleavage are considered to be potential molecular contributors of sink strength (Herbers and Sonnewald, 1998). Two classes of enzymes namely, sucrose synthase and invertase play key roles in sucrose cleavage. Sucrose synthase (EC 2.4.1.13) catalyzes the reversible cleavage of sucrose into fructose and UDP-glucose, with a stronger tendency towards sucrose cleavage in comparison to sucrose synthesis. Invertases (EC 3.2.1.26), catalyze the irreversible cleavage of sucrose into glucose and fructose, and produce two-fold more hexoses compared to sucrose synthase, outlining a possible higher contribution of invertases in hexose signaling pathways.

Invertases can be classified into insoluble acid (cell wall), soluble acid (vacuolar) and soluble neutral (cytosolic) invertases, based on their solubility, optimum pH of function and cellular localization. The various isoforms of invertases are said to regulate the entry of sucrose into different utilization pathways (Sturm, 1999). The acid invertases (Fig. 1-1), namely cell wall invertases (CWINs) and vacuolar invertases (VINs) are similar on the molecular level with highly conserved NDPNG domain close to the N-terminal

and the WECXDF domain close to the C-terminal (Sturm, 1999) of the amino acid sequence. They also possess a putative signal peptide and a propeptide at the N-terminal (Sturm and Chrispeels, 1990; Unger et al., 1994). It has been suggested that these propeptides play a role in protein folding, targeting (Klionsky et al., 1988) and control of enzyme activity (Hasilik and Tanner, 1987). Vacuolar invertases, possess a much complex N-terminal propeptide region containing a transmembrane domain (Ji et al., 2005; Ji et al., 2007) found to be essential for membrane anchoring and sorting (Xiang and Van den Ende, 2013), and an additional short hydrophobic C-terminal peptide for vacuolar targeting (Unger et al., 1994). The transport of acid invertases through plasma membrane or the tonoplast is suggested to be enabled through N-glycosylation of acid invertases at multiple positions, their molecular weights ranging from 55 kDa to 70 kDa after glycosylation (Tymowska-Lallane and Kreis, 1998). The neutral invertases are biochemically different from the acid invertases, lacking similarities in key domains of their amino acid sequence. Unlike acid invertases, they are not N-glycosylated, and have a molecular mass of 54 kDa to 65 kDa (Sturm, 1999).

In the past, vacuolar invertases (VINs) have been attributed to roles in cell elongation of seedling hypocotyls in *Arabidopsis* (Sergeeva et al., 2006), fiber cell elongation in cotton (Wang et al., 2010), and rapidly expanding tissues in carrot taproot (Tang et al., 1999) and sugar beet petioles (Gonzalez et al., 2005). It has been suggested that VIN regulates the sink size by driving cell expansion, owing to a turgor generated by influx of osmotic solutes in response to an increase in hexoses (Koch, 2004; Sergeeva et al., 2006). It has also been considered that VINs drive cell expansion based on availability of carbohydrates (Koch, 2004). Further, role of VINs in determination of hexose-to-sucrose ratio in potato (Zrenner et al., 1996) and tomato (Klann et al., 1996) suggests the importance of sink sugar composition in regulation of the sink size (Klann et al., 1996). In addition to its role in facilitating sink expansion, VINs have also been found to play a major role in early plant development in carrot (Tang et al., 1999) and *Arabidopsis* (Leskow et al., 2016). Through its regulation of composition of sugars, it has been found to play a key role in fruit ripening in tomato (Qin et al., 2016); and the regulation of stomatal opening in *Arabidopsis* (Ni et al., 2012).

Many studies also report the induction of VINs under cold stress. In potato, the unfavourable cold-induced sweetening was attributed to a VIN gene, suppression of which was found to prevent this characteristic (Bhaskar et al., 2010; Wiberley-Bradford et al., 2014). In *Arabidopsis*, VIN activity was demonstrated to

be key in stabilizing the central energy supply under cold stress and combined cold/high light conditions (Weiszmann et al., 2017).

Critical roles of VIN in key developmental processes, as demonstrated in the previous studies, marks a need for its tight regulation, which could be achieved transcriptionally or post-translationally. Transcriptionally, they are said to be regulated by various signals (Proels and Roitsch, 2009), mainly sugars (Burch et al., 1992; Xu et al., 1996; Trouverie et al., 2004) and phytohormones (Roitsch et al., 2004), whereby different patterns of induction and repression were observed based on the intrinsic sugar and hormone levels. Post-translational control is exercised by polypeptide vacuolar inhibitor sequences, closely related to the pectin methylesterase family (Hothorn et al., 2004), with evidence for VIN inhibition by inhibitors previously demonstrated in potato (Greiner et al., 1999; Brummell et al., 2011) and tomato (Qin et al., 2016).

The current study outlines key physiological roles of two VIN isoforms, *OsINV2* and *OsINV3*, for the first time in rice, a C3 crop, with respect to sink size, cell expansion, non-structural carbohydrates (NSC) allocation and dry matter partitioning differences. Differences in various other phenotypic characteristics at the seedling, tillering and reproductive stages, are also recorded and discussed. Role of the rice VIN in cold stress and its regulation by sugars and ABA, to isolate a possible mechanism for cold-stress tolerance imparted by *OsINV3* at the seedling stage, has also been studied and discussed. In addition, performance of multiple varieties of sorghum, a C4 crop, has also been determined in terms of sugar accumulation potentials under local environmental conditions. Various plant growth parameters have also been scored for correlation with the stem brix values, in addition to determination of roles of *SbINV1* and *SbINV2* in sugar content in sorghum stems.

Objectives of the study undertaken

With a view of attaining better understanding of vacuolar invertases in two major crop species rice and sorghum, the present study was conducted with the following main objectives-

1. To isolate key physiological roles of vacuolar invertase isoforms *OsINV2* and *OsINV3* in rice, using *Tos-17* retrotransposon insertion mutants. (Chapter 2)
2. To study the regulation of *OsINV2* and *OsINV3* by sugars and ABA, and identify the significance of vacuolar invertase in imparting cold tolerance during the seedling stage in rice. (Chapter 3)
3. To evaluate the performance of sorghum varieties for sugar accumulating potential under local conditions, and study the role of vacuolar invertase isoforms *SbINV1* and *SbINV2* in determination of sucrose content in its stems. (Chapter 4)

Through this study we also aim to isolate any major differences in roles of vacuolar invertase between C3 and C4 crops, in terms of their activity in major sinks.

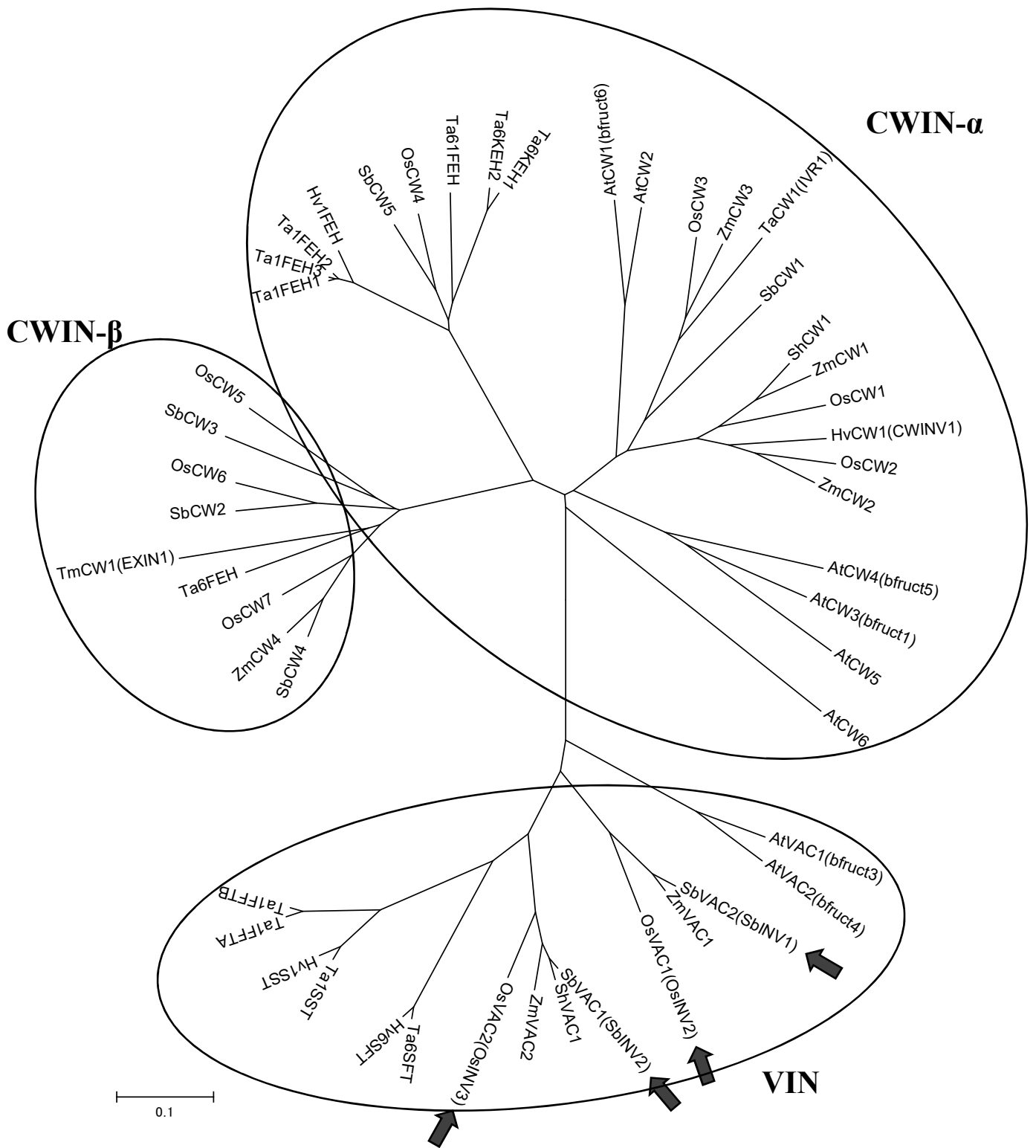


Fig. 1-1. Phylogeny of functional acid invertases across major crop species comprising Arabidopsis and major crop species namely rice, wheat, maize, barley, sorghum and sugarcane, using the Neighbor-Joining method (Saitou and Nei, 1987). The evolutionary distances were computed using the Poisson correction method (Zuckerkanndl and Pauling, 1965). All positions containing gaps and missing data were eliminated. Evolutionary analyses were conducted in MEGA6 (Tamura et al., 2013). The optimal tree with the sum of branch length = 6.82081190 is shown. The tree is drawn to scale, with branch lengths in the same units as those of the evolutionary distances used to infer the phylogenetic tree. Genes used in the study are marked by arrows referred to as *OsINV2* (Os04g0535600), *OsINV3* (Os02g0106100), *SbINV1* (Sb06g023760) and *SbINV2* (Sb04g000620), where the rice VINs *OsINV2* and *OsINV3* were found to be homologous to the sorghum VINs *SbINV1* and *SbINV2*.

CHAPTER 2

MUTANT ANALYSIS OF TWO VACUOLAR INVERTASE GENES,

OsINV2 AND *OsINV3* IN RICE

2-1 Introduction

Carbon that is assimilated by plants through photosynthesis is partitioned among various tissues based on their competitive ability to import assimilates. This ability is commonly termed as sink strength and has been previously described to be dependent on physical as well as physiological capacity of the sinks (Ho, 1988; Marcelis, 1996, Herbers and Sonnewald, 1998; Bihmidine et al., 2013). While sink size determines the physical capacity, sink activity involving assimilate transport, utilization and storage by the sink cells, determines the physiological capacity (Ho 1988; Herbers and Sonnewald, 1998). In crops, an increase in sink strength directly translates to an increase in yield, mainly due to a higher assimilate partitioning into the sinks co-ordinated by an increased sink size. With respect to rice (*Oryza sativa* L.), an important cereal crop that feeds a majority of the global population, there is a pressing need to increase the sink strength in order to achieve global food security and enable sustenance by ensuring food for the rapidly growing population.

In rice, eight neutral invertases (NINs), nine cell wall invertases (CWINs) and two vacuolar invertases (VINs) have been identified (Ji et al., 2005). Till date, CWINs have been found to play a primary role in assimilate partitioning, thus regulating the grain weight in crops including rice (Cheng et al., 1996; Hirose et al., 2002; Wang et al., 2008; Tang et al., 2016; Li et al., 2013). For example, two of rice CWIN isogenes, *OsCIN1* and *OsCIN2*, play a role in determination of sink strength by regulation of assimilate partitioning, where *OsCIN1* was found to play a role during the early grain filling stages, and *OsCIN2* in the regulation of grain size and weights (Hirose et al., 2002; Wang et al., 2008).

Roles of CWINs as contributors to sink strength, exhibiting a role in phloem unloading have been extensively studied in maize and fava bean (Miller and Chourey, 1992; Weber et al., 1995), and a CWIN *OsCIN2* (*GIF1*) has been previously reported to play a key role in phloem unloading in rice (Wang et al., 2008). However, establishing role of VINs in terms of sucrose import by sinks has not been a research focus in recent times. This chapter presents results for characterization of VIN isogenes, *OsINV2* and *OsINV3*, in

rice, using *Tos17* retrotransposon insertion mutants, highlighting key physiological roles in regulation of growth, assimilate partitioning, sink size and activity, yield and its components, and NSC content. Data for temporal and spatial expression studies using the *promoter::GUS* lines, and reconfirmation of the phenotypic differences observed between the wild-type (WT) and the mutant using complementation tests have also been discussed.

2-2 Materials and Methods

2-2.1 Plant material and genotyping

To elucidate the physiological function of a vacuolar invertase isoform, *OsINV3*, the gene disruption lines were screened from the population of mutants carrying insertions of the *Tos17* retro-transposon, which were obtained from the National Institute of Agrobiological Sciences, Ibaraki, Japan. Detailed procedure for generation of the insertion mutants are as previously described (Miyao et al., 2003). PCR-screening was conducted using DNA pools prepared with three-dimensional sampling method from approximately 40,000 plants bearing *Tos17* insertion (Agrawal et al., 2005). Nested PCR was carried out with PrimeStar GXL DNA polymerase (Takara Bio Inc., Shiga, Japan) according to manufacturer's instructions using combinations of primers specific to *Tos17* and *OsINV2* (Table 2-1A), and *Tos17* and *OsINV3* (Table 2-1B) sequences. Positive products were sequenced after gel-purification to identify the location of insertions in the rice genome. Insertion lines NC8085 and NG6411 were isolated with a *Tos17* insertion in the first exon of *OsINV2* (Os04g0535600) (Fig. 2-1A) and the second exon of *OsINV3* (Os02g0106100) respectively (Fig. 2-1B). The initial screening to isolate the insertion lines was performed by Drs. Tatsuro Hirose, Akio Miyao and Hirohiko Hirochika; and kindly provided to us. The WT and mutants were segregated from the same *Tos17* insertion lines following genotyping using the primer sets F7/R7 and F1/R1 for WT alleles of *OsINV2* and *OsINV3* respectively, and R7/T6 and F1/T6 for the mutant alleles of *OsINV2* and *OsINV3* respectively (Tables 2-1A and B) by multiplex PCR (Multiplex PCR Assay kit, Takara Bio Inc.). Genotyping for confirmation of complementation in *OsINV3* was performed using the T5 primer instead of the T6 primer. Genomic DNA isolation from leaves was performed by first pulverizing the samples with the extraction buffer (1 M KCl, 100 mM Tris-HCl (pH 8.0), and 10 mM EDTA), and incubating at room temperature (RT) for 15 minutes, after a thorough vortex. Following this, the mixture was centrifuged at 15,000 rpm for 10 minutes at RT, and the supernatant mixed with equal amounts of isopropanol. At the end of the incubation period the mixture was centrifuged at 15,000 rpm for 10 minutes at 4°C, and the pellet washed with 80% ethanol. The washed pellet was resuspended in 30 µl of sterile distilled water (SDW) after drying at RT for 5-10 minutes. 1 µl of the genomic DNA template was used for PCR with PrimeStar GXL DNA polymerase (Takara Bio Inc.) according to manufacturer's instructions.

2-2.2 Generation of complement lines

The full-length ORF of *OsINV2* along with 2107 bp upstream of the putative translation start site, and of *OsINV3* along with 2212 bp upstream of the putative translation start site was isolated by PCR using a high-fidelity DNA polymerase (PrimeStar GXL, Takara Bio Inc.) and primer sets PL1/cds3T and PL2/R7T respectively (Tables 2-1A and B) with genomic DNA from a rice cultivar, Nipponbare, as the template. The resultant DNA fragment was cloned into a binary vector, pZH2B (Kuroda et al. 2010) using In-Fusion HD cloning kit (Takara Bio Inc.) according to manufacturer's instructions. The complement lines were generated by incorporation of this vector into the homozygous *Tos17* mutant using *Agrobacterium* (EHA105) mediated transformation (Toki et al., 1997). Successful complementation was assessed by genotyping using F7, R7 and T6, and F1, R1 and T5 primers (Table 2-1B) for *OsINV2* and *OsINV3* respectively. Out of the 16 complementation lines isolated, the assessed lines were selected and propagated to T1 generation, solely based on availability of grain. The T1 plants were used for complementation tests.

2-2.3 Growth conditions and grain size analyses for controlled experiments

Seeds were sown in nursery soil in a plastic tray following chemical sterilization with 2.5% sodium hypochlorite for 30 minutes, an elaborate wash and imbibition with water at 30°C for three days. They were placed in a growth chamber at 27°C/22°C, 14 hr-light/10 hr-dark cycle, 65% relative humidity and a light intensity of 900 $\mu\text{mol}\cdot\text{m}^{-2}\cdot\text{s}^{-1}$. One-week old seedlings were transferred to 1/4-strength Yoshida nutrient solution (Yoshida et al., 1976) for growth analyses, whereby shoot and root lengths, and fresh weights were determined at 14 days after sowing (DAS), 21 DAS and 25 DAS, while remaining seedlings were transplanted to bigger plastic pots at around 20 DAS and grown under the same conditions for the grain size analyses. Plants for monoculm culture were grown under the above-mentioned growth conditions, where a single stem was maintained for all plants, by physical removal of young new tillers.

Grain length, width and area for ten respective grains from each of the three replicate plants from *OsINV3* WT, mutant and the T1 complement (C4) lines were determined using a digital microscope (VHX-6000, Keyence, Osaka, Japan) in concert with ImageJ 1.46r (Schneider et al., 2012).

2-2.4 Scanning Electron Microscopy (SEM) analysis

Spikelet hulls for *OsINV3* WT, mutant and C4, at 2 days before heading (DBH) were sampled and processed as previously described (Li et al., 2011) followed by dehydration in isoamyl alcohol. The samples were dried with a critical-point drier (JEOL JCPD-5, Tokyo, Japan) and coated with Pt/Pd using a sputter coater (Hitachi E-1030, Tokyo, Japan). The SEM (Hitachi S-4800, Tokyo, Japan) was operated at 2 kV, with an aperture of 15 mm, and magnification of 120X and 200X for lemma and palea respectively. Cell density was determined as number of cells/unit area for the outer surface, and the cell area, width and height were determined for the cells on the inner surface of palea and lemma using ImageJ. Mean and SE were determined for 9 spikelet hulls for each line, with cell size analyses for 10 characteristic cells from palea and lemma of each of the 9 spikelets.

2-2.5 Promoter::*GUS* assay

OsINV2 promoter>::GUS construct: A genomic DNA fragment that covers -2107 to +18 nucleotides of the translation start site of *OsINV2*, was amplified by PCR with primers INV2-PL1 and -ATG, having restriction sites *Ase*I and *Sac*I, respectively, at the 5' end of each primer (Table 2-1A).

OsINV3 promoter>::GUS construct: A genomic DNA fragment that covers -1930 to +30 nucleotides of the translation start site of *OsINV3*, was amplified by PCR with primers PINV3-L2H and -R2X, having restriction sites *Hind*III and *Xba*I, respectively, at the 5' end of each primer (Table 2-1B).

Following the double restriction digestion, the genomic DNA fragments were cloned into a binary vector, pZH2B-GUS (Kuroda et al. 2010), with a pre-existing insertion of the beta-glucuronidase (*GUS*) gene. Eventually, two plasmid constructs with the *GUS* gene, one flanked by 18 nucleotides downstream of the translation start site of *OsINV2*, expected to be driven by the *OsINV2* promoter (Fig. 2-5.1 A), and the other flanked by 30 nucleotides downstream of the translation start site of *OsINV3* and an interconnecting *Xba*I (six nucleotides) site, expected to be driven by the *OsINV3* promoter were obtained (Fig. 2-5.2 R). The *GUS* lines of *OsINV2* and *OsINV3* were generated by incorporation of this vector into the WT lines segregated from NC8085 and NG6441 respectively, using transformation techniques mentioned above. The plasmid constructs for *OsINV2* and *OsINV3 promoter-GUS* were prepared and provided by Dr. Tatsuro Hirose. Following genotyping using INV2-PL1 and INV2-ATG (Table 2-1A), and PINV3-L2H and PINV3-R2X (Table 2-1B) for *OsINV2* and *OsINV3* respectively, 3 lines were isolated and propagated to

T1 generation. The T1 plants that tested positive for staining were isolated and their grain used for further analyses.

Plant tissues to be analyzed were sampled in ice cold 90% acetone (v/v), on ice. Samples were incubated at room temperature for 20 minutes, followed by wash with 50 mM phosphate buffer (pH 7.0) which was repeated thrice to eliminate the acetone completely. Following this, the GUS staining was performed similar to the methods previously described (Hirose et al. 2014). Observation was carried out using a stereo microscope (SMZ745T, Nikon, Tokyo, Japan).

2-2.6 Field trials and determination of yield and its components

Plants were grown in an experimental paddy field at the Institute for Sustainable Agro-ecosystem Services (ISAS), The University of Tokyo (35.73°N, 139.53°E, 58m above sea level), in Tokyo, Japan. Cultivation was carried out between the months of May and October 2015 and 2016, where one-month old seedlings were transplanted to the field on May 28, 2015 and May 25, 2016. Hills were spaced at 0.3 m × 0.15 m with one seedling per hill, leading to a planting density of 22.2 hills m⁻². Basal dressing of fertilizer was applied at 50 g.m⁻² with a N:P₂O₅:K₂O of 12:16:18. Three sub-plots were maintained for each of the lines, their positions alternating with one another. Five biological replicates from each of the three sub-plots for both WT and mutant were used for assessment of yield and its components. The yield component data were obtained using methods previously described (Hirose et al., 2013).

2-2.7 Growth analyses, dry weight and photosynthesis rate measurements for field grown plants

Plant height and the number of tillers were determined for field grown WT and mutants at various stages from 28 days after transplant (DATr) to heading (82 DATr), and 29 DATr to harvest (131 DATr) in 2015 and 2016 respectively. Plant height was measured from the stem base to the tip of the uppermost fully expanded leaf. SPAD and leaf area were determined in 2015, with SPAD readings measured at 26 DBH and heading using a chlorophyll meter (SPAD-502, Minolta Corporation Ltd., Osaka, Japan) for five biological replicates from each of the three sub-plots, and leaf area determined at 28 DBH (panicle initiation) for at least 7 respective plants in each line. Panicle initiation was identified by the appearance of

first internode at 28 DBH, where young panicles (~3-4 cm in length) at the base of the stem were isolated and sampled.

Leaves, stem, panicles and dead plant tissue from each plant were sampled separately and dried at 80 °C for at least one week before weighing them. Five biological replicates from each of the three sub-plots for each line were used for dry weight estimation at panicle initiation (28 DBH), heading, 10 DAH, 20 DAH and harvest (40 DAH). Dry matter partitioning to panicles or vegetative tissues was estimated on per panicle basis, as the ratio of total dry weight of panicles or vegetative tissues to the total dry weight of the plant.

Photosynthesis rates for the flag leaves of the main stem of *OsINV3* WT and the mutant (KO) were measured at panicle initiation, heading and late ripening stages using CIRAS-3 Photosynthesis Systems (PP systems, Amesbury, MA, USA) between 1100 and 1200 hours. The leaf chamber was set to 30°C, photosynthetic photon flux density of 1500 $\mu\text{mol}\cdot\text{m}^{-2}\cdot\text{s}^{-1}$ and CO₂ concentration of 390 $\text{ml}\cdot\text{L}^{-1}$.

2-2.8 Panicle and grain size analyses for field grown panicles

The panicles from WT and mutant lines were harvested post-maturity (40 DAH) and air-dried for two weeks before analyses. The length of the panicles was measured from the tip to base for all panicles in three replicate plants for both the lines, and the number of primary and secondary rachis branches were determined for the same sample set.

Grain length, width and area were determined for ten corresponding grains from each of the three replicate plants for both the WT and the mutant using ImageJ. For the grain thickness distribution curve, the whole grain set for three replicate plants were analyzed. The grains were made to pass through a series of sieves sized from 1.8 mm to 2.4 mm, and the grains trapped in each of these sieves were counted and weighed. The average weight per grain was obtained as the ratio of the total weight to total number of the grains corresponding the particular grain thickness.

2-2.9 Quantitative Real-time PCR

Young panicles (~3-4 cm in length) from *OsINV3* WT, mutant and C4 were sampled in liquid nitrogen and pulverized cryogenically using a Multi-beads shocker (Yasui Kikai, Osaka, Japan) at 2000 rpm for 15

seconds. RNA was isolated using the RNeasy Plant Mini kit (QIAGEN, Germany), followed by reverse transcription using a PrimeScript RT reagent kit with gDNA eraser (Perfect Real Time, Takara Bio). 1 µl of the cDNA synthesized was used for real-time PCR using SYBR Premix Ex Taq II (Tli RNase H Plus, Takara Bio) in a thermocycler (ABI7300, Thermo Fisher Scientific, Waltham, MA, USA). Primers specific to *OsINV2*, *OsINV3* and polyubiquitin gene *RUBIQ1* (Wang et al., 2000) are listed in Tables 2-1A and B. mRNA transcript abundance was determined in terms of %*RUBIQ* using the following formula

$$\text{mRNA abundance} = 2^{[\Delta\text{Ct}(\text{RUBIQ}) - \Delta\text{Ct}(\text{gene of interest})]} * 100$$

Confirmation of aberrant transcripts in *OsINV3* KO was done using two sets of primers F5/R5 and F6/R6, the former amplifying region downstream of the *Tos-17* insertion site, and the latter amplifying region spanning the *Tos-17* insertion (Table 2-1B).

2-2.10 Plant sampling and pulverization

Mature leaf, leaf sheath and culm from *OsINV2* and *OsINV3* WT and mutants with at least three biological replicates for each line, were sampled at heading and harvest, while whole panicles from field grown plants for *OsINV3* WT and mutant with at least six biological replicates, were sampled at panicle initiation (28 DBH), heading, 5 DAH, 10 DAH, 20 DAH, 30 DAH and harvest (40 DAH), on dry ice. Samples were then pulverized cryogenically as mentioned above, and weighed separately for NSC determination and the enzyme assay.

2-2.11 Determination of starch and soluble sugar contents, and invertase enzyme assay

NSC (Starch, sucrose, glucose and fructose) contents were determined as follows.

Extraction

To approximately 30 mg of cryogenically pulverized sample (refer 2-2.10 for details), 1 ml of 80% ethanol was added, vortexed thoroughly, and incubated at 80°C for 10 minutes. This was centrifuged at 12,000 rpm for 5 minutes at RT, and the supernatant collected in a fresh 1.5 ml tube. The pellet was resuspended in 500 µl of 80% ethanol, following the incubation and the centrifugation steps mentioned above. The supernatants

were pooled and dried in a vacuum evaporator, and used for the sugar assay. The pellets remaining behind after the extraction were used for the measurement of starch after drying.

Measurement of starch

To the dried pellet obtained 1 ml of SDW was added and incubated at 105°C for 1.5-3 hours, with elaborate mixing every 30 minutes. To this, 200 µl of 50 U/ml glucoamylase was added and incubated at 40°C with shaking for a minimum of 4 hours, to hydrolyze the starch. The tubes were centrifuged at 15,000 rpm for 5 minutes at 4°C before measurement by F-kit (Boehringer Mannheim/R-Biopharm) according to manufacturer's instructions. The starch content was determined in terms of glucose generated.

Measurement of sugars

The vacuum dried pellet was resuspended in 500 µl of SDW and centrifuged at 15,000 rpm for 5 minutes at 4°C before measurement by F-kit (Boehringer Mannheim/R-Biopharm) according to manufacturer's instructions.

Invertase enzyme assay

Preparation of crude extract, and the soluble and insoluble enzyme assay were performed similar to the methods previously described (Ishimaru et al., 2005), with the following modifications. The reaction buffer for acid invertase contained 100 mM of sodium acetate (pH 4.5) and 20 mM sucrose, to which 50 µl aliquot of the crude extract was added to initiate the reaction. The reaction volume was maintained at 200 µl. The reaction progressed at 37 °C for 30 minutes and was stopped by the addition of 20 µl of 1 M HEPES-NaOH (pH 7.5) and boiling at 98 °C for 2 minutes. Neutral invertase assay was performed same as above, except that the reaction buffer used contained 100 mM HEPES-NaOH (pH 7.5) instead of the acid buffer. The enzyme activity was determined as V_{max} in terms of glucose generated by the reaction measured by the F-kit (Boehringer Mannheim/R-Biopharm) according to manufacturer's instructions.

2-2.12 Statistical analyses

Unpaired student's t-test statistic (Microsoft Excel 2016) was used to determine significance in differences between WT and the mutants from minimum 3 independent biological replicates. For analyses with the complementation lines one-way ANOVA with a post-hoc analysis (Tukey's test) was used (SPSS 13.0 for Windows). P values ≤ 0.05 , ≤ 0.01 and ≤ 0.001 were indicated by *, ** and *** respectively, and considered significant. Year and variety differences and their interactive effects on the variables were determined using two-way ANOVA (SPSS 13.0 for Windows).

The GenBank database accession numbers for *OsINV2* and *OsINV3* used in this study are AF276703.1 and AF276704.1 respectively.

2-3 Results

2-3.1 Verification of the mutants

Genotypic verification of the WT and mutants was carried out, confirming the presence of WT and KO alleles, showing bands corresponding to 304 bp, 180 bp, 350 bp and 250 bp for *OsINV2* WT, *OsINV2* KO, *OsINV3* WT and *OsINV3* KO respectively (Fig. 2-1C). In terms of VIN enzyme activity in leaf blades, significant reduction in both *OsINV2* and *OsINV3* mutants was observed, demonstrating a 69.32% (Fig. 2-1D) and a 45.16% (Fig. 2-1E) decrease respectively, in comparison to the WT.

2-3.2 Growth analysis

Seedling stage

Shoot and root length differences were not found in *OsINV2* WT and KO (Fig. 2-2A), however, existent in *OsINV3* WT and KO, with KO having shorter shoots at 21 DAS and 25 DAS (Fig. 2-2C).

Tillering to harvest stage

While plant height and number of tillers weren't different in the mutants for *OsINV2* (Fig. 2-2B and E), *OsINV3* mutant was consistently found to be shorter (2-2D and F), with higher number of tillers during the grain filling stage (Fig. 2-2F). A compensatory trend for the number of tillers in *OsINV3* mutants was observed, where the number of tillers that was lower at the beginning of the tillering stage was found to significantly increase in progressive growth stages (Fig. 2-2D and F) in both 2015 and 2016.

SPAD values were not different between the WT and KO of both *OsINV2* and *OsINV3* at panicle initiation and heading stages (Fig. 2-2G). Leaf area at panicle initiation was also not found to be different between the WT and the KO of *OsINV2* and *OsINV3* (Fig. 2-2H).

2-3.3 Total plant weight and tissue-wise dry matter partitioning

Seedling stage

Differences in seedling shoot, root and total fresh weight for the *OsINV2* WT and KO was not observed (Fig. 2-3A), however both the shoot and the root fresh weights at 25 DAS were found to be lower in the *OsINV3* KO thus, contributing to a significantly lower total fresh weight in comparison to the WT at this stage (Fig. 2-3B).

Tillering to harvest stage

OsINV2 KO didn't differ with the WT in terms of total dry weights and tissue-wise dry weights measured in terms of per panicle basis at all the stages tested i.e. vegetative (Fig. 2-3G), panicle initiation (Fig. 2-3C and H), heading (Fig. 2-3D and I), 10 DAH (Fig. 2-3J), 20 DAH (Fig. 2-3E and K) and 40 DAH (Fig. 2-3F and L). *OsINV3* KO, on the other hand showed consistently smaller dry weights at all the growth stages. While, the leaf dry weights were significantly smaller until 20 DAH (Figs. 2-3C-E and 2-3G-K), stem dry weights ceased to be different after heading (Fig. 2-3D-E and 2-3I-K). Panicle dry weights were consistently lower, as a key contributor for lower total dry weight in the *OsINV3* KO at 20 DAH and 40 DAH (Figs 2-3E-F and 2-3K-L).

The total dry weights measured on whole plant basis, revealed smaller dry weight for *OsINV3* KO at the panicle initiation stage, where the differences ceased to exist as the plants entered the reproductive stage (Fig. 2-3M). The KOs showed an increase in dry matter partitioning to vegetative tissues (Fig. 2-3N), with a compromised partitioning to the panicles (Fig. 2-3O) from heading to harvest. The photosynthesis rates however, at panicle initiation (Fig. 2-3P), heading (Fig. 2-3Q) and late ripening (Fig. 2-3R) were not different between the WT and KO.

The year and variety interactions on tissue dry weights per panicle, from panicle initiation to harvest were not present for *OsINV2* WT and KO, with the exception of leaf dry weight at harvest that tended to be higher in the KO (Table 2-2.1). A higher stem dry weight in the *OsINV2* KO was also observed at harvest in comparison with the WT (Table 2-2.1). In *OsINV3* KO the total dry weight per panicle was consistently smaller than the WT at all growth stages (panicle initiation to harvest) with a similar trend observed in both years, where the stem and leaf tended to show a compensatory recovery in dry weights following heading with lower panicle weight being a significant phenotype in the mutants (Table 2-2.2).

2-3.4 Yield and its components

Field trials conducted in 2015 and 2016 for assessment of yield and its components didn't show any significant differences between the *OsINV2* WT and KO, nor were any year and variety interactions observed (Table 2-3.1). However, *OsINV3* KO showed a marked decrease in yield, owing to a lower 1000 grain weight and lower % of grain filling in both years (Table 2-3.2) with absence of year and variety interactions for those factors. Thus, it could be said that *OsINV3* regulates the grain yield, by influencing the 1000-grain weight and the % of grain filling.

2-3.5 Panicle and grain size analyses

The mutant panicles were significantly shorter (Fig. 2-4A), however, with no differences in the number of primary or secondary rachis branches when compared to the WT (Fig. 2-4B). The weight of the panicle after threshing was also not different between the WT and KO (Fig. 2-4A). The mutant grains, both unhulled and hulled were found to be smaller in size than the WT (Fig. 2-4C). The length, width and area of filled grains were all found to be significantly smaller for the mutant when compared to the WT (Fig. 2-4D). Further, the distribution of grain number and grain weight for a corresponding grain thickness revealed a significantly shorter peak and a smaller area under the distribution curve for the mutant (Fig. 2-4E), with the single grain weight for a corresponding grain thickness significantly smaller in the mutants (Fig. 2-4F).

2-3.6 GUS assay

2-3.6.1 *OsINV2*

The flag leaf (FL), first (-1C), second (-2C) and third (-3C) internodes, first (-1LS) and second (-2LS) leaf sheath, and the panicles (P), analyzed for *OsINV2* expression at harvest revealed no expression of *OsINV2* at this stage (Fig. 2-5.1 B). The spatio temporal expression of *OsINV2* in young panicles revealed a strong expression in the early stages of panicle initiation, starting from panicles smaller than 1cm in length (Fig. 2-5.1 top). Expression was strongly observed in the elongating rachis branches, anther, rudimentary glume, awn, palea, lemma and nerves in the early stages, however ceasing to express at the FL stage until heading (Fig. 2-5.1 C bottom).

2-3.6.2 *OsINV3*

OsINV3 promoter::GUS assay for panicles at progressing stages of panicle development were studied to isolate the temporal and spatial expression pattern in the panicles. Early panicle development stages of young panicles, 0.5cm – 1cm in length, showed no GUS activity except for in the bract hair (Fig. 2-5.2 N). Expression of *OsINV3* was first observed in panicles ~3cm in length, in the rudimentary glume, pedicel and the empty glumes in the spikelets in upper position (Fig. 2-5.2 A and a), following a similar expression pattern in the spikelets in lower position along the progressing stages of development. The expression in rachilla and spikelet was observed basipetally along the progressing stages of panicle development (Fig. 2-5.2 B-F, 2-5.2 b-f). A strong staining in the anthers was also observed in all stages, pointing towards a possible role in development of anthers and pollen in the initial stages, and anther dehiscence just before flowering (Fig. 2-5.2 b-f). Further observations of the anther revealed expression in the epidermal cells as well as the pollen (Fig. 2-5.2 Q). Strong expression was observed in the dorsal end of the ovary following fertilization until 6 days after flowering (DAF) (Fig. 2-5.2 G-K). However, no expression in the developing endosperm or maternal tissues of hulled grain was observed following this stage (Fig. 2-5.2 L-M).

2-3.7 NSC content and enzyme activity

2-3.7.1 In panicles

The amounts of NSCs in the whole panicles of field grown *OsINV3* WT and KO plants were estimated at stages from panicle initiation to maturity (Fig. 2-6.1 (A-I)). While levels of starch in both the WT and the mutant were not different (Fig. 2-6.1 H), significant differences in the sugar levels were determined till 20 days after heading (DAH) (Fig. 2-6.1 A-G), characterized by higher sucrose and lower hexose levels until 10 DAH (Fig. 2-6.1 A-D). At 20 DAH, sucrose and hexoses were found to be lower in the mutant than in the WT (Fig. 2-6.1 E). After this stage, no differences between the WT and the mutant were observed until maturity (Fig. 2-6.1 F and G). The differences in the sugar composition were reflected in the hexose-to-sucrose ratios, where, although the trend was maintained from heading to harvest for both WT and mutants, the ratio was found to be significantly lower for the mutants between heading to 10 DAH, which signifies the pre-storage phase of grain filling (Fig. 2-6.1 I). However, a stark difference in hexose-to-sucrose ratio between the WT and the mutant was observed at panicle initiation stage (Fig. 2-6.1 I) usually characterized

by high hexose levels, mainly due to a higher sucrose and negligible hexose levels in the mutants (Fig. 2-6.1 A).

The VIN activity at the panicle initiation stage (Fig. 2-6.1 J) was not found to be different between the WT and the KO, neither were the NIN (Fig. 2-6.1 K) and the CWIN (Fig. 2-6.1 L) activities. However, the *OsINV2* mRNA levels were found to be significantly higher in the *OsINV3* KO than in the WT (Fig. 2-6.1 M).

2-3.7.2 In vegetative tissues

NSC (Sucrose, glucose, fructose and starch) content in the leaf blade (LB), leaf sheath (LS) and culm (C) in the *OsINV2* (Fig. 2-6.2 A-H) and *OsINV3* (Fig. 2-6.2 I-P) WT and KO were measured at heading and harvest. No significant differences were found in sucrose (Fig. 2-6.2 A and E), glucose (Fig. 2-6.2 B and F), fructose (Fig. 2-6.2 C and G) and starch (Fig. 2-6.2 D and H) levels in LB, LS or culm of *OsINV2* WT and KO at heading and harvest. However, the hexoses tended to be slightly higher in the LB and LS of the KO at harvest (Figs. 2-6.2 F and G). Similar tendency was observed in *OsINV3* KO that didn't show any differences in their sucrose (Fig. 2-6.2 I), glucose (Fig. 2-6.2 J), fructose (Fig. 2-6.2 K) and starch (Fig. 2-6.2 L) levels in the tissues tested at heading. However, the hexose levels in the LB of the *OsINV3* KO tended to be lower than the WT at harvest (Figs. 2-6.2 N and O), while the sucrose (Fig. 2-6.2 M), glucose (Fig. 2-6.2 N), fructose (Fig. 2-6.2 O) and starch (Fig. 2-6.2 P) content in all other tissues were unchanged. The total NSC in the vegetative tissues were not different between the WT and mutants of *OsINV2* and *OsINV3* at heading (Fig. 2-6.2 Q) and harvest (Fig. 2-6.2 R), however the total sugar was found to be significantly higher in the *OsINV2* KO, and significantly lower in the *OsINV3* KO (Fig. 2-6.2 R).

Significant differences in the VIN activity between the WT and the mutants of *OsINV2* (Figs. 2-6.2 S and T) and *OsINV3* (Figs. 2-6.2 U and V) were not observed, with the exception of the LS of the *OsINV2* KO that showed a lower VIN activity at harvest (Fig. 2-6.2 T).

2-3.8 Complementation tests

2-3.8.1 *OsINV2*

Genotyping of the WT, mutant and the complementation lines C1, C2, C3, C5, C7, C10 and C11 confirmed the successful incorporation of *OsINV2* gene in the mutant lines, enabling an effective complementation (Fig. 2-7A). Complementation test for *OsINV2* was performed using two methods.

Monoculm growth conditions

The total soluble sugars (sucrose, glucose and fructose) in the culm of the complement lines were found to be lower, while in the LS tended to be higher than the WT and KO, that didn't differ between each other (Fig. 2-7D). Total starch content was found to be higher in both C and LS in the comp lines (Fig. 2-7E). Although the hexose levels were found to be higher in both the C (Fig. 2-7B) and the LS (Fig. 2-7C) of the comp lines, sucrose in the culm tended to be lower (Fig. 2-7B), while in the LS, it was found to be higher (Fig. 2-7C) than the WT and KO. While the total NSC was not different between the WT and the KO, the comp lines showed higher NSC content (Fig. 2-7F), owing to a higher starch content in the C and LS (Fig. 2-7E).

The panicles of the comp lines were longer than that of the WT and KO (Figs. 2-7G and H). However, no differences in the grain size parameters - area, width and height, were found (Fig. 2-7I). The grain number was found to be higher, with a compromise in the grain weight in the comp lines in comparison to the WT and KO (Fig. 2-7J).

Greenhouse conditions

Contrary to the data obtained from field grown *OsINV2* WT and mutants at harvest (Figs. 2-6.2 F and G), the hexose content in the LS of the KO tended to be lower than the WT, while in the FL was not significantly different (Figs. 2-7L and M). The hexose content in the C5 lines in all the tissues was significantly higher (Figs. 2-7L and M), while the sucrose levels remained unchanged between the lines (Fig. 2-7K). The total starch content was also found to be different between the lines (Fig. 2-7N). Total NSC in the comp lines tended to be higher, owing to a higher total sugar content (Fig. 2-7O).

Although, successful complementation was achieved, role of *OsINV2* in regulating the sugar content in the vegetative tissues could not be established.

2-3.8.2 *OsINV3*

Role of OsINV3 in reproductive stage

Genotyping of the WT, mutant and the complementation lines C3, C4 and C13 confirmed the successful incorporation of *OsINV3* gene in the mutant lines, enabling an effective complementation (Fig. 2-8A). The mRNA transcript levels revealed through real-time PCR showed an overexpression in the C4 line (Fig. 2-8B). The presence of aberrant transcript in the mutants was reconfirmed by semi-quantitative PCR using primers F6 and R6 spanning the *Tos17* insertion, that showed an absence of amplicon in the mutants (Fig. 2-8H), while primers F5 and R5 targeting the region downstream of the *Tos17* insertion showed a presence of amplicon, however, lighter in intensity (Fig. 2-8I), coinciding with the real-time data (Fig. 2-8B). The enzyme activity in the mature leaves of the mutant lines was found to be lower by 28.8% relative to the WT, suggesting a reduction in soluble acid invertase activity in the mutants, with observed recovery in the C4 line (Fig. 2-8C). It was observed that the panicles of the mutants were shorter than that of the WT, with displayed recovery of the trait upon complementation (Fig. 2-8D). Grain length and width of unhulled grain was also found to be smaller in the mutant when compared with the WT, with significant recovery observed for both the traits in C4 (Fig. 2-8E). Similar results were obtained for the area of both filled and unfilled spikelets, where smaller area of the mutants was significantly recovered in the C4 lines (Fig. 2-8F). In addition to smaller grain size and panicle height, average single grain weight was also found to be lower in the mutant lines, displaying an absolute recovery for the trait in C4 (Fig. 2-8G). These results indicate a significant role for *OsINV3* in the regulation of panicle height, grain size and grain weight.

In order to isolate the role of *OsINV3* in spikelet cell expansion, spikelets at 2 days before heading (DBH) from WT, mutant and the C4 lines were analyzed using SEM. The cell density in mutant on the outer surface of both palea and lemma were significantly higher than the WT, with observed recovery in the C4 line (Fig. 2-8J, K and L). The cells were stacked closer in the mutants when compared to the WT and the C4 lines. For an observed 23.5% decrease in spikelet area (Fig. 2-8F), a 24.3% increase in the cell density (Fig. 2-8L) was established suggesting a possible lack of difference in cell number. However, cell size on the outer surface of the spikelets of mutant was considerably smaller (Fig. 2-8J and K). The epidermal cells on the inner surface of palea and lemma were analyzed, with decreased cell area, cell width and cell length in the

mutant, and recovery for these traits in the C4 lines (Fig. 2-8M and N). Although absolute recovery in the cell length, and cell area in the lemma of C4 was observed; cell width and cell area in the palea, although significant, were only partially recovered. Thus, the role of *OsINV3* in cell expansion in regulation of spikelet size was established.

Role of OsINV3 in seedling stage

Consistent data with respect to *OsINV3* regulation of shoot height and root length could not be obtained, where no significant differences between the WT, KO and C4 lines were observed (Fig. 2-8O). However, in terms of shoot and root dry weights, KO tended to show lower shoot and root dry weights in comparison to the WT, with observed recovery in the C4 lines, after 19 DAS (Fig. 2-8P). Thus, isolating a role for *OsINV3* in dry matter production during the seedling stage.

2-4 Discussion

Role of OsINV2 and its functional importance

Despite, an increase in total sugar content observed in the *OsINV2* mutants at harvest (Fig. 2-6.2R), complementation tests failed to reaffirm this proposed role of *OsINV2* in regulating the sugar content in vegetative tissues at harvest (Figs. 2-7F and 2-7O). However, the complement lines showed a significant increase in the total NSC content both under monocult (Fig. 2-7F) and greenhouse conditions (Fig. 2-7O). This increase in total NSC could be due to lack of regulation of *OsINV2* as otherwise in the WT, which may be attributed to an absence of regulatory elements upstream or downstream of the gene introduced in the mutants used for complementation. The complementation lines under the monocult conditions also showed longer panicles (Fig. 2-7H), demonstrating that the size of the panicle was strictly owing to turgor generated by the hexoses generated. However, the size of the spikelet was unaffected (Fig. 2-7I), conserving the function of spikelet size regulation by *OsINV3*. A trade-off between the number of spikelets and the grain weight was observed (Fig. 2-7J), where the complement lines were found to have a higher spikelet number, but decreased grain weight, further conserving the function of grain weight regulation by *OsINV3*. Although the *OsINV2* complement lines, failed to establish a concrete role for *OsINV2*, they helped reconfirm the key regulatory roles of *OsINV3* in grain size and weight determination.

Key role of OsINV3 in determination of spikelet size and its influence on grain weight

The *OsINV3* mutants demonstrated smaller sinks by displaying shorter panicle and smaller grain phenotypes, owing to smaller cell size in both the inner and outer surfaces of palea and lemma of the mutant spikelets as demonstrated by the SEM analysis (Fig. 2-8J-N). Role of vacuolar invertases in cell expansion by generation of a turgor in the cell has previously been suggested in *Arabidopsis* roots (Sergeeva et al., 2006), developing petioles and primary roots of carrot (Sturm et al., 1995) and has been widely accepted (Tang et al., 1999; Roitsch and Gonzalez, 2004; Gonzalez et al., 2005; Ruan et al., 2010). The expression of *OsINV3* in the spikelet as observed in the *promoter::GUS* lines in the palea, lemma and the nerves during the panicle development stages (Fig. 2-5.2D-F and d-f) and the early grain filling stages (Fig. 2-5.2 O), reiterates the role of *OsINV3* in cell expansion in the spikelet. Size of the spikelet hull, was found to play a

crucial role in determination of final grain weight, as reported previously (Wang et al. 2008; Song et al. 2015), mainly by modifying the grain filling rate, eventually affecting the grain weight (Wang et al. 2008).

OsINV3 regulates assimilate partitioning into the sinks by modulating the hexose-to-sucrose ratio

The lower grain yield for the mutants, was primarily owing to the lower percentage of grain ripening and lower grain weight (Table 2-3.2). A lower grain ripening could be attributed to failure in normal development of anthers and pollen, and the process of flowering, as observed in *promoter::GUS* lines beginning from the early panicle development stages until after anthesis, where a strong expression of *OsINV3* in anthers (Fig. 2-5.2a-f, and Fig. 2-5.2Q, left) and pollen (Fig. 2-5.2Q, right), and the lodicules (Fig. 2-5.2P) was found. This prospect is co-incident with recent findings (Wang and Ruan 2016, Goetz et al. 2017), and a previous study that isolated a decrease in *OsINV3* transcript levels in the later stages of pollen development of the male sterile lines (Kong et al., 2007). While the size restriction of the grain could be stated as one of the reasons for smaller grain weight, a lower assimilate partitioning to grain was also observed (Fig. 2-3 O), indicating an impaired transport of sucrose from source to sink tissues. In rice, sucrose transport from the source to maternal sinks along the phloem is largely believed to be symplasmic, driven by a sucrose gradient owing to the osmotic potential at the unloading site from the SE/CC complex (Aoki et al. 2012). Modifications in the sugar composition, thus the osmotic potential at the site of unloading could lead to altered capacities of sucrose import by sinks.

Hexose-to-sucrose ratio has long been considered to play a major role in modulating the osmotic gradient, thus, regulating the sink strength during the period of grain filling (Herbers and Sonnewald 1998). This ratio is found to increase during the pre-storage phase, followed by its drastic decrease, characterizing the beginning of the active storage phase of grain filling (Herbers and Sonnewald 1998). In our study, although this ratio from heading to harvest was maintained equally between the WT and the mutants, it tended to be significantly lower in the mutants during the pre-storage phase of grain filling (Fig. 2-6.1I), with an increased sucrose concentration, which diminished the sucrose gradient along the site of unloading, facilitating a lower sucrose influx thus, a lower availability of sucrose for unloading into the filial tissues. The *promoter::GUS* studies revealed a strong *OsINV3* expression at the dorsal ovary immediately after fertilization until 6 DAF (Fig. 2-5.2G-M), serving as the critical point for directing sucrose import.

Thus, the lower assimilate partitioning to the sinks during the reproductive stage, and the lower dry matter in both shoots and roots of the *OsINV3* mutants in the seedling stage (Fig. 2-7P), are demonstrative of the role of *OsINV3* as a sink strength determinant.

Functional redundancy of vacuolar invertase

Key biochemical functions are redundantly encoded in various isoforms to ensure normal development upon failure of one of the isoforms. Rice consists of two isoforms of vacuolar invertase, *OsINV2* and *OsINV3* (Ji et al. 2005). In terms of yield (Tables 2-3.1 and 2-3.2) and dry matter partitioning (Fig. 2-3C-F and 2-3G-L), no key defects with respect to grain yield were observed in the mutants of *OsINV2*, however, *OsINV3* mutants demonstrated smaller and lighter grain (Fig. 2-8A-G) with lower partitioning to the grain (Fig. 2-3O). This could be attributed to the functional redundancy between *OsINV2* and *OsINV3*, where *OsINV3* substituted for *OsINV2* in its absence but, *OsINV2* failed to fulfil the key regulatory roles of *OsINV3* in terms of maintaining the hexose-to-sucrose ratios and grain size in the *OsINV3* mutants. The complementary expression pattern of these two VINs in the panicles from panicle initiation to grain filling stages (Fig. 2-5.1 C and Fig 2-5.2 A-M) could be attributed to this inability of *OsINV2* to fulfil key roles of *OsINV3*, where, *OsINV2* was found to be functional in the early stages, *OsINV3* played a key role in the later stages with increased expression levels in the spikelet (Fig. 2-5.2 d-f). However, in the vegetative tissues, drastic differences in the NSC content (Fig. 2-6.2 Q-R) and VIN activities (Fig. 2-6.2 S-V) between the WT and mutants wasn't observed, possibly owing to a satisfactory substitution by the other isoform.

In the developing panicles of *OsINV3* mutants, although the development of sinks was not defective, they were reduced in size (Figs. 2-8D and E), owing to the lower ratios of hexose to sucrose in comparison to the WT (Fig. 2-6.1 I). Lack of differences in the VIN activity (Fig. 2-6.1 J) failed to account for the reduced hexose levels in the young developing panicles (Fig. 2-6.1A). This could be attributed to the functional redundancy of VINs, where *OsINV2* was overexpressed under the absence of *OsINV3*, owing to a greater demand of hexoses in the rapidly expanding tissues; which was confirmed by an increase in mRNA transcript levels of *OsINV2* in the tissues of the *OsINV3* mutants (Fig. 2-6.1 M). Despite this overexpression, *OsINV2* failed to substitute for the key physiological roles of *OsINV3*, in maintaining the hexose to sucrose ratios (Fig. 2-6.1 I). We suggest two possible rationale to explain this finding. First, the higher V_{max} of

510 nkat mg⁻¹ for OsINV2 when compared to 20.5 nkat mg⁻¹ for OsINV3 (Ji et al. 2007), outlines a stronger possibility of the former being regulated post-translationally by inhibitors, as reported in CWINs (French et al. 2014 (in rice); Jin et al. 2009 (in tomato)). However, lack of studies on mode of regulation by VIN inhibitors deems it difficult to replicate this in *in vitro* assays as observed in our study (Fig. 2-6.1 J). Second, differences in cellular or sub-cellular localization of the two isoforms could explain the inadequate substitution by OsINV2 for physiological roles of OsINV3. However, further studies need to be carried out to establish this proposition.

Primers	Sequence (5'-3')	Size of the amplicon (bp)	
Genotyping			
F7	CTCTGCTTCCCGAGACGA	304	
R7	GAGTTGGTCCAGGCGTAGTC		
T6	AGGTTGCAAGTTAGTTAAGA	180	
Complementation			
PL1	CAACATATGCCTAAAGTCCATGC	8318	
cds3T	CTAGTCTACATATGGACGGA		
<i>Promoter::GUS</i>			
INV2-PL1	CAACATATGCCTAAAGTCCATGC	2125	
INV2-ATG	GGAGATGGCCGGGATCAT		
Real-time PCR			
<i>OsINV2</i>	F2	GGCAGCTTGGTACCTGTGCTA	n/a
	R2	GCAGAGTTCAGCTCCCAAATC	
<i>RUBIQ</i>	F4	GGAGCTGCTGCTGTTCTTGG	
	R4	CACAATGAAACGGGACACGA	

Table 2-1A. *OsINV2* primer sequences. n/a – not applicable

Primers	Sequence (5'-3')	Size of the amplicon (bp)	
Genotyping			
F1	AGATTCTTCCAGCCCCATTT	350	
R1	GTACCACTGGTCGGGAACC		
T5	CATCGGATGTCCAGTCCATTG	315	
Complementation			
PL2	GCAGCTAGCCTTTTTCTCTT	5575	
R7T	CTAGGCCATGTAGGCTTGGT		
<i>Promoter::GUS</i>			
PINV3-L2H	CCCAAGCTTACACACGCATGTTGCTGA	1978	
PINV3-R2X	CCCTCTAGAGGCGTCGGCGACGTC		
Real-time PCR			
<i>OsINV3</i>	F3	GACCGCCGTGTACTTCTACG	n/a
	R3	GACGACCCTCTTGACGATGT	
<i>RUBIQ</i>	F4	GGAGCTGCTGCTGTTCTTGG	
	R4	CACAATGAAACGGGACACGA	
Semi-quantitative PCR			
F5	AAGACCTTCTACGATCCGGC	107	
R5	AGCTGGAGGGAAGCCCAA		
F6	ATGAACGATCCCAACGGTCC	170	
R6	TACCACTGGTCGGGAACCAT		

Table 2-1B. *OsINV3* primer sequences. n/a – not applicable

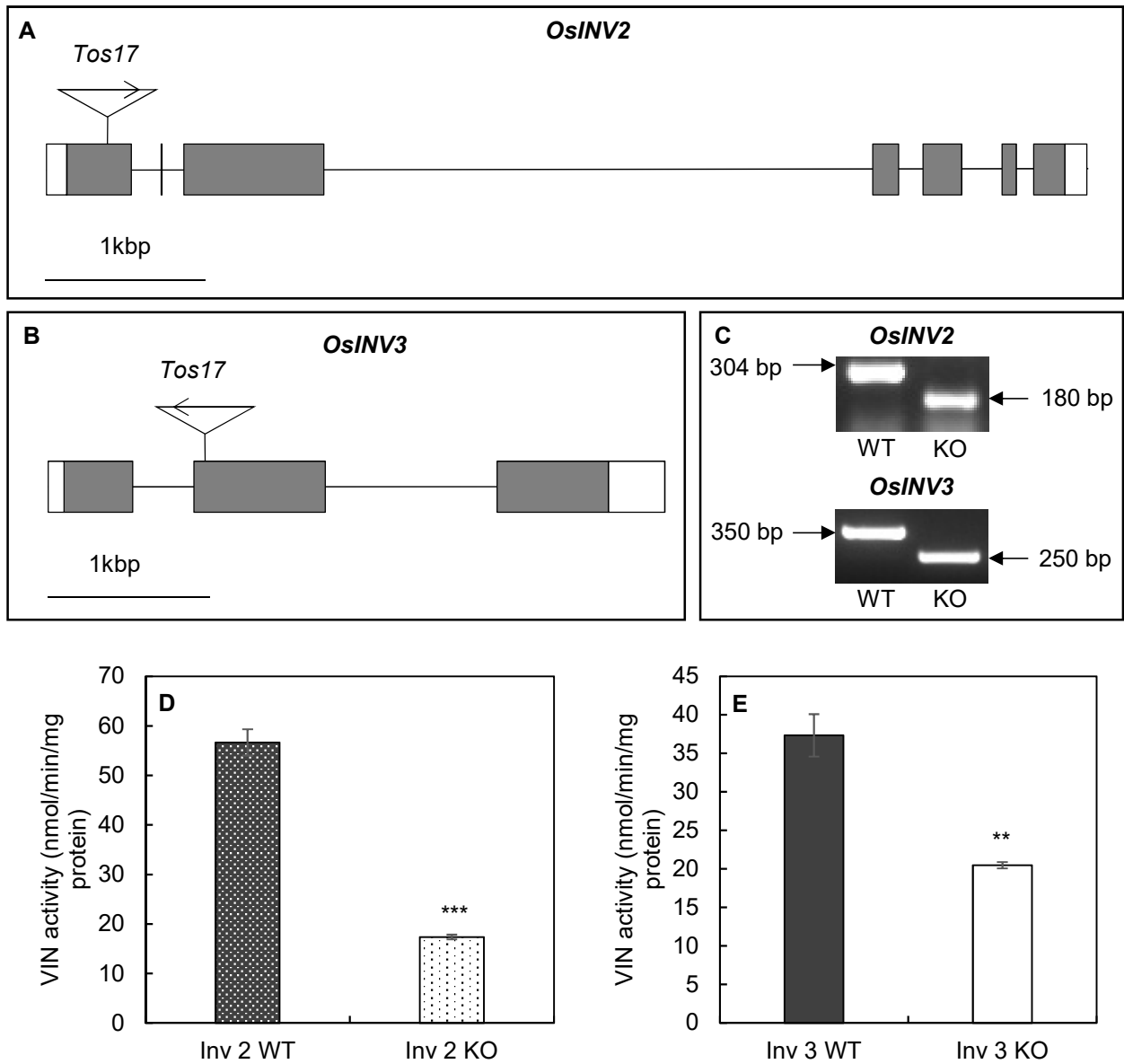


Fig. 2-1 (A) *OsINV2* and (B) *OsINV3* genes in 5'-3' direction with the *Tos17* insertion in the corresponding exons in forward and reverse orientation respectively. Grey boxes denote exons separated by lines that denote introns, white boxes indicate 5'(left) and 3'(right) UTRs. (C) Gel data showing the presence of WT and KO alleles in *OsINV2* and *OsINV3* WT and KO lines, and the decrease in vacuolar invertase (VIN) activity in the flag leaf of (D) *OsINV2* and (E) *OsINV3*, WT and mutants (KO) at the heading stage. Data represent the mean \pm SE (n=3). Asterisks indicate statistical significance of difference using Student's T-statistic with **-p<0.01 and ***-p<0.001.

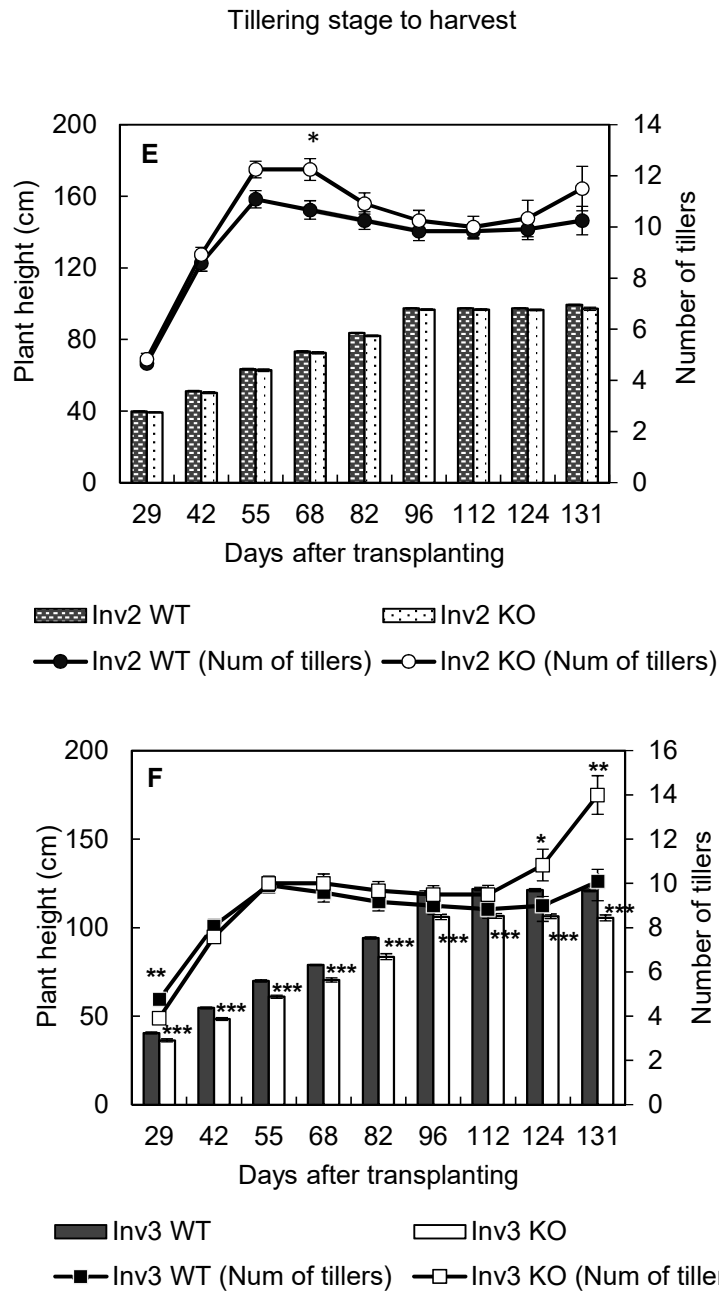


Fig. 2-2 (E-F). Growth analysis, including plant height and number of tillers for (E) *OsINV2* and (F) *OsINV3* WT and mutants (KO) from tillering to harvest stage. Data represent the mean \pm SE (n=12). Asterisks indicate statistical significance of difference using Student's T-statistic with *-p<0.05, **-p<0.01 and ***-p<0.001. Field data shown for 2016.

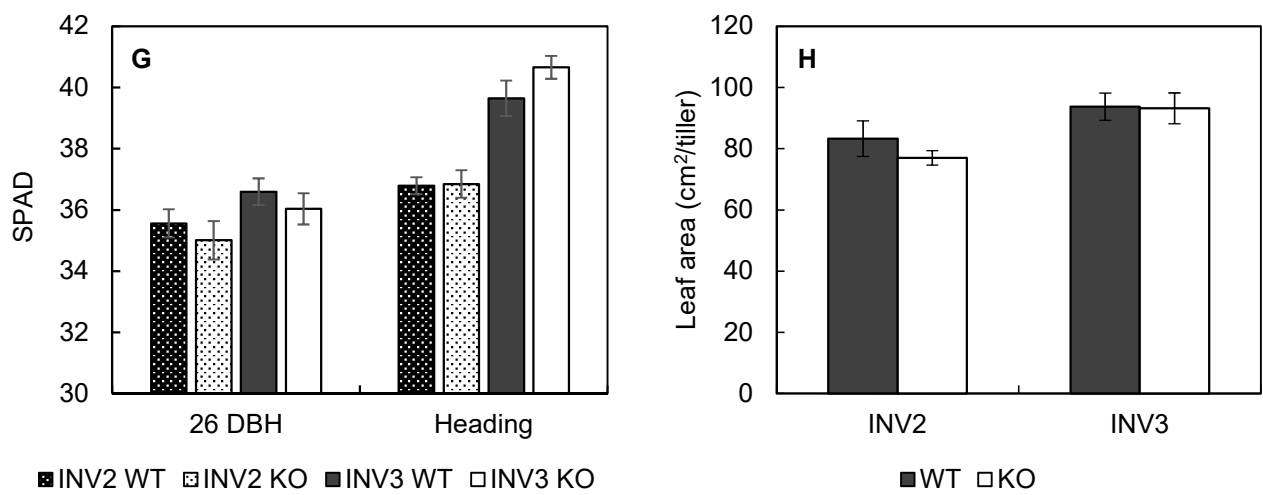


Fig. 2-2 (G-H). (G) SPAD at 26 DBH and heading (n=15), and (H) Leaf area index (LAI) (n=9) for *OsINV2* and *OsINV3* WT and mutants (KO). Data represent the mean \pm SE. Field data obtained in 2015.

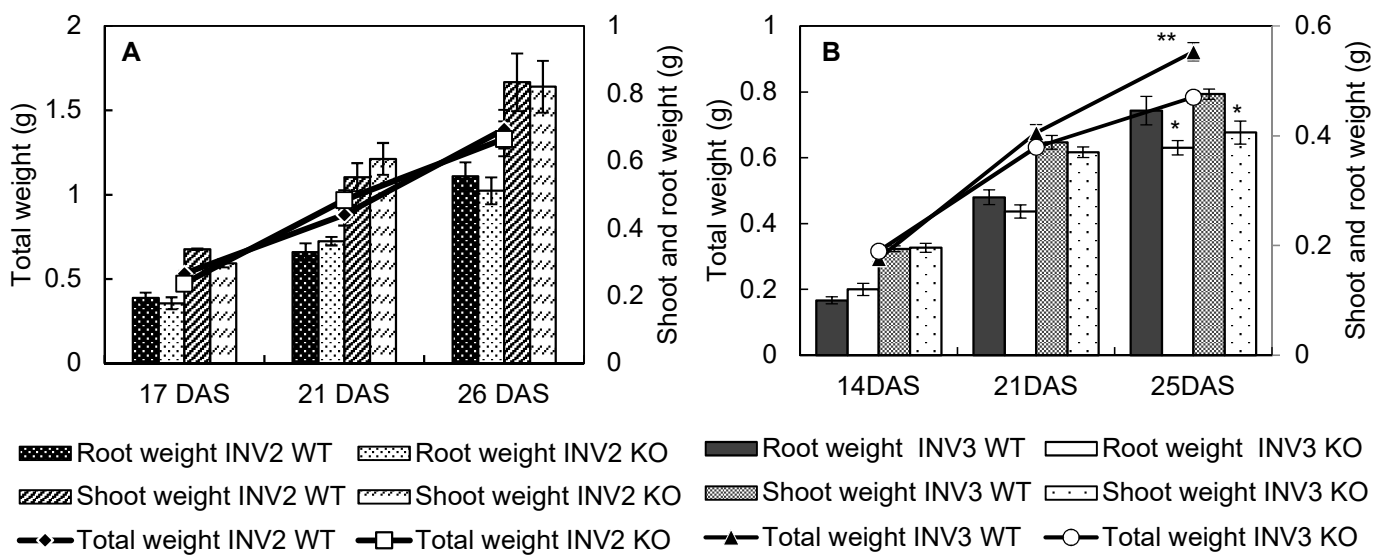


Fig. 2-3 (A-B). Seedling total fresh weight, shoot and root fresh weights for WT and mutants (KO) of (A) *OsINV2* and (B) *OsINV3*. Data represent the mean \pm SE (n=9). Asterisks indicate statistical significance of difference using Student's T-statistic with *-p<0.05 and **-p<0.01.

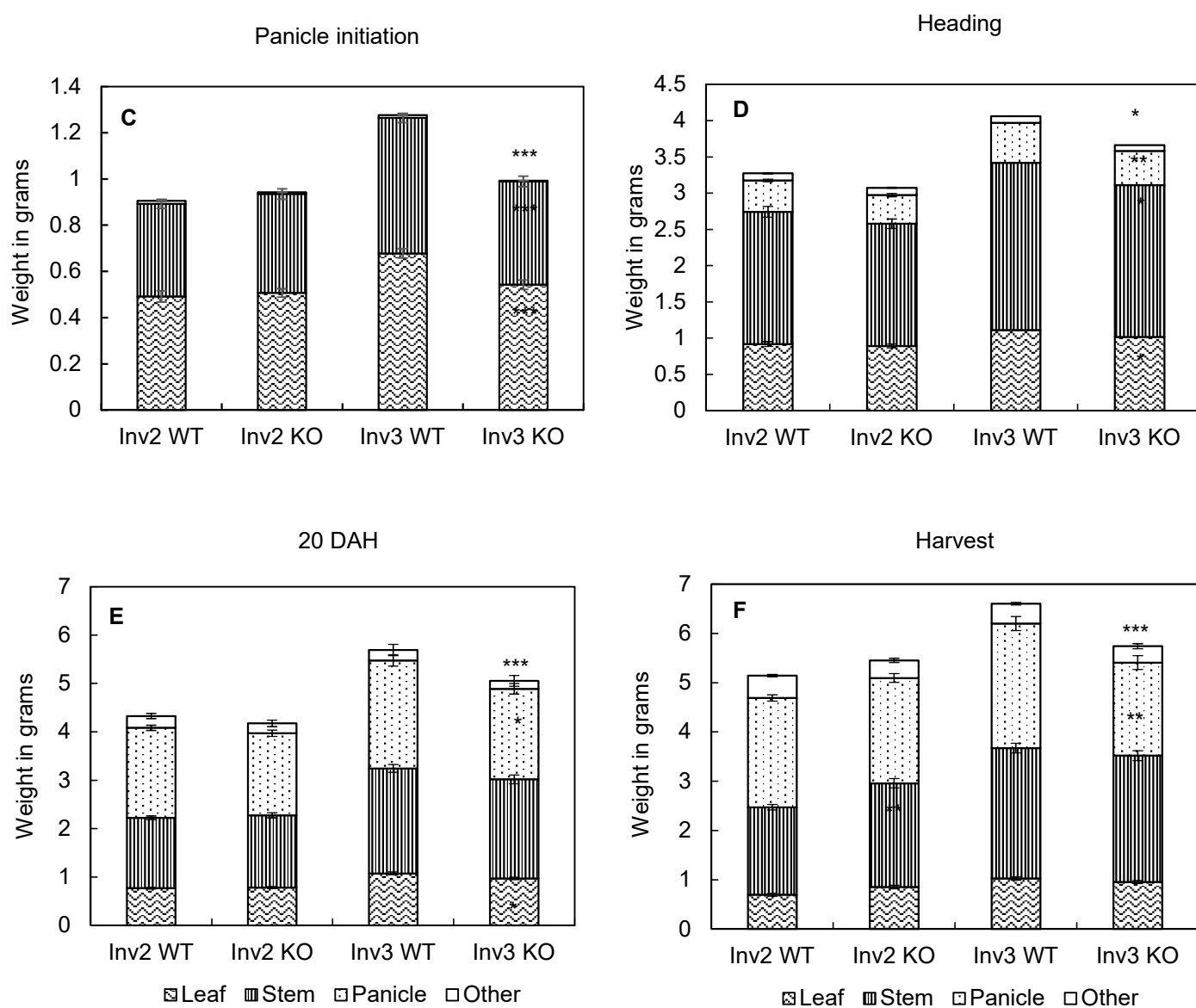


Fig. 2-3 (C-F). Tissue-wise dry weight partitioning expressed in grams per panicle for *OsINV2* and *OsINV3* WT and mutants (KO) at (C) panicle initiation, (D) heading, (E) 20 DAH and (F) 40 DAH (harvest). Data represent the mean \pm SE (n=9). Asterisks indicate statistical significance of difference using Student's T-statistic with *-p<0.05, **-p<0.01 and ***-p<0.001. Field data shown for 2015

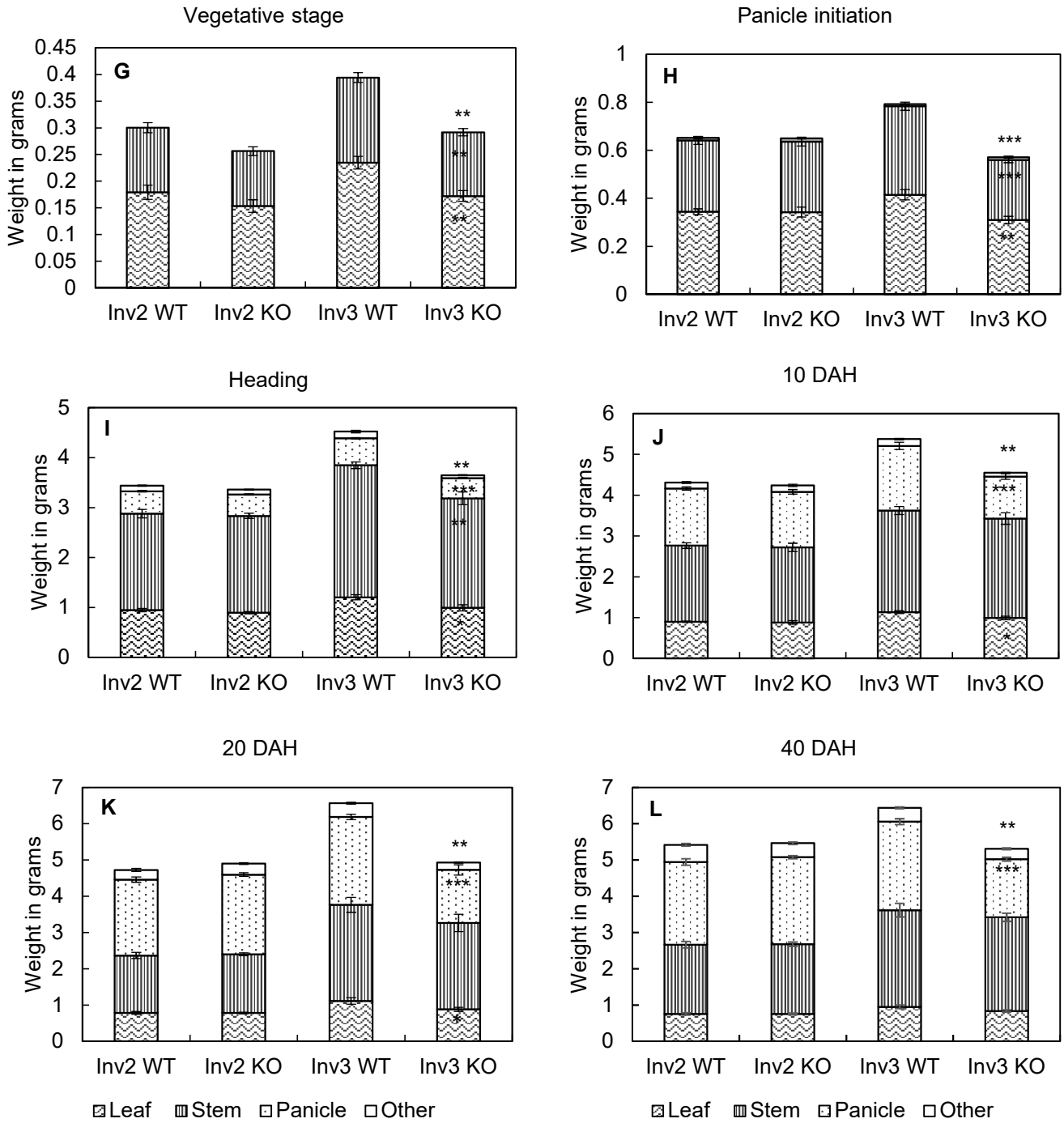


Fig. 2-3 (G-L). Tissue-wise dry weight partitioning expressed in grams per panicle for *OsINV2* and *OsINV3* WT and mutants (KO) at (G) vegetative stage, (H) panicle initiation, (I) heading, (J) 10 DAH, (K) 20 DAH and (L) 40 DAH (harvest). Data represent the mean \pm SE (n=9). Asterisks indicate statistical significance of difference using Student's T-statistic with *-p<0.05, **-p<0.01 and ***-p<0.001. Field data shown for 2016

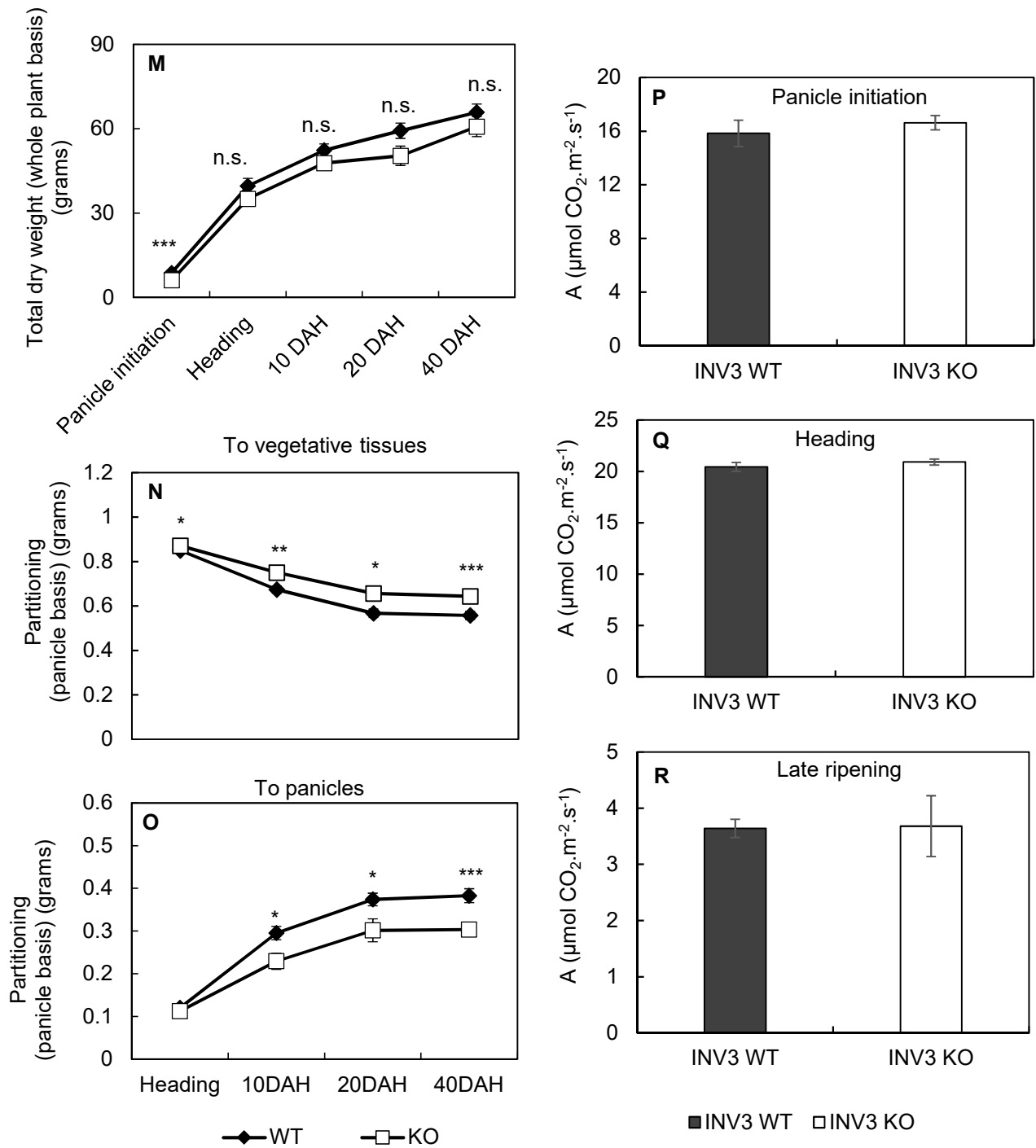


Fig. 2-3 (M-R). Dry weight differences and photosynthesis rates in *OsINV3* WT and the mutants (KO). (M) Total dry weights measured on a whole plant basis (N) Dry matter partitioning to the vegetative tissues and (O) panicles, on per panicle basis for *OsINV3* WT and KO (n=9). Photosynthesis rates (A in $\mu\text{mol CO}_2\cdot\text{m}^{-2}\cdot\text{s}^{-1}$) for the *OsINV3* WT and the mutant (KO) at 30°C, PARi 1500 $\mu\text{mol}\cdot\text{m}^{-2}\cdot\text{s}^{-1}$ and CO_2 concentration of 390 $\text{ml}\cdot\text{L}^{-1}$ at (P) Panicle initiation (Q) Heading (R) Late ripening, were measured using CIRAS-3 Photosynthesis Systems (PP systems, Amesbury, MA, USA) (n=6). Data represent the mean \pm SE. Asterisks indicate statistical significance of difference using Student's T-statistic with *-p<0.05, **-p<0.01 and ***-p<0.001; and n.s. – not significant. X-axis – representative of stage, and not scaled to number of days.

	Year	Variety	Leaf (g)	Stem (g)	Dried tissue (g)	Total (g)	
Panicle initiation (28 DBH)	2015	Inv2 WT	0.49±0.02	0.40±0.02	0.01±0.002	0.91±0.04	
		Inv2 KO	0.51±0.02	0.43±0.02	0.01±0.001	0.94±0.04	
	2016	Inv2 WT	0.34±0.01	0.3±0.02	0.01±0.005	0.65±0.03	
		Inv2 KO	0.34±0.02	0.29±0.02	0.01±0.002	0.65±0.04	
	Average	Inv2 WT	0.42	0.35	0.01	0.78	
		Inv2 KO	0.43	0.36	0.01	0.8	
	ANOVA	Year	***	***	n.s.	***	
	Variety	n.s.	n.s.	n.s.	n.s.		
	Year*Variety	n.s.	n.s.	n.s.	n.s.		
<hr/>							
	Year	Variety	Leaf (g)	Stem (g)	Panicle (g)	Dried tissue (g)	Total (g)
Heading	2015	Inv2 WT	0.92±0.05	1.82±0.08	0.43±0.02	0.1±0.01	3.27±0.13
		Inv2 KO	0.89±0.03	1.69±0.05	0.4±0.01	0.1±0.01	3.07±0.1
	2016	Inv2 WT	0.95±0.03	1.93±0.09	0.45±0.02	0.11±0.01	3.44±0.12
		Inv2 KO	0.89±0.02	1.94±0.05	0.43±0.01	0.1±0.01	3.36±0.08
	Average	Inv2 WT	0.94	1.88	0.44	0.11	3.36
		Inv2 KO	0.89	1.82	0.42	0.1	3.22
	ANOVA	Year	n.s.	*	n.s.	n.s.	n.s.
	Variety	n.s.	n.s.	n.s.	n.s.	n.s.	
	Year*Variety	n.s.	n.s.	n.s.	n.s.	n.s.	
<hr/>							
	Year	Variety	Leaf (g)	Stem (g)	Panicle (g)	Dried tissue (g)	Total (g)
20 DAH	2015	Inv2 WT	0.77±0.02	1.45±0.04	1.86±0.05	0.24±0.02	4.34±0.09
		Inv2 KO	0.78±0.02	1.49±0.05	1.7±0.07	0.2±0.01	4.34±0.09
	2016	Inv2 WT	0.78±0.04	1.58±0.08	2.09±0.07	0.26±0.04	4.72±0.19
		Inv2 KO	0.78±0.02	1.62±0.04	2.19±0.05	0.30±0.03	4.9±0.11
	Average	Inv2 WT	0.78	1.52	1.98	0.25	4.53
		Inv2 KO	0.78	1.56	1.95	0.25	4.62
	ANOVA	Year	n.s.	*	***	*	***
	Variety	n.s.	n.s.	n.s.	n.s.	n.s.	
	Year*Variety	n.s.	n.s.	*	n.s.	n.s.	
<hr/>							
	Year	Variety	Leaf (g)	Stem (g)	Panicle (g)	Dried tissue (g)	Total (g)
Harvest (40 DAH)	2015	Inv2 WT	0.7±0.03	1.77±0.06	2.22±0.06	0.45±0.03	5.14±0.13
		Inv2 KO	0.85±0.04	2.1±0.1	2.14±0.09	0.36±0.04	5.35±0.21
	2016	Inv2 WT	0.76±0.03	1.91±0.09	2.28±0.09	0.47±0.03	5.42±0.16
		Inv2 KO	0.75±0.02	1.92±0.06	2.4±0.04	0.39±0.04	5.46±0.1
	Average	Inv2 WT	0.73	1.84	2.25	0.46	5.28
		Inv2 KO	0.8	2.01	2.27	0.38	5.41
	ANOVA	Year	n.s.	n.s.	*	n.s.	n.s.
	Variety	*	*	n.s.	*	n.s.	
	Year*Variety	*	n.s.	n.s.	n.s.	n.s.	

Table 2-2.1. Tissue-wise dry weights per panicle for *OsINV2* WT and mutant (KO). Data represent the mean ± SE (n=9-15). Asterisks indicate statistical significance of difference with *-p<0.05, **-p<0.01 and ***-p<0.001. Year and variety effects and interaction on individual tissue dry weights were determined using 2-way ANOVA test.

	Year	Variety	Leaf (g)	Stem (g)	Dried tissue (g)	Total (g)		
Panicle initiation (28 DBH)	2015	Inv3 WT	0.68±0.02	0.59±0.02	0.01±0.004	1.28±0.04		
		Inv3 KO	0.54±0.02	0.45±0.02	0.003±0.001	0.99±0.04		
	2016	Inv3 WT	0.41±0.02	0.37±0.02	0.01±0.002	0.79±0.04		
		Inv3 KO	0.31±0.02	0.25±0.01	0.01±0.004	0.57±0.03		
	Average	Inv3 WT	0.55	0.48	0.01	1.04		
		Inv3 KO	0.43	0.35	0.007	0.78		
	ANOVA	Year		***	***	n.s.	***	
		Variety		***	***	n.s.	***	
		Year*Variety		n.s.	n.s.	n.s.	n.s.	
		Year	Variety	Leaf (g)	Stem (g)	Panicle (g)	Dried tissue (g)	Total (g)
Heading	2015	Inv3 WT	1.11±0.03	2.31±0.07	0.55±0.02	0.09±0.01	4.06±0.12	
		Inv3 KO	1.01±0.03	2.1±0.06	0.47±0.02	0.08±0.01	3.66±0.11	
	2016	Inv3 WT	1.20±0.05	2.64±0.07	0.54±0.01	0.13±0.03	4.52±0.11	
		Inv3 KO	0.99±0.06	2.19±0.13	0.40±0.01	0.06±0.01	3.65±0.19	
	Average	Inv3 WT	1.16	2.48	0.55	0.11	4.29	
		Inv3 KO	1	2.15	0.44	0.07	3.66	
	ANOVA	Year		n.s.	*	*	n.s.	n.s.
		Variety		**	***	***	**	***
		Year*Variety		n.s.	n.s.	n.s.	*	n.s.
		Year	Variety	Leaf (g)	Stem (g)	Panicle (g)	Dried tissue (g)	Total (g)
20 DAH	2015	Inv3 WT	1.07±0.03	2.17±0.08	2.23±0.12	0.22±0.02	4.39±0.09	
		Inv3 KO	0.97±0.03	2.05±0.09	1.87±0.11	0.16±0.01	4.3±0.09	
	2016	Inv3 WT	1.11±0.09	2.65±0.2	2.43±0.07	0.38±0.03	6.57±0.32	
		Inv3 KO	0.88±0.06	2.38±0.24	1.46±0.14	0.2±0.02	4.93±0.29	
	Average	Inv3 WT	1.09	2.41	2.33	0.3	5.48	
		Inv3 KO	0.93	2.22	1.67	0.18	4.62	
	ANOVA	Year		n.s.	**	n.s.	***	n.s.
		Variety		**	n.s.	***	***	***
		Year*Variety		n.s.	n.s.	*	**	*
		Year	Variety	Leaf (g)	Stem (g)	Panicle (g)	Dried tissue (g)	Total (g)
Harvest (40 DAH)	2015	Inv3 WT	1.02±0.03	2.65±0.1	2.53±0.14	0.4±0.03	5.39±0.21	
		Inv3 KO	0.95±0.03	2.56±0.1	1.89±0.14	0.33±0.05	5.44±0.21	
	2016	Inv3 WT	0.95±0.05	2.66±0.19	2.44±0.08	0.38±0.03	6.44±0.25	
		Inv3 KO	0.84±0.03	2.58±0.11	1.6±0.05	0.28±0.02	5.31±0.2	
	Average	Inv3 WT	0.99	2.66	2.49	0.39	5.92	
		Inv3 KO	0.9	2.57	1.75	0.31	5.38	
	ANOVA	Year		*	n.s.	n.s.	n.s.	n.s.
		Variety		*	n.s.	***	*	***
		Year*Variety		n.s.	n.s.	n.s.	n.s.	n.s.

Table 2-2.2. Tissue-wise dry weights per panicle for *OsINV3* WT and mutant (KO). Data represent the mean ± SE (n=9-15). Asterisks indicate statistical significance of difference with *-p<0.05, **-p<0.01 and ***-p<0.001. Year and variety effects and interaction on individual tissue dry weights were determined using 2-way ANOVA test.

Year	Variety	No. of productive panicles	No. of spikelet/panicle	% of filled grain	1000 grain weight	Yield (kg/10a)
2015	INV2 WT	10.2±0.35	106.73±3.17	74.06±1.93	24.03±0.18	430.31±24.53
	INV2 KO	10.47±0.274	102.85±1.91	76.44±1.3	24.19±0.2	442.83±18.0
	INV2 WT/KO	n.s.	n.s.	n.s.	n.s.	n.s.
2016	INV2 WT	9.33±0.33	99.8±1.39	85.66±0.88	25.81±0.1	456.73±17.32
	INV2 KO	9.21±0.44	98.74±1.84	85.36±1.09	26.08±0.16	447.89±21.12
	INV2 WT/KO	n.s.	n.s.	n.s.	n.s.	n.s.
Average	INV2 WT	9.77	103.27	79.86	24.92	443.52
	INV2 KO	9.84	100.8	80.9	25.14	445.36
ANOVA	Year	**	*	***	***	n.s.
	Variety	n.s.	n.s.	n.s.	n.s.	n.s.
	Year*Variety	n.s.	n.s.	n.s.	n.s.	n.s.

Table 2-3.1. Yield and its components for *OsINV2* WT and mutant (KO). Data represent the mean ± SE (n=12-15). Asterisks indicate statistical significance of difference with *-p<0.05, **-p<0.01 and ***-p<0.001. Year and variety dependence on individual yield components were determined using 2-way ANOVA tests.

Year	Variety	No. of productive panicles	No. of spikelet/panicle	% of filled grain	1000 grain weight	Yield (kg/10a)
2015	INV3 WT	8.25±0.27	121.84±3.34	85.23±0.82	26.24±0.21	499.93±23.28
	INV3 KO	9.75±0.55	113.21±3.82	68.47±1.89	19.62±0.71	364.32±26.88
	INV3 WT/KO	*	n.s.	***	***	**
2016	INV3 WT	9.3±0.4	112.4±2.1	76.6±2.8	27.7±0.1	491.8±25.2
	INV3 KO	9.2±0.4	107.8±2.8	63±2.2	19.3±0.1	256.2±18.7
	INV3 WT/KO	n.s.	n.s.	***	***	***
Average	INV3 WT	8.79	117.11	80.91	26.98	495.86
	INV3 KO	9.46	110.49	65.23	19.46	310.26
ANOVA	Year	n.s.	*	**	*	*
	Variety	n.s.	n.s.	***	***	***
	Year*Variety	n.s.	n.s.	n.s.	n.s.	n.s.

Table 2-3.2. Yield and its components for *OsINV3* WT and mutant (KO). Data represent the mean ± SE (n=12-15). Asterisks indicate statistical significance of difference with *-p<0.05, **-p<0.01 and ***-p<0.001. Year and variety dependence on individual yield components were determined using 2-way ANOVA tests.

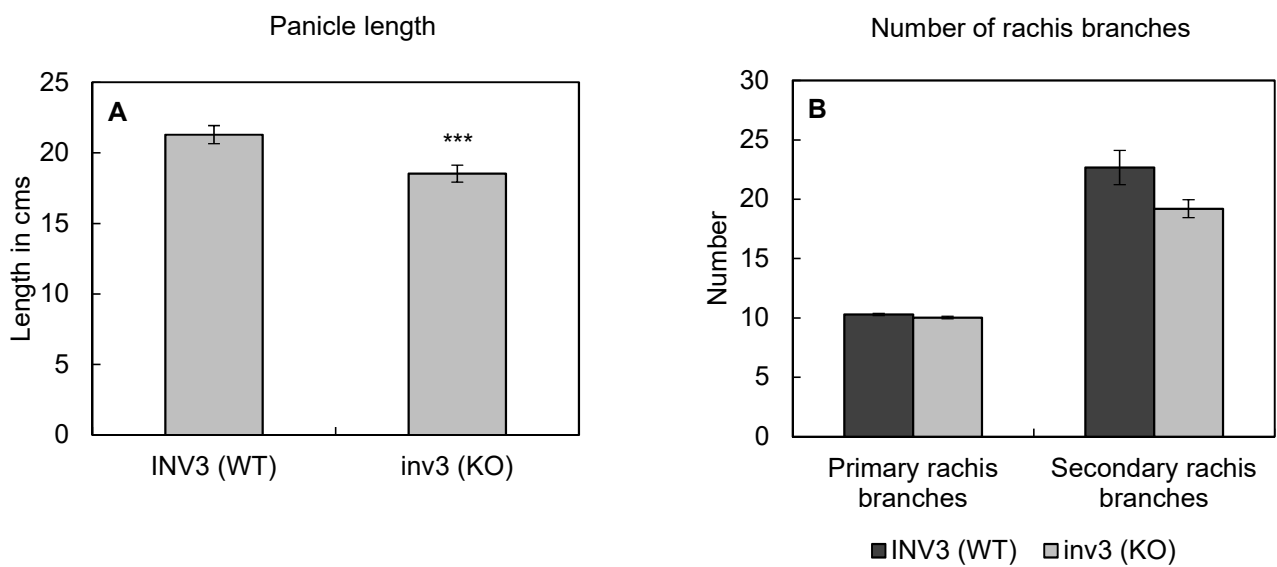


Fig. 2-4 (A-B). Panicle analysis for field grown *OsINV3* mutants (KO). (A) Panicle length, and weight after threshing (n=29), and (B) Number of rachis branches for *OsINV3* WT and KO are shown. Data represent the mean \pm SE (n=3 plants). Asterisks indicate statistical significance of difference using Student's T-statistic with ***-p<0.001.

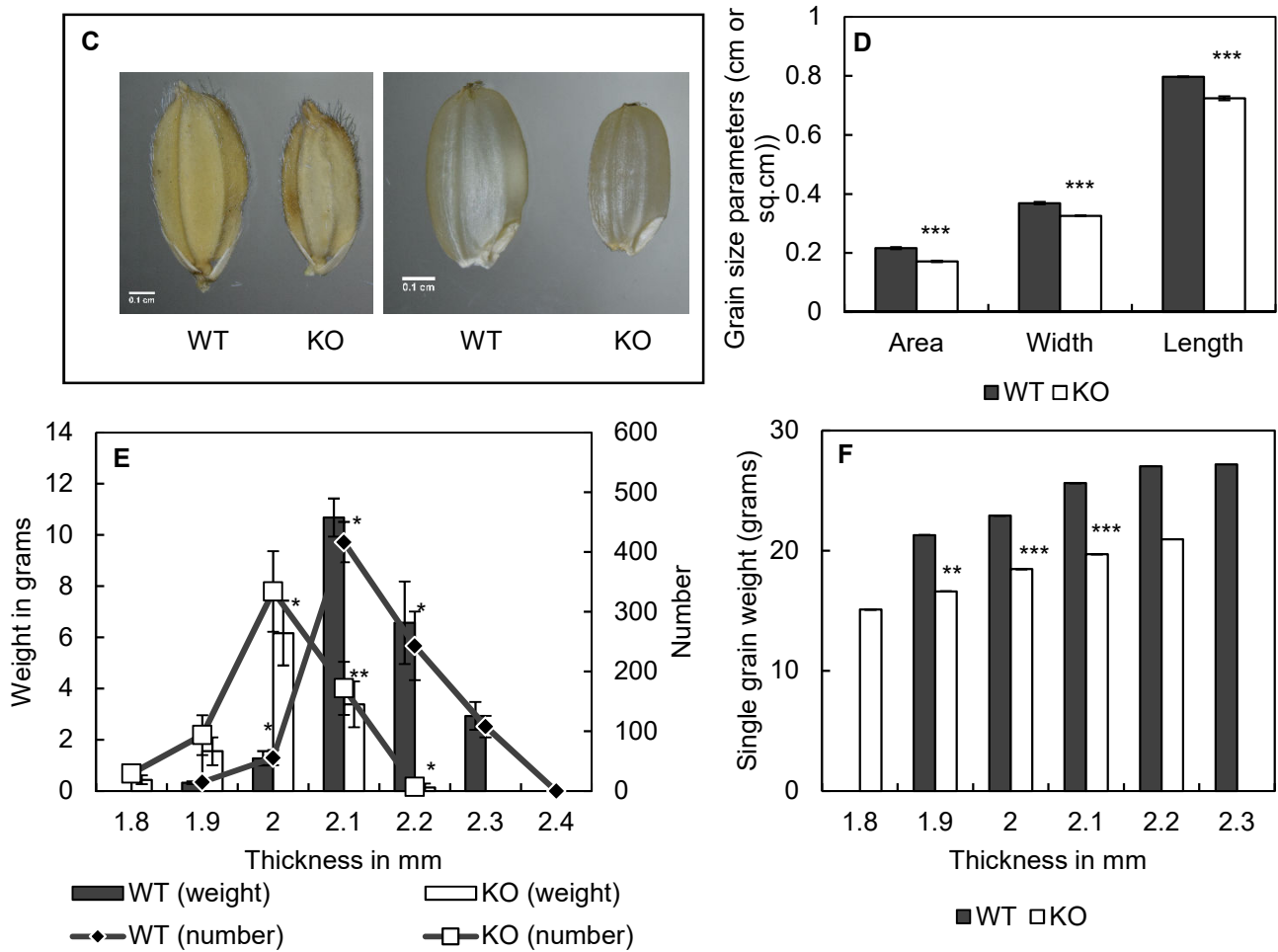


Fig. 2-4 (C-F). Grain size analysis for field grown mutants (KO). (C) Grain size differences, unhusked (left) and husked (right), (D) grain size parameters of unhusked grain (N=30), (E) grain number and weight for corresponding grain thickness, (F) single grain weight for corresponding grain thickness are shown. Data represent the mean \pm SE (n=3 plants). Asterisks indicate statistical significance of difference using Student's T-statistic with *-p<0.05, **-p<0.01 and ***-p<0.001. Horizontal bars represent 1 mm.

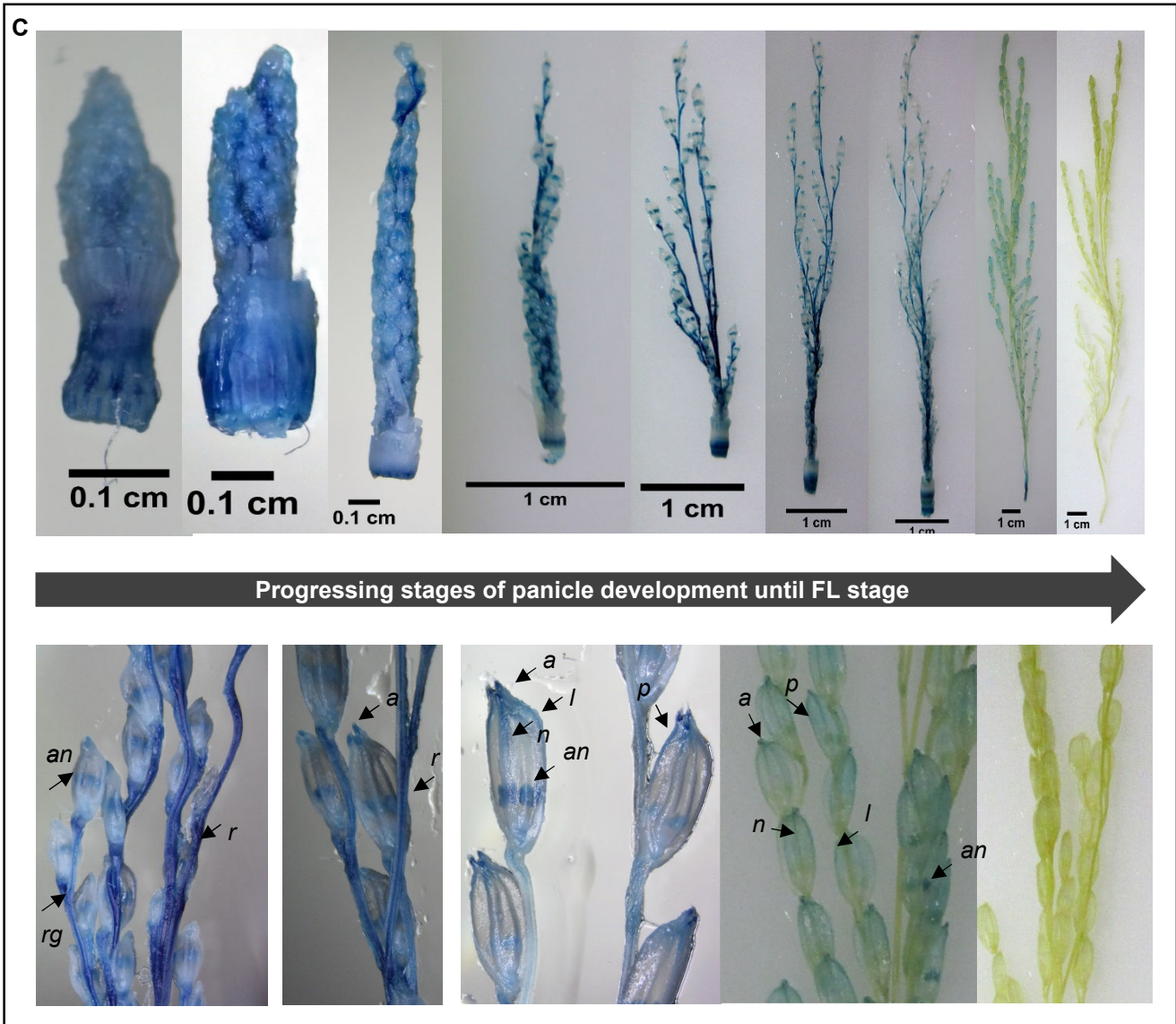


Fig. 2-5.1 C. (C) Spatio-temporal expression of *OsINV2* in the young panicles from stages of panicle length less than 1cm to the FL stage. Top: Whole panicle images, Bottom: magnified images denoting expression of *OsINV2* in the early stages of panicle initiation. Arrows show the areas stained, isolating *OsINV2* expression in rachis branches (*r*), palea (*p*), lemma (*l*), nerves (*n*), anther (*an*), rudimentary glume (*rg*) and awn (*a*).

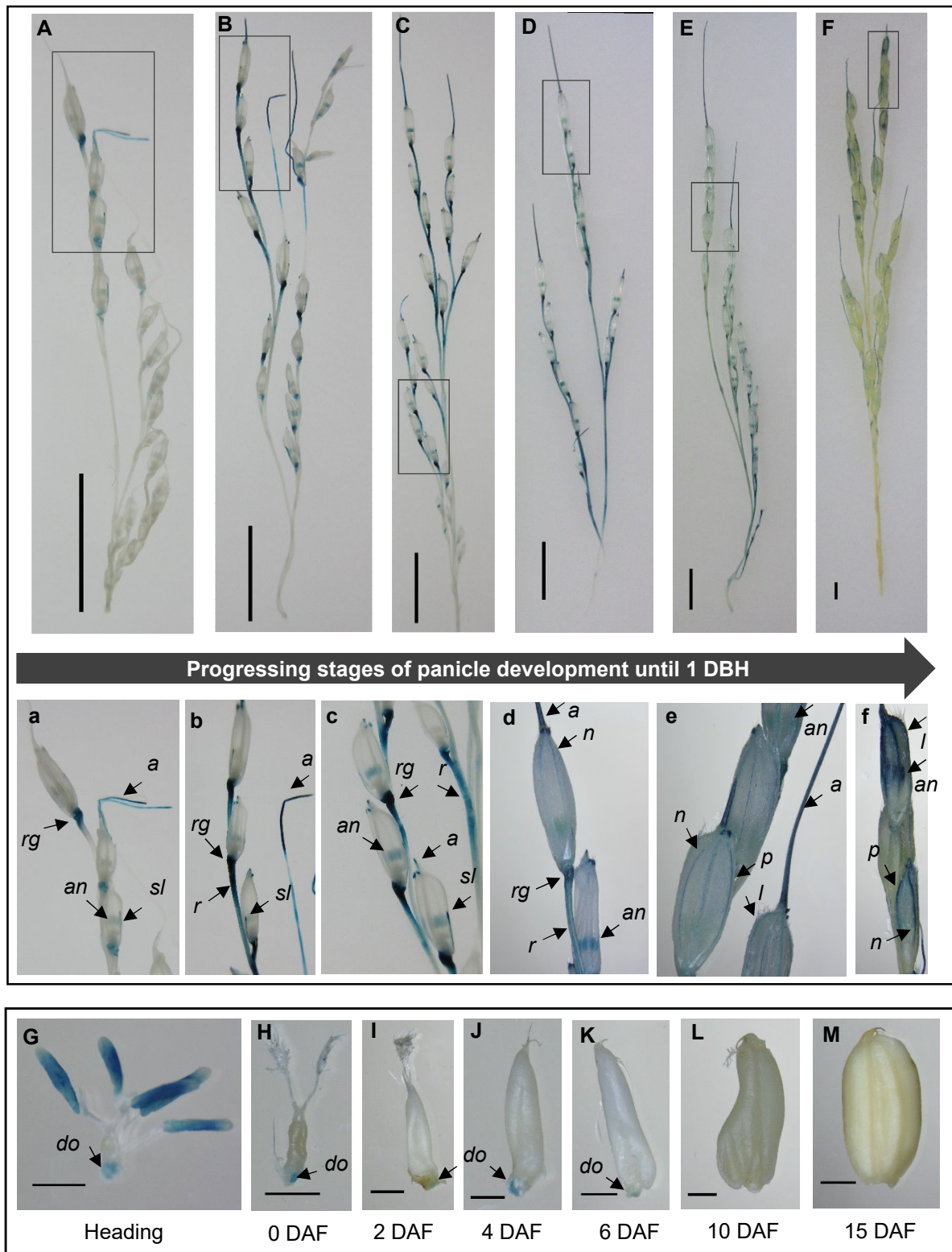


Fig. 2-5.2 (A-M). Spatio-temporal expression of *OsINV3* in the panicle using *promoter::GUS* lines. (A)-(F) *GUS* stained panicles at different progressing stages of panicle development until 1 DBH; (a)-(f) magnified images of the area marked in (A)-(F). (G)-(M) *Promoter::GUS* expression in the developing endosperm at heading, 0 DAF, 2 DAF, 4 DAF, 6 DAF, 10 DAF and 15 DAF respectively. Vertical bars indicate 1 cm and horizontal bars indicate 1 mm. Arrows show the areas stained, isolating a vascular trace of *OsINV3* expression in rachis branches (*r*), palea (*p*), lemma (*l*), nerves (*n*), anther (*an*), sterile lemmas (*sl*), rudimentary glume (*rg*), awn (*a*) and the dorsal end of the ovary (*do*).

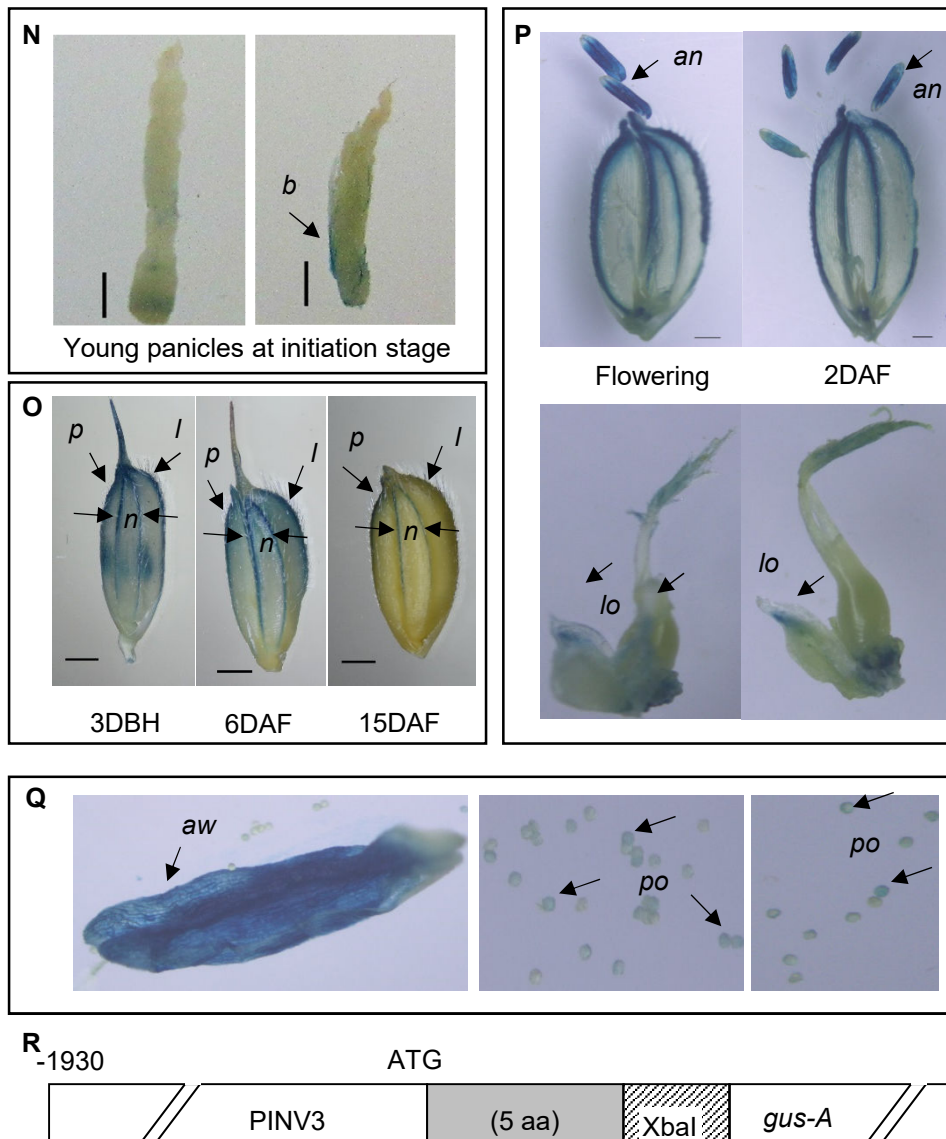


Fig. 2-5.2 (N-R). *OsINV3 promoter::GUS* expression in the (N) young panicles (smaller than 1cm) at the beginning of panicle initiation stage, (O) spikelet at progressing developmental stages from 3 DBH to 15 DAF, and (P) anthers and the lodicules at flowering and 2 DAF, (Q) Magnified images of the stained anther and the pollen, (R) The construct used for generating *OsINV3-GUS* lines, with *gus-A* driven by the *OsINV3* promoter. Bars indicate 1 mm. Arrows show expression in the bract hair (*b*), palea (*p*), lemma (*l*), nerves (*n*), anther (*an*), lodicule (*lo*), anther walls (*aw*) and pollen (*po*).

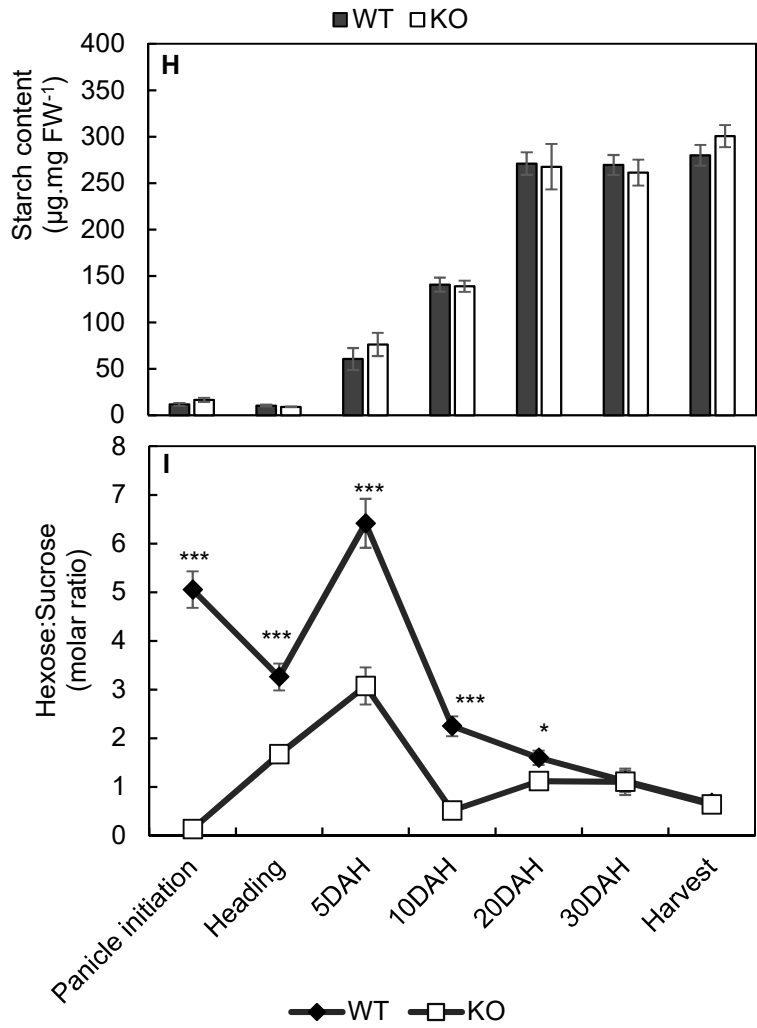
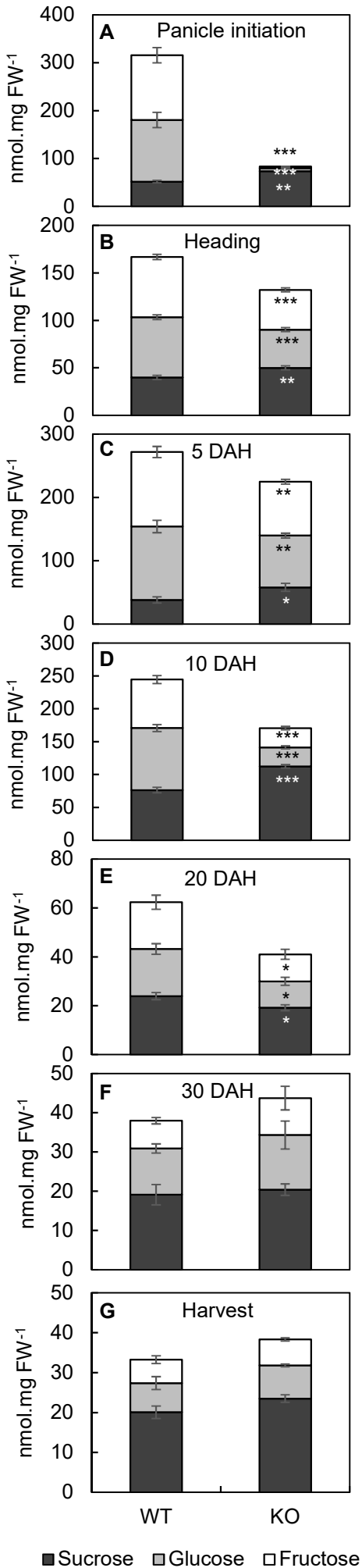


Figure 2-6.1 (A-I). NSC profile of panicles of the *OsINV3* WT and the mutant (KO) during growth stages from panicle initiation to harvest.

(A-G). Concentration of sugars in the panicle at panicle initiation, 5 DAH, 10 DAH, 20 DAH, 30 DAH and harvest; (H). Starch content in the panicles; (I). Hexose-to-sucrose ratio in the panicles of WT and the mutant at similar growth stages as mentioned above. Data represent the mean \pm SE (n=6). Asterisks indicate statistical significance of difference using Student's T-statistic with *-p<0.05, **-p<0.01 and ***-p<0.001. X-axis – representative of stage, and not scaled to number of days.

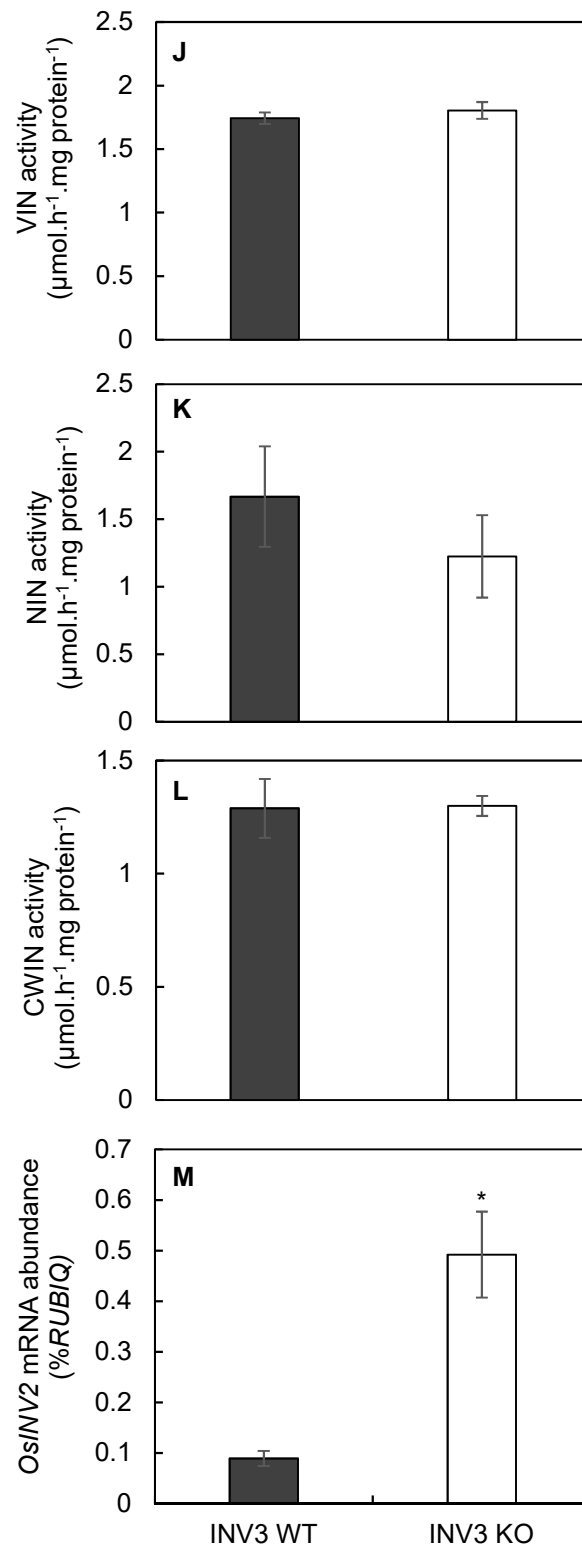


Figure 2-6.1 (J-M). (J) Vacuolar invertase activity, (K) Neutral invertase activity, (L) Cell wall invertase activity and (M) mRNA abundance of OsINV2 (%RUBI/Q), in young panicles (~ 4-5 cm in length) of *OsINV3* WT and mutant (KO). Data represent the mean \pm SE (n=3-5). Asterisks indicate statistical significance of difference using Student's T-statistic with $*-p<0.05$.

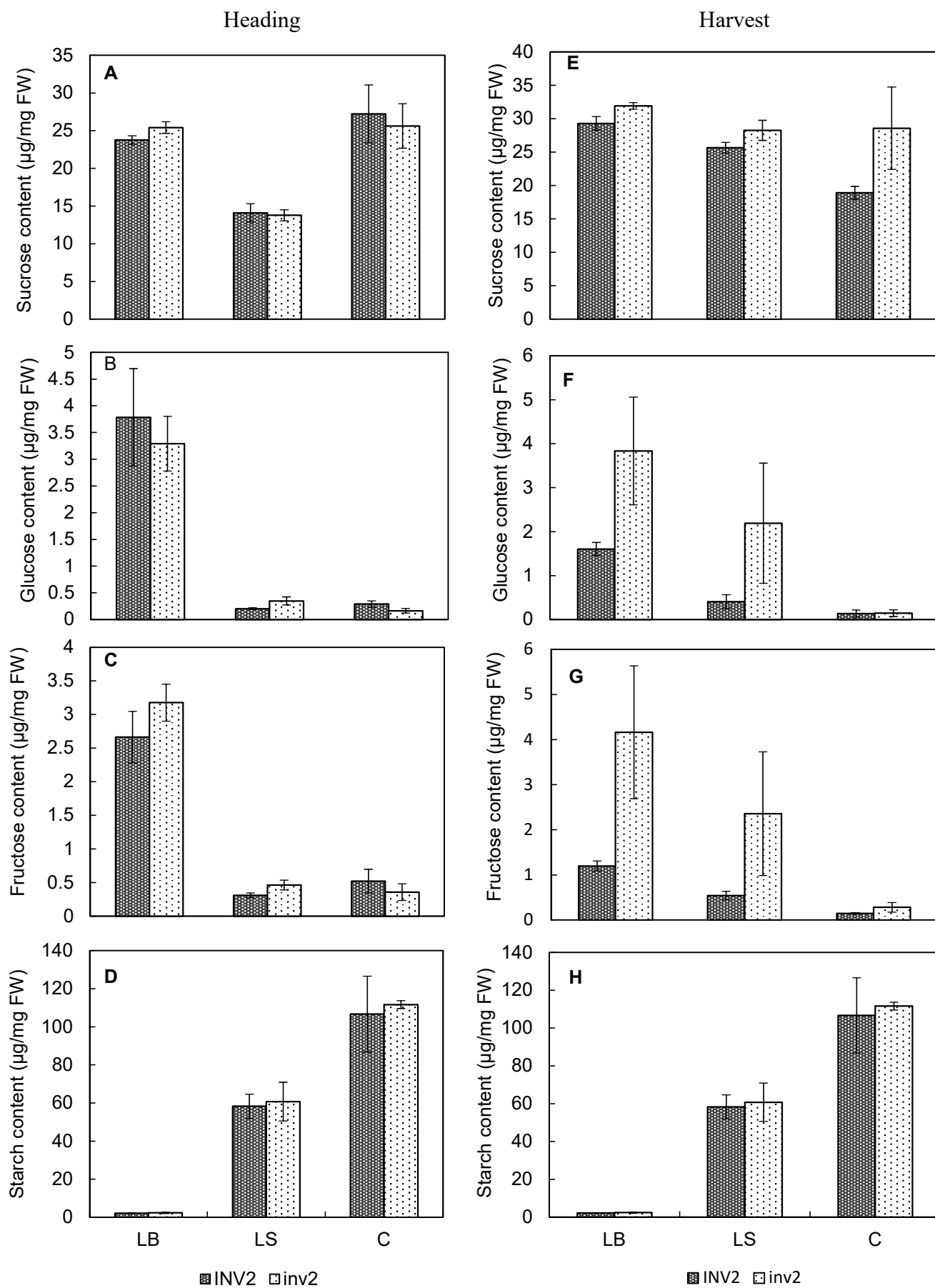


Figure 2-6.2 (A-H). NSC profile of *OsINV2* WT and KO at heading and harvest in LB, LS and C. (A), (B), (C) and (D) indicate sucrose, glucose, fructose and starch content respectively at heading; while, (E), (F), (G) and (H) indicate sucrose, glucose, fructose and starch content respectively at harvest in the *OsINV2* WT and KO. Data represent the mean \pm SE (n=4).

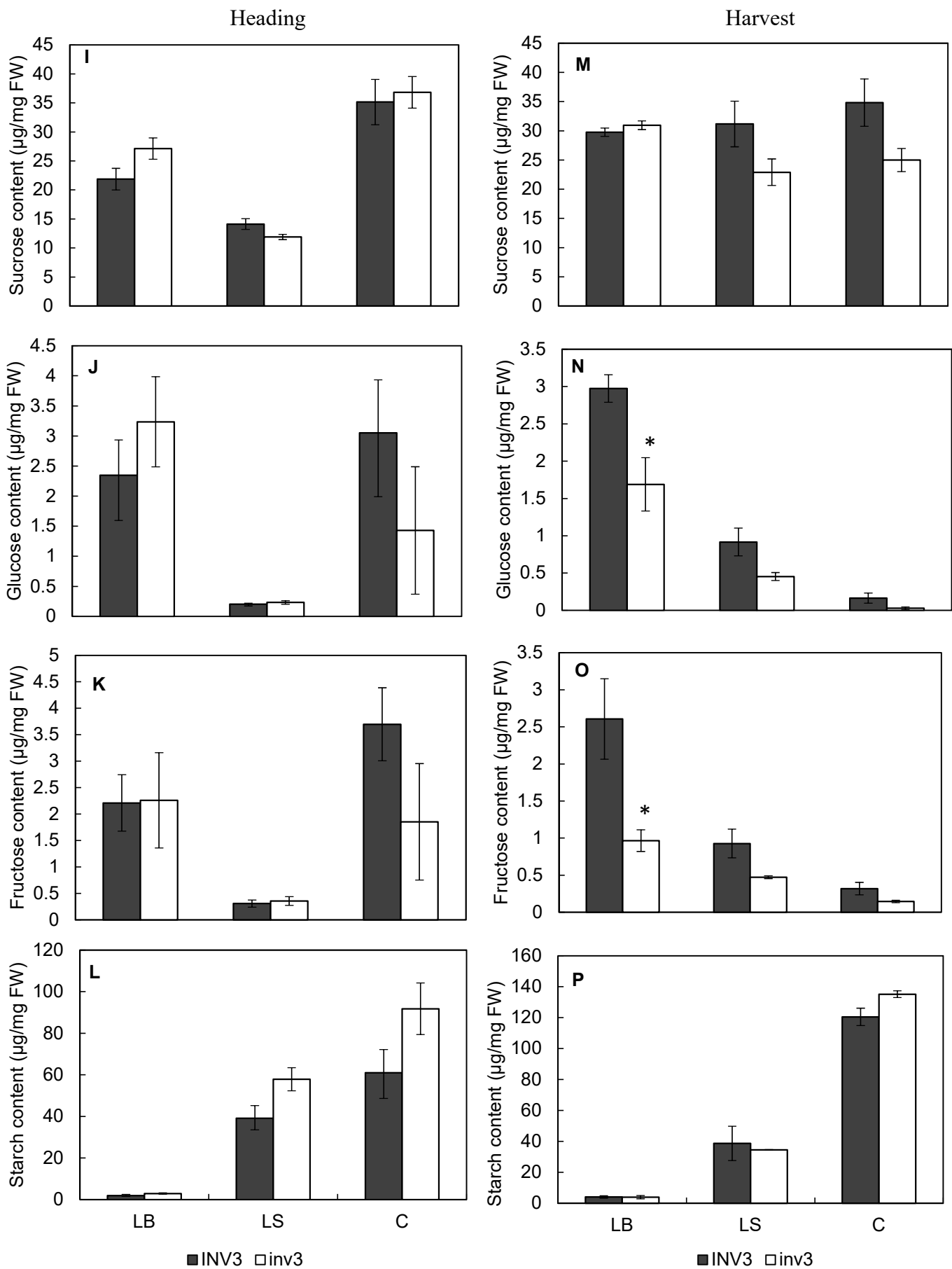


Figure 2-6.2 (I-P). NSC profile of *OsINV3* WT and KO at heading and harvest in LB, LS and C. (I), (J), (K) and (L) indicate sucrose, glucose, fructose and starch content respectively at heading; while, (M), (N), (O) and (P) indicate sucrose, glucose, fructose and starch content respectively at harvest, in the *OsINV3* WT and KO. Data represent the mean \pm SE (n=4). Asterisks indicate statistical significance of difference using Student's T-statistic with *-p<0.05.

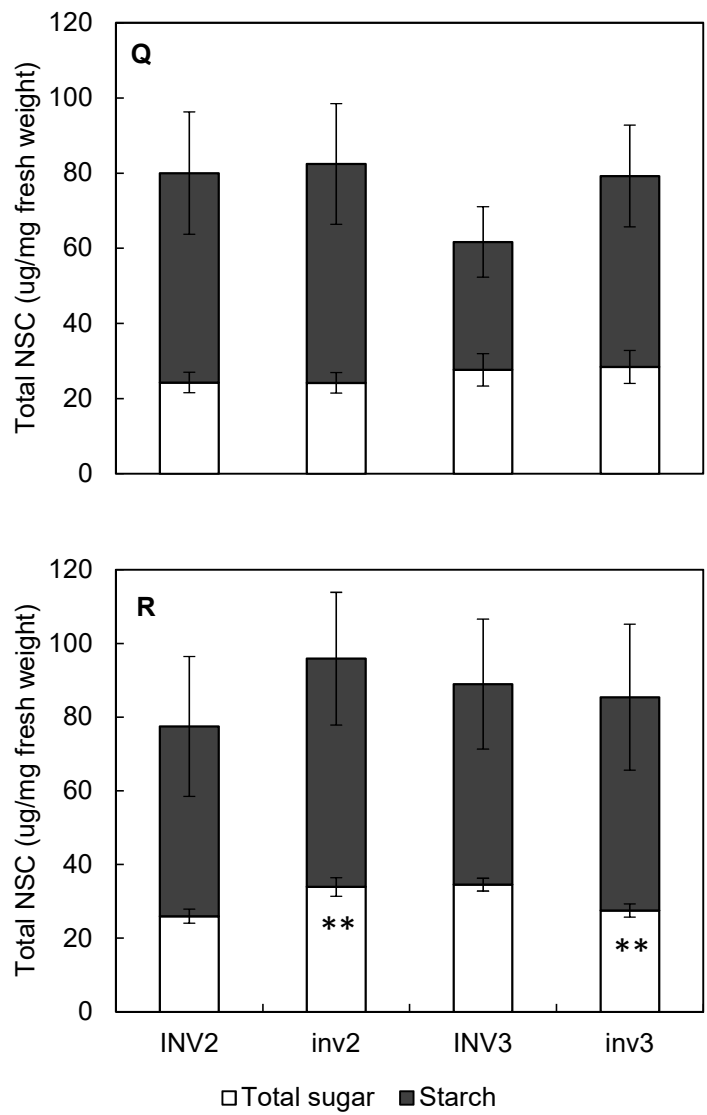


Figure 2-6.2 (Q-R). Total NSC in *OsINV2* and *OsINV3* WT and KO at (Q) heading and (R) harvest respectively. Data represent the mean \pm SE (n=4). Asterisks indicate statistical significance of difference using Student's T-statistic with **-p<0.01.

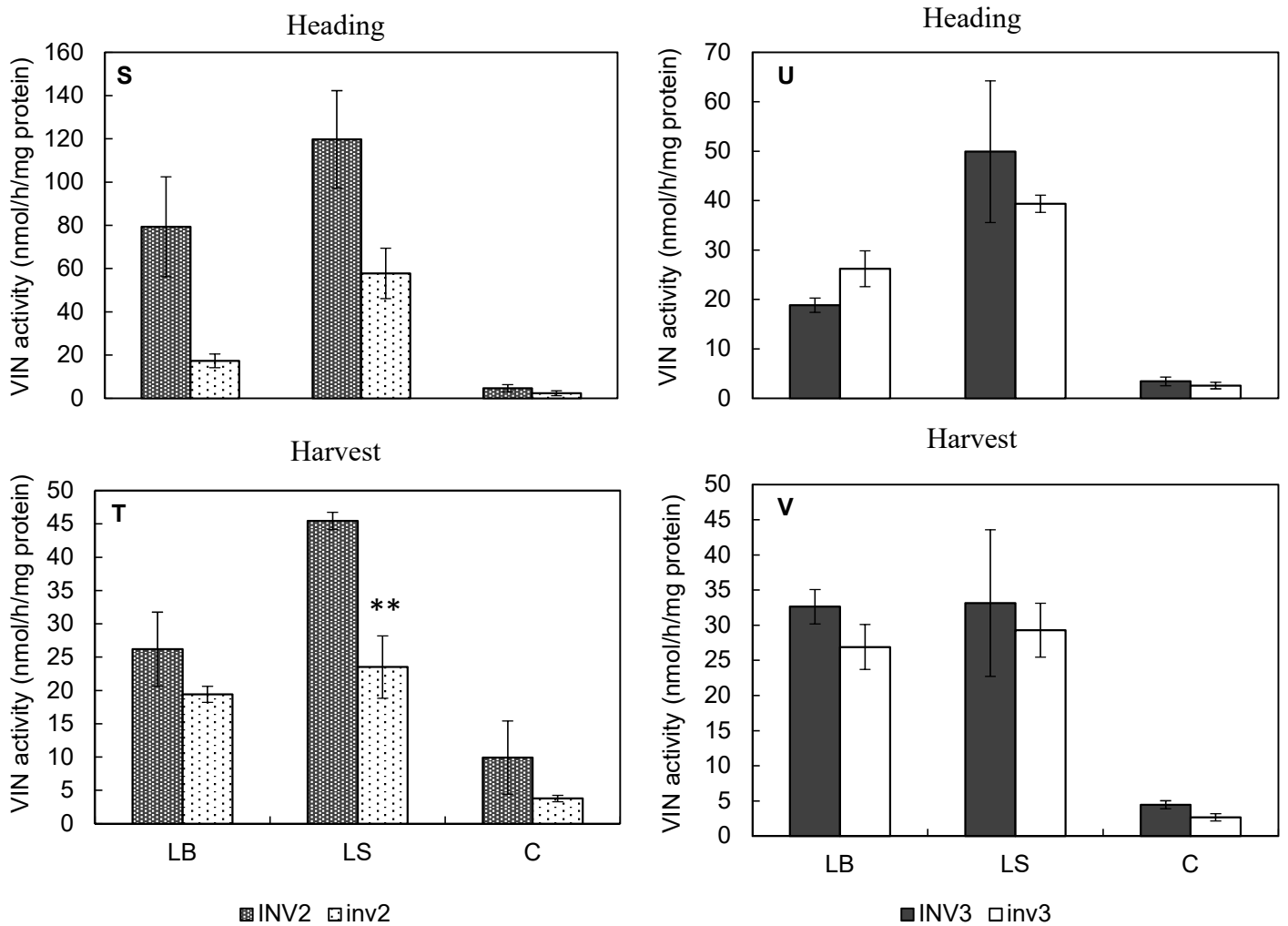


Figure 2-6.2 (S-V). Vacuolar invertase activity in LB, LS and C for *OsINV2* WT and KO, and *OsINV3* WT and KO. (S) and (T) show VIN activity at heading and harvest respectively for *OsINV2* WT and KO, while (U) and (V) show VIN at heading and harvest for *OsINV3* WT and KO. Data represent the mean \pm SE (n=4). Asterisks indicate statistical significance of difference using Student's T-statistic with $*-p<0.05$.

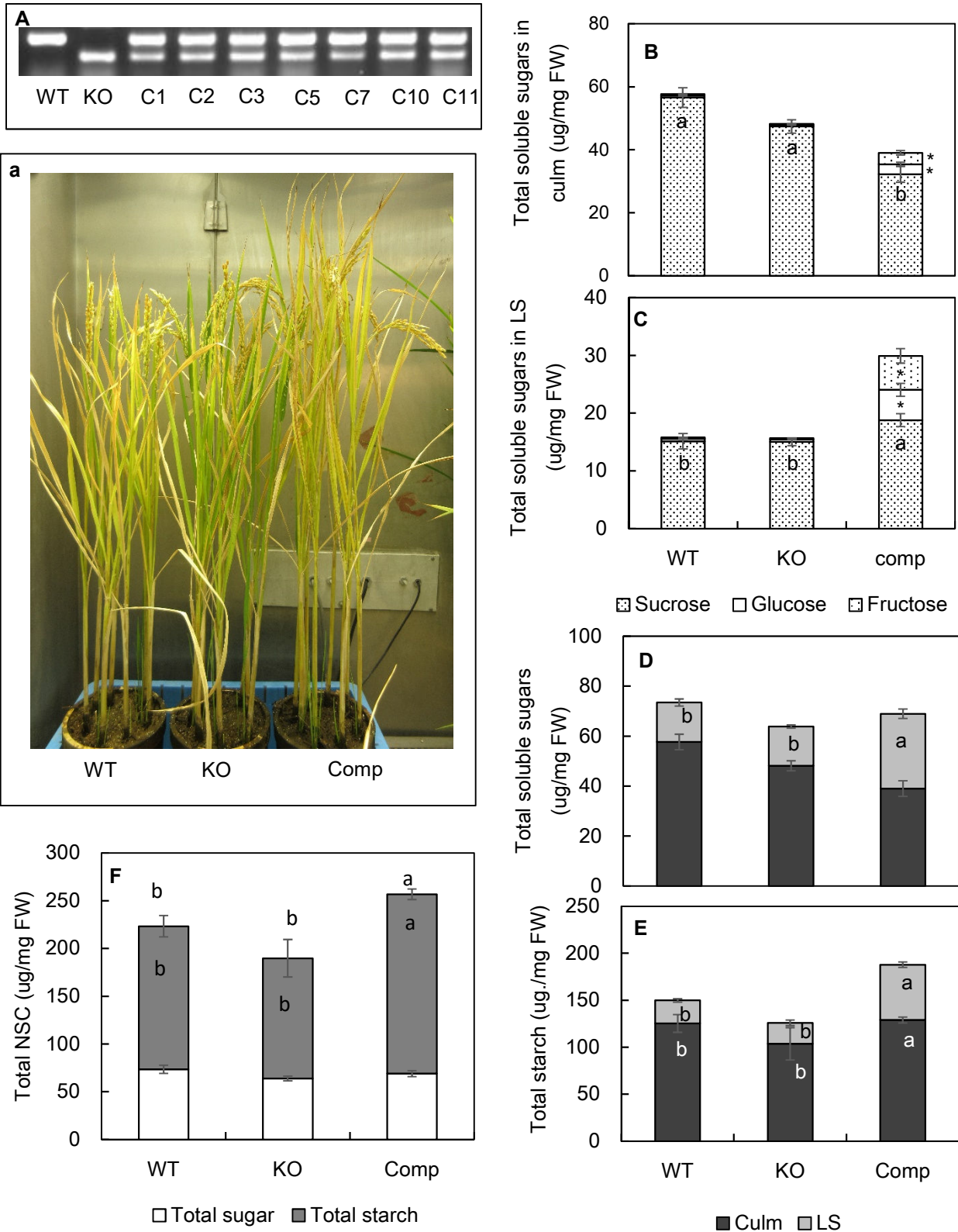


Fig. 2-7 (A-F). (A) Gel data showing the presence of WT and KO alleles in WT, KO and complement lines. (a) showing the monoculm plants at harvest, (B)-(F) shows the NSC content in the LS and Culm of *OsINV2* WT, KO and complement lines (C1, C2, C3, C5, C7, C10, C11) grown in monoculm conditions, with (B) and (C) showing the total sugar content in the culm and LS respectively, (D), (E) and (F) showing the total sugars, total starch, and total NSC content in the stems of WT, KO and complement lines respectively. Data represent the mean \pm SE (n=6). Same letters indicate insignificant differences between the lines.

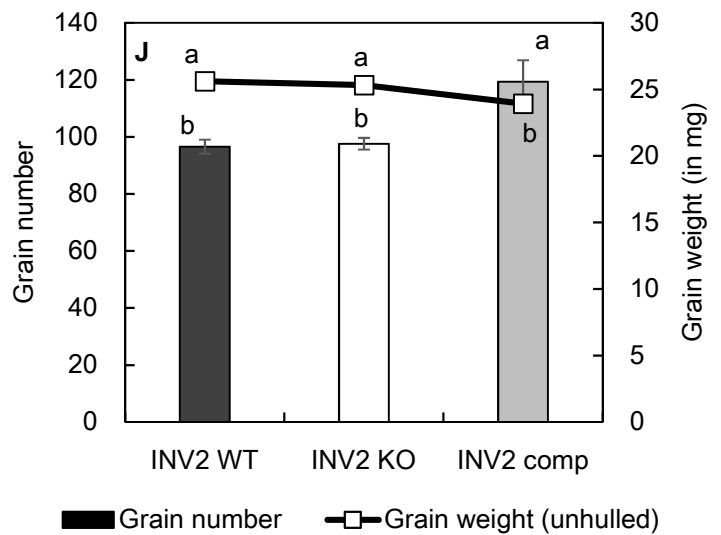
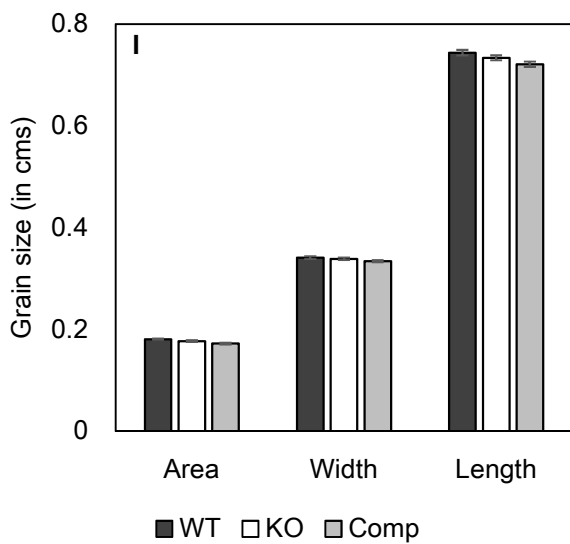
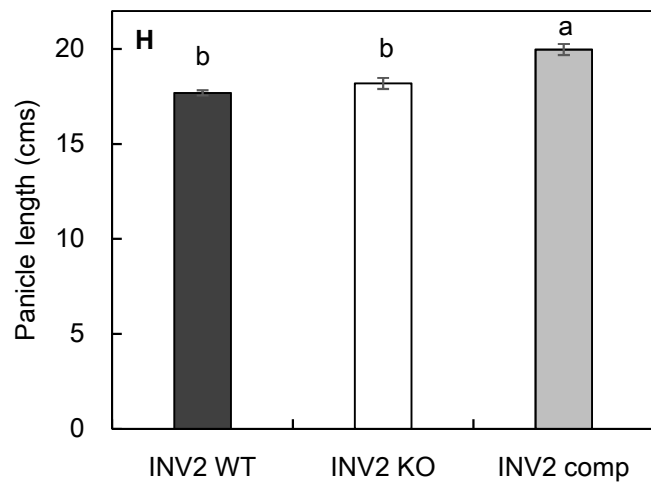


Fig. 2-7 (G-J). Panicle and grain size analysis for *OsINV2* WT, KO and Comp lines grown under monocolm conditions (G) and (H) show differences in panicle length between WT, KO and comp lines. (I) Grain size (n=30), (J) grain number and grain weight differences between the lines are also indicated. Data represent the mean \pm SE (n=6). Same letters indicate insignificant differences between the lines.

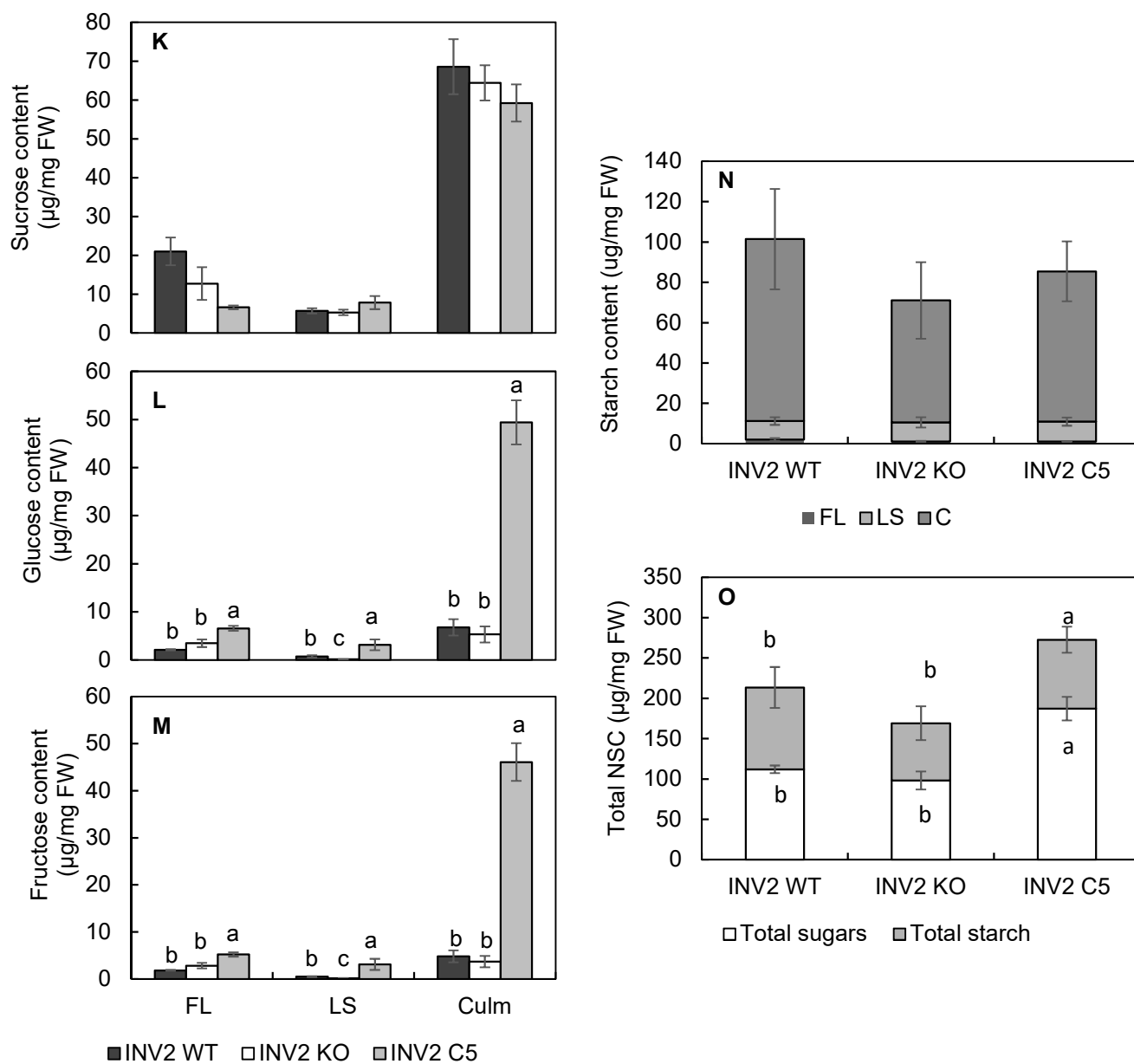


Fig. 2-7 (K-O). The NSC content in the FL, LS and Culm of *OsINV2* WT, KO and C5 lines grown in controlled conditions is shown, with (K), (L) and (M) showing the sucrose, glucose and fructose content, (N) and (O) showing the total starch and total NSC content respectively. Data represent the mean \pm SE (n=5). Same letters indicate insignificant differences between the lines.

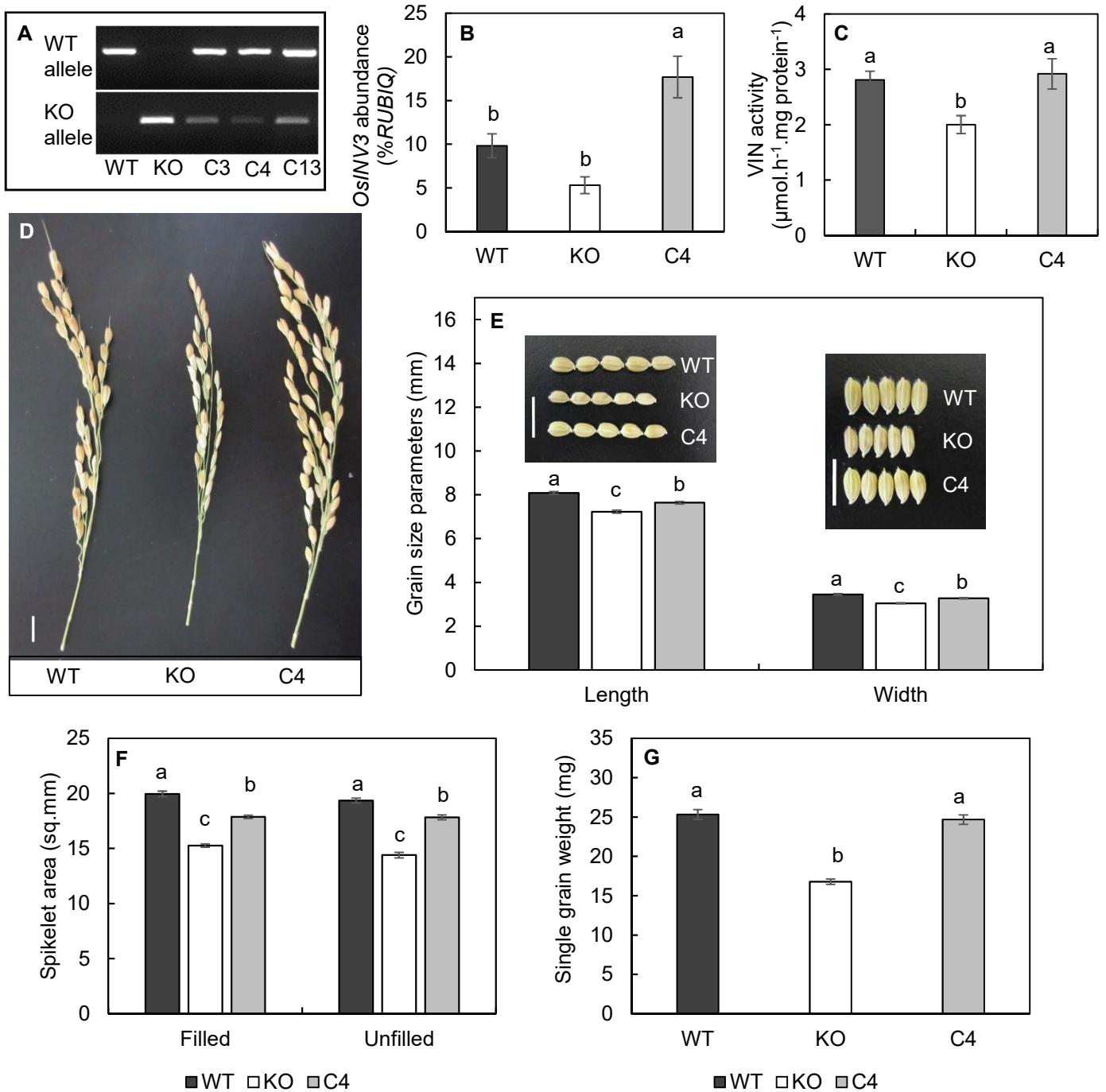


Figure 2-8 (A-G). Complementation test for *OsINV3* by determination of panicle and grain size and weight parameters. (A) Gel data showing the presence of WT and KO alleles in WT, KO and complement lines, (B) mRNA transcript level of *OsINV3* relative to *RUB1Q* (n=3) and (C) Vacuolar invertase activity expressed as V_{max} (n=5), in mature leaf at the seedling stage of WT, KO and C4, (D) Panicles from WT, KO and C4 lines, (E) Grain length and width parameters for WT, KO and C4 (n=12), (F) Spikelet area for filled and unfilled spikelets from WT, KO and C4 lines (n=12), (G) average weight per grain, for WT, KO and C4 lines (n=whole grain set from 3 plants). Data represent the mean \pm SE. Same letters indicate insignificant differences between the lines. Vertical white bars indicate 1 cm.

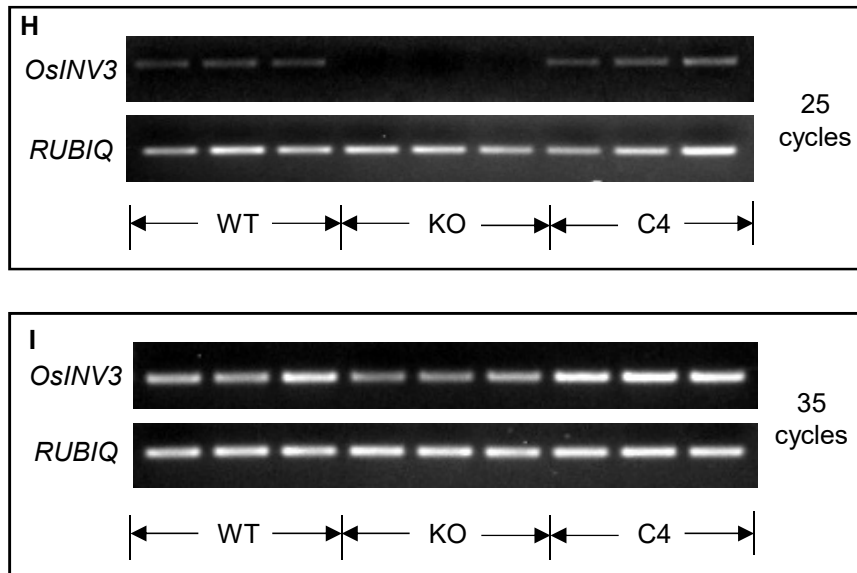


Figure 2-8 (H-I). Semi-quantitative PCR gel images for 300ng of starting RNA concentration from mature leaves of WT, mutant (KO) and C4, using (H) primers F6 and R6, spanning the *Tos17* insertion site, and (I) primers F5 and R5 downstream of the *Tos17* insertion site, confirming the presence of an aberrant transcript in the mutants.

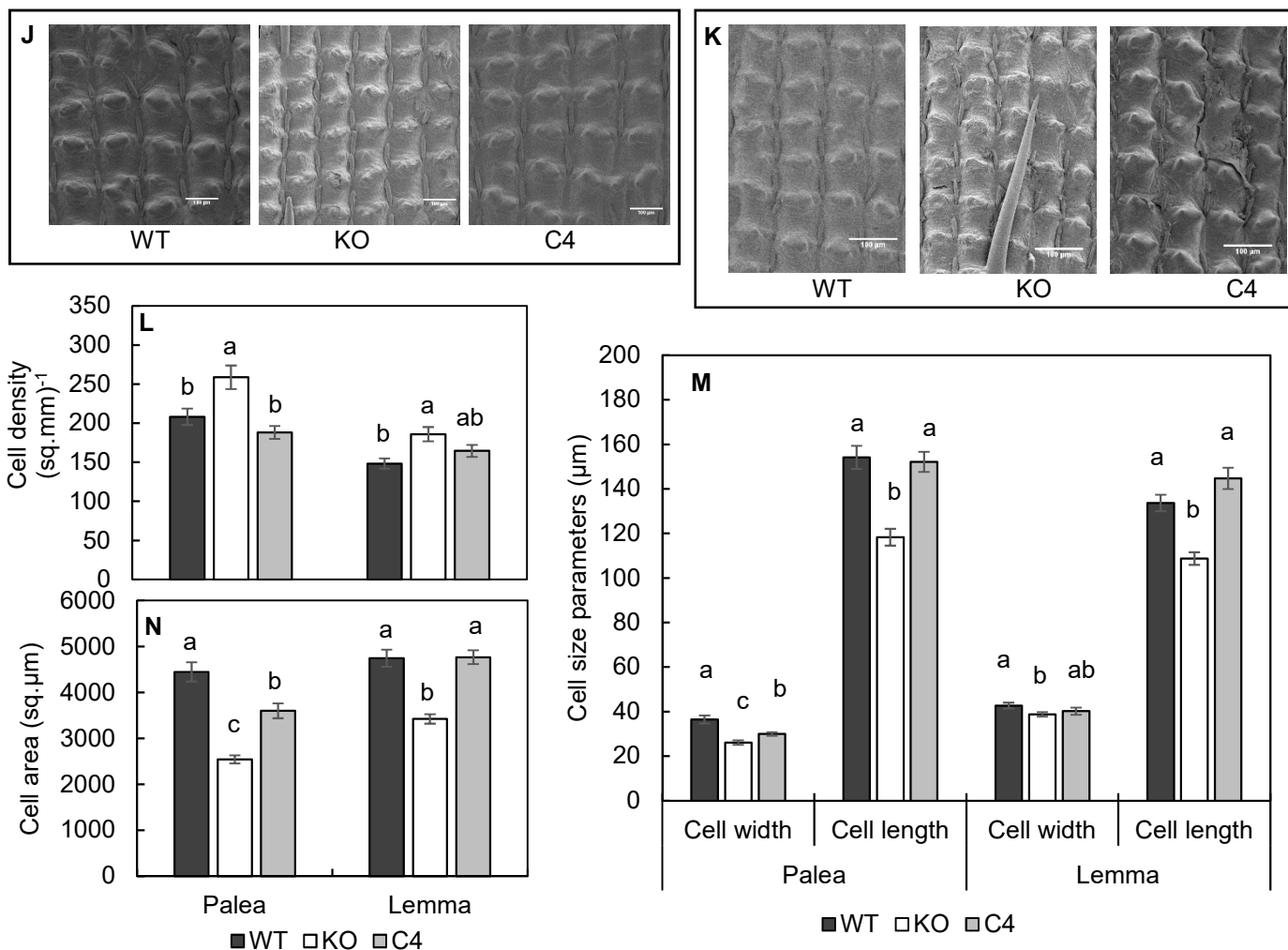


Figure 2-8 (J-N). Complementation test for *OsINV3* by determination of spikelet cell number and size analysis using SEM. Cell density for a fixed area in the outer surface of (J) palea and (K) lemma for WT, mutant (KO) and C4. (L) Cell density expressed as number of cells/sq.mm of the outer surface of palea and lemma for WT, KO and C4. (M) Cell size parameters, depicting cell width and cell length and (N) Cell area in sq.μm, for the inner surface of palea and lemma. Data represent the mean ± SE (n=12). Same letters indicate insignificant differences between the lines. Horizontal bars represent 100 μm.

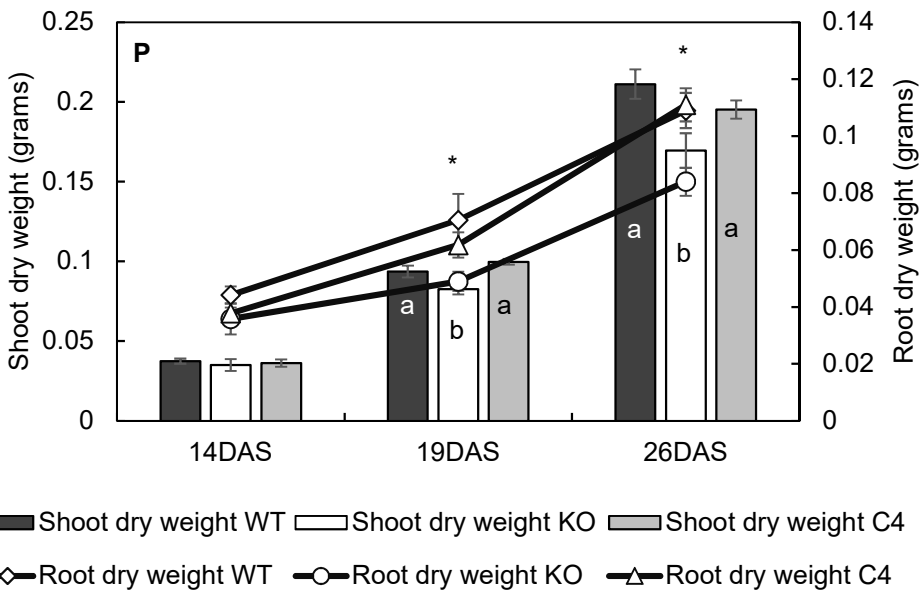
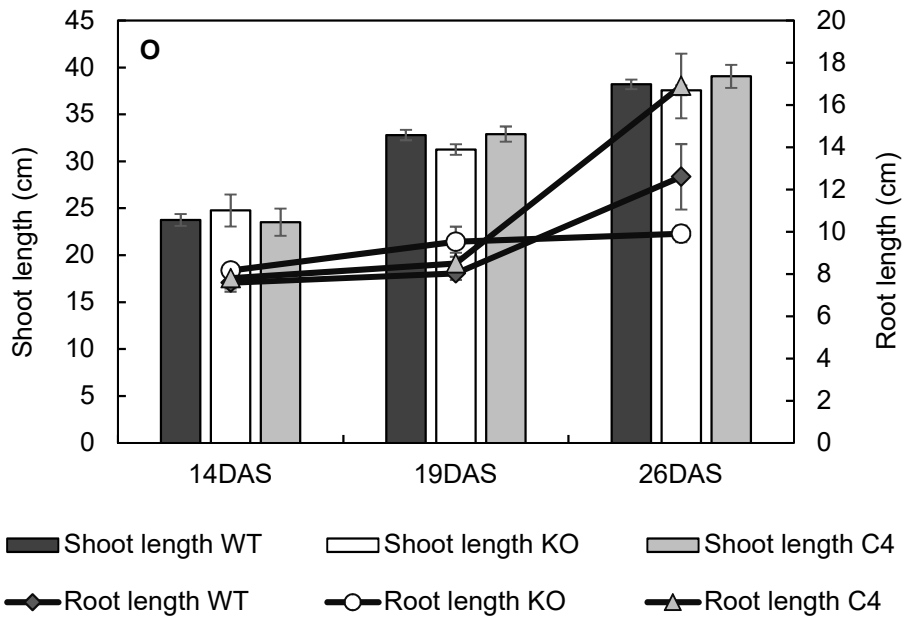


Figure 2-8 (O-P). Complementation test for *OsINV3* at seedling stage. (O) indicates the shoot and root length, and (P) indicates the shoot and root dry weights, for *OsINV3* WT, KO and C4 lines. Data represent the mean \pm SE (n=5). Same letters indicate insignificant differences between the lines for bar graph; while * indicates significant differences in KO when compared with WT and C4 lines, for line graph.

CHAPTER 3

ROLE OF *OsINV3* IN COLD STRESS RECOVERY DURING THE SEEDLING STAGE IN RICE

3-1 Introduction

Having its origin in the tropical and sub-tropical regions, rice is highly susceptible to cold stresses in the temperate regions, leading to a decrease in crop productivity (Zhang et al., 2014). Cold stress can be classified as chilling stress (0-15°C) and freezing stress (<0°C), and an exposure to chilling temperatures has been suggested to impart cold tolerance in temperate plants (Zhu et al., 2007), a process termed as acclimatization. Seedling and the reproductive stages are found to be the critical stages leading to cold induced losses in yield and grain quality, thus being indicated as key stages for evaluation of cultivars for cold-tolerance (Zhang et al., 2014).

Role of soluble sugars as one of the key metabolites induced by cold, in imparting protective effects under cold stress has been well studied (Wanner and Junttila, 1999; Guy et al., 2008), where they have been suggested to serve as an osmoprotectant and a cryoprotectant (Nagao et al., 2005; Shao et al., 2007; Nagele et al., 2012). Increase in hexose and sucrose contents have been associated with freezing tolerance in *Arabidopsis* (Klemens et al., 2013). However, given their multiple roles, and involvement in various metabolic and signaling pathways, the exact mechanism underlying this is not known (Tarkowski and Van den Ende, 2015).

It has been previously suggested that a balance between carbon fixation and sucrose biosynthesis is essential to maintain the photosynthetic capacity in plants (Stitt and Hurry, 2002), and invertases by their sucrose degradative ability are said to influence this balance by regulating the levels of cellular sucrose available. This not only enables recovery upon release from stress conditions by stabilizing photosynthesis, but also stabilizes cytosolic energy by supply of hexoses, as found in *Arabidopsis* (Weizmann et al., 2017). In rice, acclimation of seedlings at 12°C was found to improve cold tolerance (Sageshashi and Sato, 2015b). Further analysis of various metabolites during the acclimatization of 10-day old seedlings at 12°C, showed an increase in sugar and amino acid levels with a maximum rise in the sucrose levels, suggesting the use of sucrose as a biomarker for cold tolerance (Sagehashi and Sato, 2015a).

Sugars and phytohormones have been considered as signaling molecules, playing key roles in regulation of vacuolar invertases (Burch et al., 1992; Xu et al., 1996; Roitsch et al., 2004; Koch et al., 2004; Trouverie et al., 2004). ABA, a stress hormone and glucose have been previously found to regulate vacuolar invertase in maize (Trouverie et al., 2004) and Arabidopsis (Huang, Ph.D. dissertation, 2006). Thus, the regulatory roles of sugars and ABA in vacuolar invertase expression under cold-stress conditions, could prove vital to isolating a possible mechanism for imparting cold-tolerance.

The current chapter highlights on the role of VINs in cold stress recovery in the seedling stage of rice. Preliminary studies conducted with the rice seedlings at 12°C, revealed a sharp 16-fold increase in the transcript levels of *OsINV3*, 20 hours after treatment (HAT) in the shoots, with no differences in the roots. *OsINV2* was not found to be different at this sampling stage, although showing a slight 2-fold increase in the shoots at 112 HAT. Thus, we isolated *OsINV3* as a key candidate for testing cold acclimatization and recovery in rice seedlings. The transcriptional responses of *OsINV2* and *OsINV3* to varied concentrations of sugars (sucrose and glucose) and ABA have also been demonstrated to discuss a possible mechanism for the role of *OsINV3* in cold stress recovery in rice seedlings.

3-2 Materials and Methods

3-2.1 Plant materials

The *OsINV3* WT, KO mutants and the C4 complement lines, described in Chapter 2 were used for the cold stress experiments. The ABA regulation experiment was conducted with *OsINV3* WT, while the sugar regulation experiment was conducted with Nipponbare, the variety used for generation of mutants used in this study.

3-2.2 Growth conditions and sampling stage

Plants were grown as mentioned in Chapter 2 until the beginning of the 3-leaf stage, following which they were transferred into 1/10 MS liquid solution in a set-up mentioned previously (Kuroda and Ikenaga, 2015), and as shown in Fig. 3-2B. Following growth in the liquid solution for 1-2 days, they were moved to respective treatment conditions. The entire shoot was sampled cryogenically and stored at -80°C until analysis. The sampling stage for the sugar regulation experiment differed from the others, where samplings were done at the beginning of the 4-leaf stage in comparison to the 3-leaf stage for the other experiments in this chapter. Stage-wise variation in gene expression was eliminated by including a negative control, growing under normal nutrient conditions without any supplementation.

3-2.3 Cold stress experiments

Experiment 1: *OsINV3* WT, KO and the C4 lines were subjected to 4°C under dark conditions, at the 3-leaf stage for 13 days, following which they were transferred to normal growth conditions of 27°C/22°C, 14hr-light/10-hr dark cycle, 65% relative humidity and a light intensity of 900 $\mu\text{mol m}^{-2} \text{s}^{-1}$ for 18 days. Percentage of rescued plants was scored, along with the shoot and root dry weights following rescue. Seedlings that could produce a healthy new leaf were considered to be rescued.

Experiment 2: *OsINV3* WT and KO at the 3-leaf stage were subjected to 12°C and 4°C along with control seedlings grown under 27°C/22°C day/night temperature. Seedlings at 4°C were grown in dark, while those at 12°C were grown with 14hr-light/10-hr dark cycle, 65% relative humidity and a light intensity of 900 $\mu\text{mol m}^{-2} \text{s}^{-1}$, same as the control plants. Whole shoots were sampled cryogenically 1 day after treatment

(DAT) and 5 DAT for determination of mRNA and sugar levels. 5 DAT, plants at 12°C were transferred to 4°C for 12 days, following which both the acclimatized (12°C treated) and the continuously 4°C treated plants were returned to normal growth conditions for 17 days for recovery. However, sampling for mRNA and sugar level estimation was conducted at 10 days after treatment at 4°C, prior to recovery. Samplings for dry weights were also performed at 5 DAT and 17 days after recovery (DAR). Fig. 3-1 shows the experimental set up.

3-2.4 Sugar and ABA treatment

Seedlings at their respective growth stages were subjected to the following ABA and sugar treatments and sampled cryogenically at 0.5, 1.5, 3, 6, 24 and 48 hours after treatment (HAT) for *OsINV2* and *OsINV3* transcript level determination.

ABA treatment: T0 – 0 µM, T1 – 0.5 µM and T3 – 5 µM of ABA

Sugar treatment: T0 – 0% Sugars, T1S – 0.1% sucrose, T2S – 3% sucrose, T1G – 0.1% glucose, T2G – 3% glucose, T1M – 0.1% mannitol, T2M – 3% mannitol

Both, sugars and ABA were fed through the roots, by adding the corresponding amounts to 1/10 MS growth solution.

3-2.5 Dry weights, sugar measurement and real-time PCR

Shoot and roots sampled were placed in 80°C drying oven for a minimum of 10 days before being weighed. Soluble sugars were determined similar to the methods previously described (Chapter 2, 2-2.11). RNA isolation, cDNA synthesis and real-time PCR were performed similar to the methods previously described (Chapter 2, 2-2.9).

3-3 Results

3-3.1 Cold recovery in *OsINV3* WT, KO and C4 lines

Percentage recovery of *OsINV3* KOs was found to be markedly reduced at 35% in comparison to the *OsINV3* WT and C4 lines that displayed 90% and 100% recovery respectively, following cold stress in *Experiment 1*. Shoot density differences between the KO, and the WT and C4 lines were pronounced (Fig. 3-2B) with the shoot and root dry weights of the KO being lower than that of the WT, and observed recovery in the C4 plants, suggesting a role for *OsINV3* in cold stress recovery during the seedling stage in rice.

3-3.2 Transcript level, sugar content and dry weight differences in response to chilling stress in

Experiment 2

Shoot and root dry weight differences between the WT and the KO were absent at 5 DAT, under all conditions, with the exception of shoot dry weight of the 4°C treated seedlings, where the KO had a smaller shoot dry weight in comparison to the WT (Fig. 3-3A). Following transfer to normal growth conditions, only the seedlings acclimatized to 12°C showed signs of recovery, with visual differences in plant growth between WT and KO (Fig. 3-3B). Both, the shoot and root dry weights of the KO seedlings after recovery were found to be lower than that of the WT seedlings (Fig. 3-3C), isolating a key role for *OsINV3* in plant recovery following cold stress at the 3-leaf stage.

In *OsINV3* WT, *OsINV2* showed no change in transcript levels at 1 DAT and 5 DAT (Fig. 3-4A). However, higher transcript level than the control was observed after long term cold exposure to 4°C at 15 DAT for both the seedlings acclimatized to 12°C and those at continued 4°C exposure, where the transcript levels were higher in the seedlings acclimatized to 12°C when compared to those at continued 4°C exposure (Fig. 3-4A). On the other hand, *OsINV3* transcript levels showed a strong increase after short term exposure, in seedlings subjected to 12°C at 1 DAT, with a marked decrease upon long term exposure (Fig. 3-4B), isolating an alternate expression pattern in cold regulation of the two isoforms of vacuolar invertase in rice.

Differences in total sugar contents were determined, and the sucrose content in the acclimatized seedlings was found to be significantly higher at 5 DAT and 15 DAT, while the seedlings under continuous 4°C

exposure had sucrose levels comparable to those at control conditions (Fig. 3-4C). Both glucose and fructose showed a similar trend (Fig. 3-4D and E), with a higher level observed in acclimatized seedlings from the beginning of treatment at 1 DAT and 5 DAT, after which a sudden increase in glucose and fructose content was observed at 15 DAT. Seedlings in continuous 4°C exposure, showed no differences in sugar content in the beginning of treatment at 1 DAT and 5 DAT, however, a sudden increase was observed at 15 DAT, reaching similar levels of hexose content as the acclimatized seedlings.

3-3.3 *OsINV2* and *OsINV3* response to ABA

An increase in *OsINV2* mRNA abundance was observed at both T1 and T2 treated seedlings shortly after exposure to ABA, at 0.5 HAT, and an observed increase at 24 HAT only for the T2 treated seedlings (Fig. 3-5A). *OsINV3* showed a consistent higher mRNA abundance under T2 condition, starting from 1.5 HAT to 48 HAT, reaching a maximum at 24 HAT (Fig. 3-5B), co-incident with the maximum upregulation of *OsINV3* transcript levels at 1 DAT in the 12°C treated seedlings (Fig. 3-4B). Upregulation of *OsINV3* transcript levels in the T1 treated seedlings was observed at 6 HAT, showing a similar trend as T2 treated seedlings, reaching a maximum at 24 HAT (Fig. 3-5B).

3-3.4 *OsINV2* and *OsINV3* response to sugars

The plants were treated to 0.1% and 3% sucrose and glucose, and mannitol at similar osmotic potential in order to maintain a control for the *OsINV2* and *OsINV3* response to change in osmotic potential.

In response to sucrose treatment, *OsINV2* showed an upregulation at 1.5 HAT, in both T1S and T2S conditions, while maintaining a similar trend of transcript level as the control in all other sampling points until 48 HAT (Fig. 3-6A). The transcript levels were found to be upregulated in response to glucose, as an early response at 0.5 HAT (Fig. 3-6C), as was with mannitol treatment (Fig. 3-6E). An increase in *OsINV2* transcript levels was found at 1.5 HAT in seedlings in T2M conditions (Fig. 3-6E), despite which no differences were observed in glucose-treated seedlings at the same stage, indicating a glucose-induced repression of *OsINV2* following the early 0.5 HAT. *OsINV2* was found to be stably expressed under sucrose, glucose and mannitol treated seedlings at stages following 1.5 HAT, indicating an osmotically-independent response pattern of *OsINV2*.

In response to sucrose treatment, *OsINV3* showed a downregulation at 1.5 and 3 HAT for the T1S treatment (Fig. 3-6B), suggesting a sucrose-induced repression of *OsINV3* at low sucrose concentrations. While, osmotic response of *OsINV3* at T1M was stable at all sampling points, T2M treated seedlings showed a strong upregulation of *OsINV3* to higher osmotic potential (Fig. 3-6F) at stages after 1.5 HAT. A similar response to T2G treatment until the early 3 HAT conditions was observed, with recovery to similar levels as the control following this stage (Fig. 3-6D).

3-4 Discussion

Role of *OsINV3* in acclimatization and recovery from cold stress

Our data revealed the role of *OsINV3* in recovery from cold stress (Fig. 3-2A), with a lower dry matter production in shoots and roots after exposure to 4°C (Fig. 3-2C). Previous studies have indicated a role for vacuolar invertase in recovery from cold stress, mainly by stabilizing the supply of hexoses to the cytosol, thus reactivating photosynthesis (Weizmann et al., 2017).

Although, a role in recovery from cold stress was observed in the 4°C treated plants, transcriptional upregulation of *OsINV3* at 4°C was not observed (Fig. 3-4B). Instead, *OsINV3* responded strongly to 12°C treatment (Fig. 3-4B), highlighting its role in acclimatization, wherein only the WT seedlings acclimatized to 12°C treatment could be rescued (Fig. 3-3B and C). The sugar profile (Fig. 3-4C, D and E) also revealed a significant role of *OsINV3* in increase in the hexose content the first 5 days after exposure to 12°C. Thus, *OsINV3* was not only found to play a key role in cold recovery, but also in acclimatization to chilling stress in seedlings of rice.

***OsINV2* response to cold stress**

Our preliminary studies revealed a strong upregulation of *OsINV3* in shoots of 12 °C treated seedlings, while the *OsINV2* transcript levels were not drastically affected; the reason behind studying cold response in the *OsINV3* mutants. However, our data reveals a long-term response of *OsINV2*, 15 DAT at 4°C in both the acclimatized and the continuous 4°C treated seedlings (Fig. 3-4A), which is co-incident with the increase in the hexose levels at this stage (Fig. 3-4D and E). However, it is unclear if this response to 4°C conditions is significant to cold stress recovery, or a result of the downstream presence of *OsINV2* in the cold response pathway, thus, needing further investigation.

Transcriptional regulation of vacuolar invertase by sugars and ABA

Response to ABA

Both *OsINV2* and *OsINV3* were found to be upregulated by ABA at 24 HAT (Fig. 3-5A and B), with *OsINV3* being strongly responsive to both the lower (T1) and higher (T2) ABA treatments at 24HAT, which is the time point maximum transcript levels of *OsINV3* was observed in the cold stressed seedlings (Fig. 3-4B). Thus, establishing a significant ABA transcriptional regulation of *OsINV3*, and correlating this to its cold-induced upregulation at 12°C.

Response to sugars

OsINV2 showed an early response to glucose, at 30 minutes after treatment, being significantly upregulated (Fig. 3-6C). However, this response was co-incident with that observed in the mannitol treatment conditions (Fig. 3-6E), suggestive of an early osmotic dependence in regulation of *OsINV2* by glucose. *OsINV2* transcript levels were relatively stable even with T2M treatment following 1.5 HAT (Fig. 3-6E), while *OsINV3* was greatly upregulated across all time points following 0.5 HAT (Fig. 3-6F), indicating a strong osmotic dependency of *OsINV3* transcriptional regulation (Fig. 3-6F). The early response of *OsINV3* to glucose (T2G) was significantly co-incident with that observed under T2M at 0.5 HAT (Fig. 3-6D and E), however significantly being repressed following this time point. This indicates a glucose-induced repression of *OsINV3* expression, that could be attributed to a feedback regulation by glucose. Further, the *OsINV3* transcript levels showed an upward trend in seedlings at T2 conditions 24 HAT onwards (Fig. 3-6 D), indicating a possible long-term upregulation or a circadian control of *OsINV3* by glucose, needing further investigation. Our results also indicate an absence of glucose sensing by *OsINV2* and *OsINV3*, their transcript levels being largely driven by the osmotic potential differences at the early time points after exposure.

Response of both the isoforms to sucrose was found to be osmotically independent, however being responsive to sucrose treatment at 1.5 HAT (Figs. 3-6A and B). Under T1 treatment conditions, a sucrose induced repression of *OsINV3* was observed at early time points (Fig. 3-6B), displaying contrasting patterns with *OsINV2* that was upregulated in response to the lower sucrose T1 conditions (Fig. 3-6A). Thus, it could be suggested that in view of limiting increase in sucrose concentration, *OsINV2* and *OsINV3* show contrasting expression patterns, with *OsINV2* taking a key role in sucrose hydrolysis.

In conclusion, our results outline the possibility of *OsINV3* regulation by ABA and glucose as a mechanism for the cold-induced upregulation of *OsINV3* during acclimatization, that results in an increase in the glucose levels, causing a feedback regulation of *OsINV3* and a possible reduction in the ABA content, eventually causing an increase in sucrose levels, hence, imparting chilling stress tolerance (Fig. 3-7).

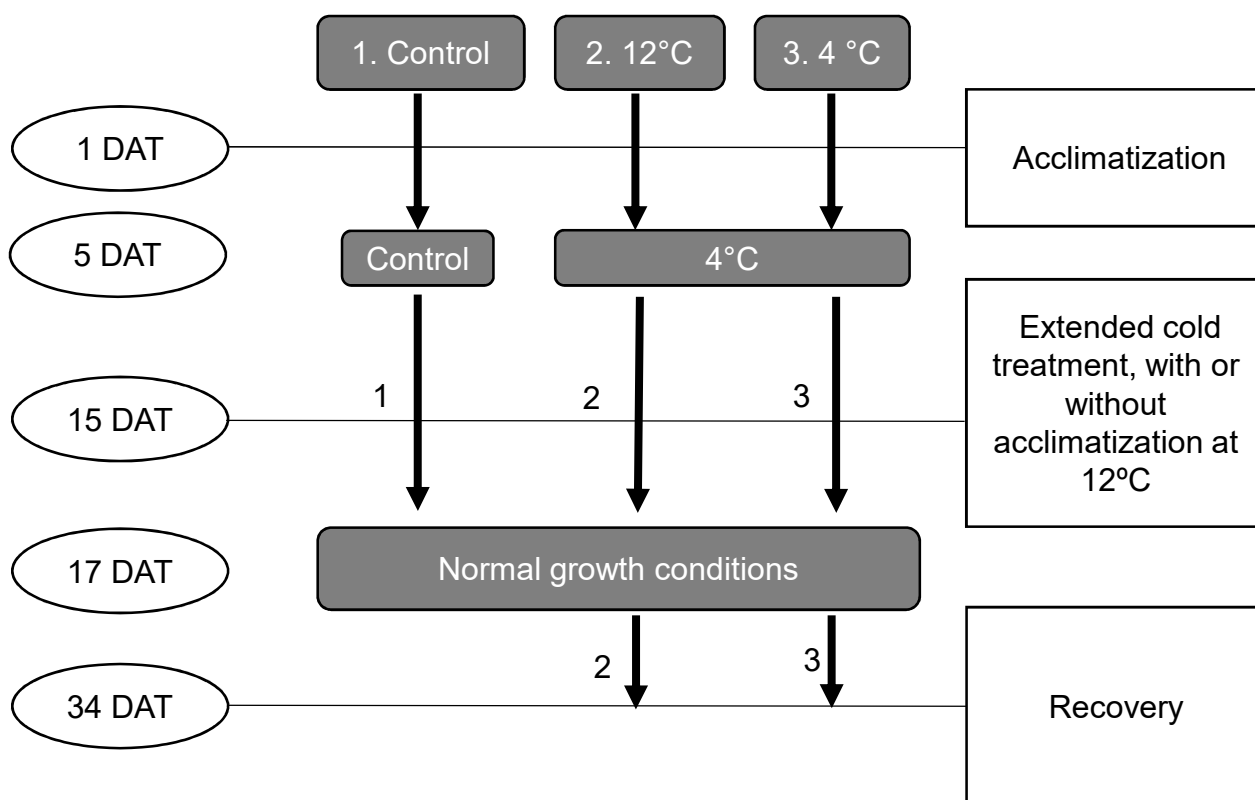


Fig. 3-1. Experimental set up showing the treatment conditions, sampling points and type of treatment in *Experiment 2*. (1) indicates rice seedlings under control conditions, (2) indicates rice seedlings with 5 days of 12°C treatment, followed by 10 days at 4°C, and (3) indicates 17 days of 4°C treatment; followed by 17 days of recovery for (2) and (3).

A

Genotype	Number of plants recovered	Total number of plants	% recovery
<i>OsINV3</i> WT	18	20	90
<i>OsINV3</i> KO	7	20	35
<i>OsINV3</i> C4	20	20	100

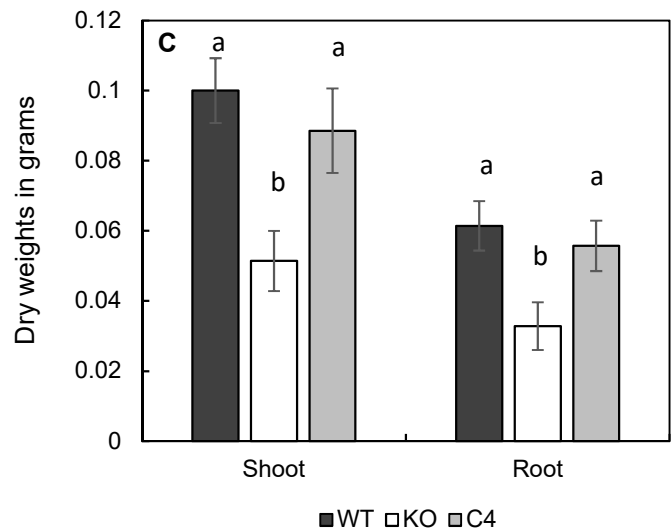
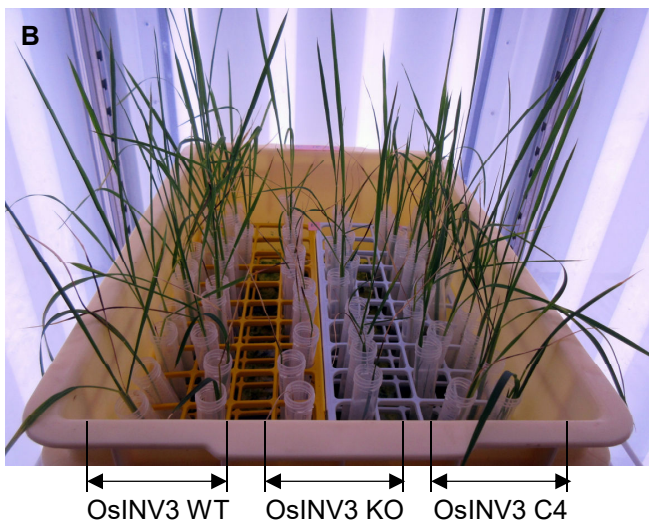


Fig. 3-2. (A) Percentage of rescued plants, (B) visual differences in shoot density, and (C) shoot and root dry weights for *OsINV3* WT, KO and C4 lines after recovery in *Experiment 1*, with treatment at 4°C for 13 days and recovery for 18 days. Data represent the mean \pm SE (n=7). Same letters indicate insignificant differences between the lines.

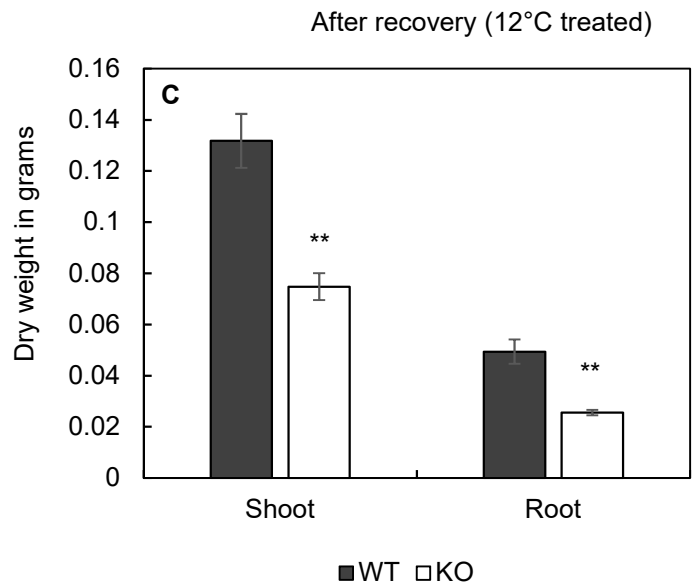
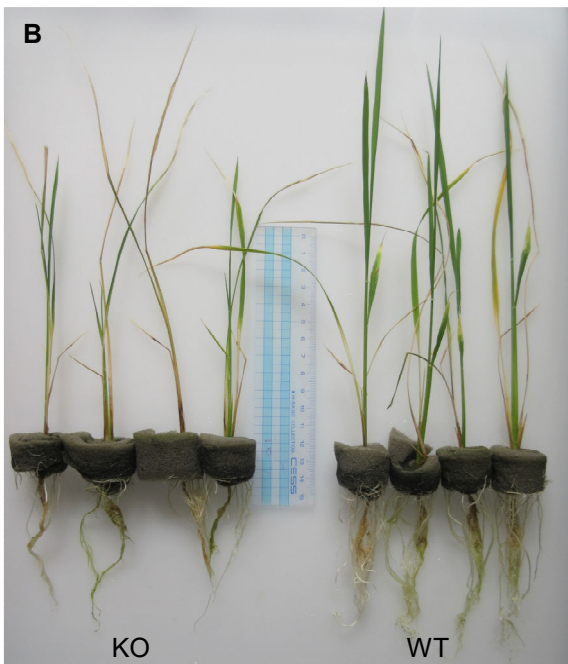
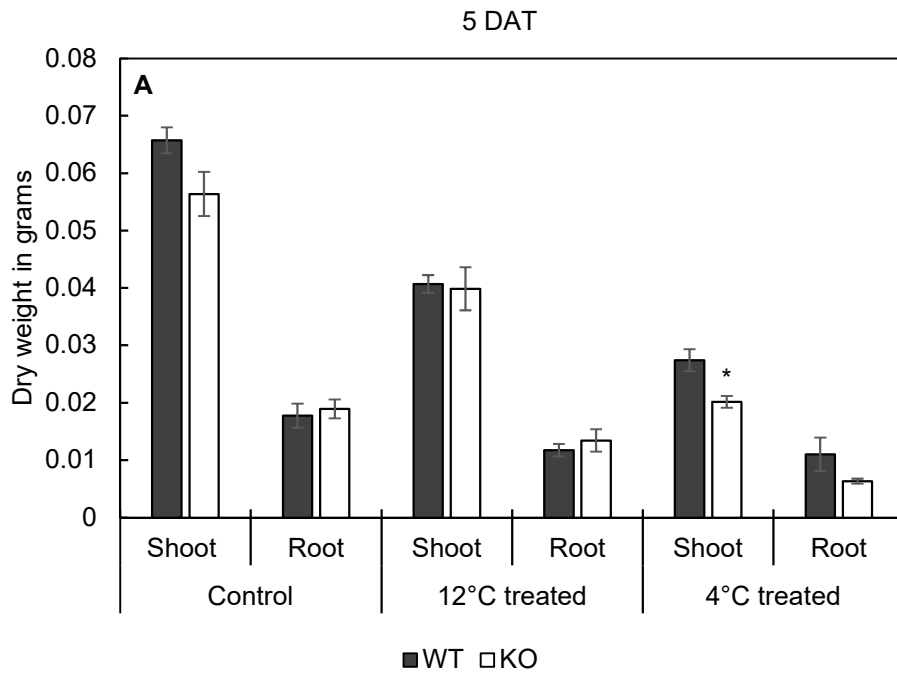


Fig. 3-3 (A-C). Shoot and root dry weights at (A) 5 DAT for control, 12°C treated and 4°C treated seedlings and (B) after recovery for the 12°C treated plants. (C) shows the visual differences between the WT and the KO for the 12°C treated seedlings, that could be rescued. Data represent the mean \pm SE (n=3). Asterisks indicate statistical significance of difference using Student's T-statistic with *-p<0.05 and **-p<0.01.

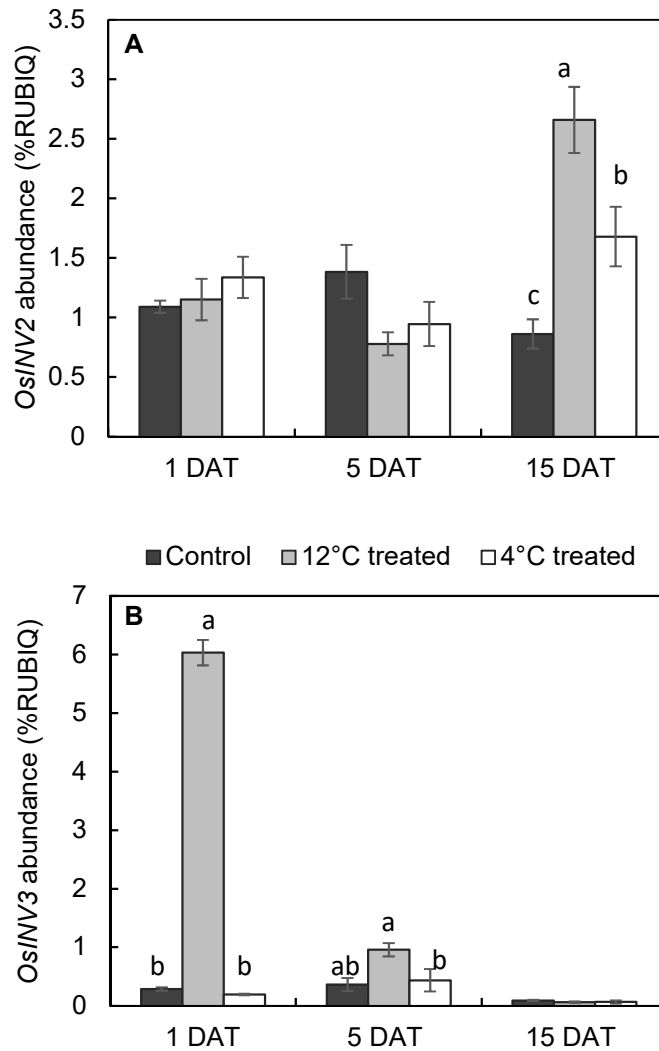


Fig. 3-4 (A-B). mRNA abundance of (A) *OsINV2* and (B) *OsINV3* in the shoots of *OsINV3* WT under control, 12°C treated and the 4°C treated plants at 1 DAT, 5 DAT and 15 DAT. Data represent the mean \pm SE (n=3). Same letters indicate insignificant differences between treatments in *Experiment 2*.

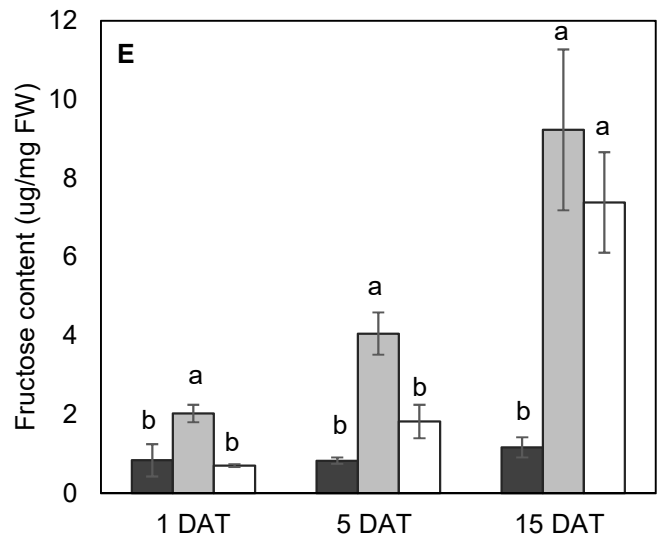
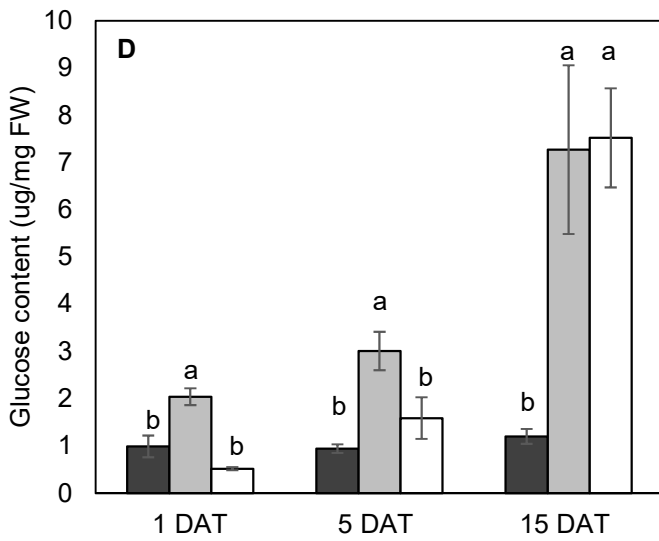
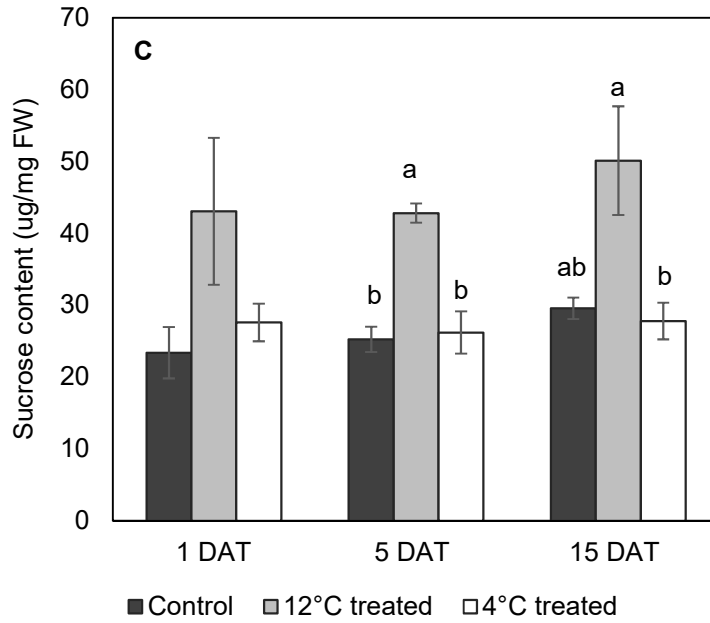


Fig. 3-4 (C-E). Total soluble sugars (C) sucrose, (D) glucose and (E) fructose, in the shoots of *OsINV3* WT under control, 12°C treated and the 4°C treated plants at 1 DAT, 5 DAT and 15 DAT in *Experiment 2*. Data represent the mean \pm SE (n=3). Same letters indicate insignificant differences between treatments.

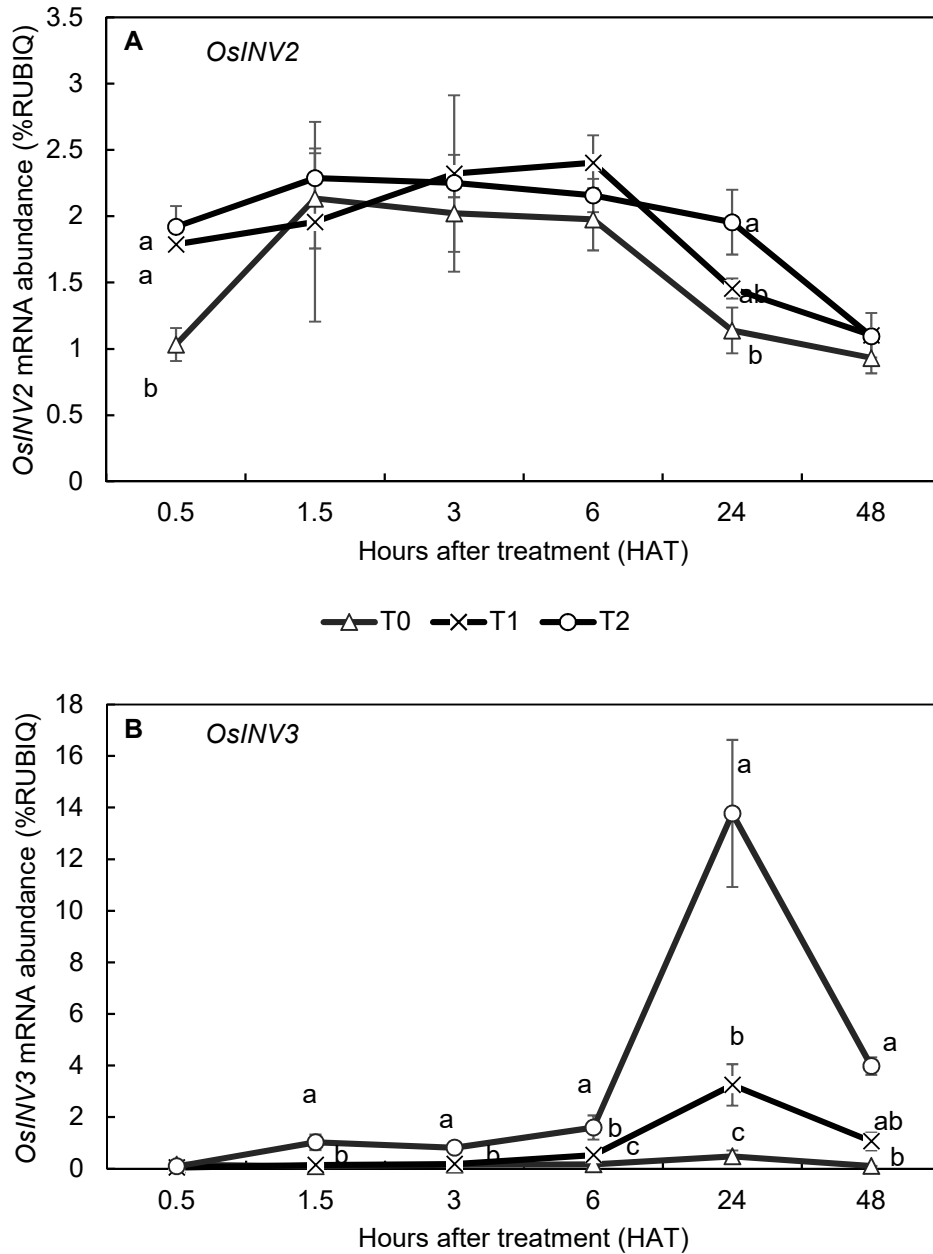
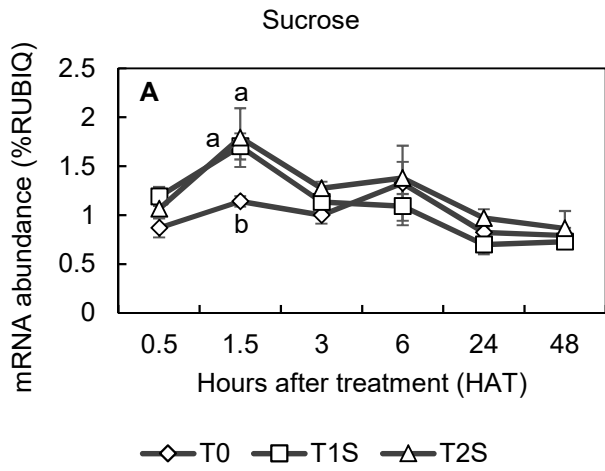


Fig. 3-5. Response of (A) *OsINV2* and (B) *OsINV3*, to ABA at T0 (0 μ M), T1 (0.5 μ M) and T2 (5 μ M) conditions at 0.5, 1.5, 3, 6, 24 and 48 hours after treatment. Data represent the mean \pm SE (n=3). Same letters indicate insignificant differences between the lines.

Response of *OsINV2*



Response of *OsINV3*

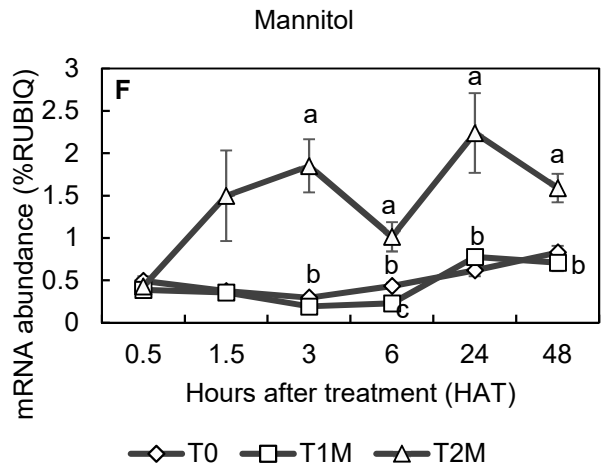
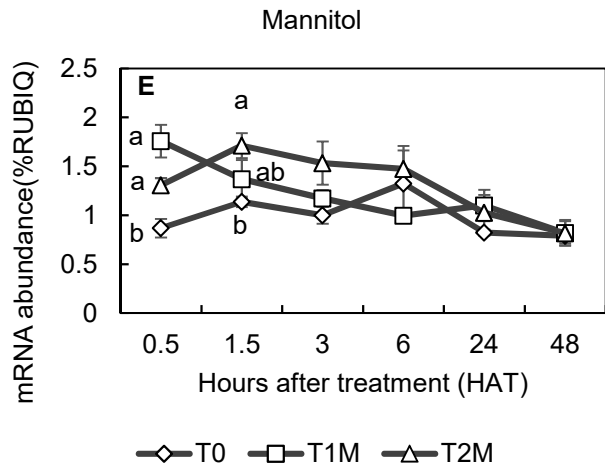
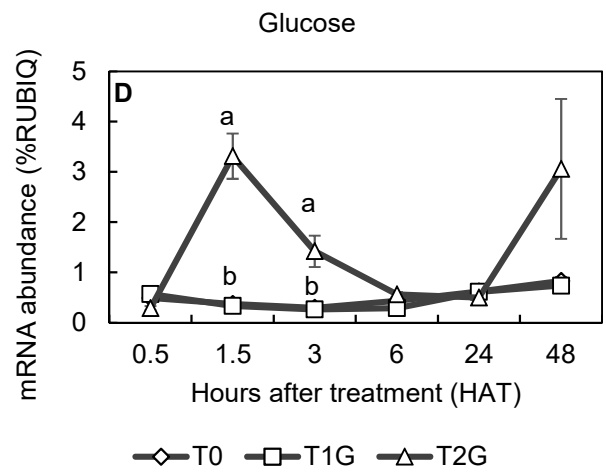
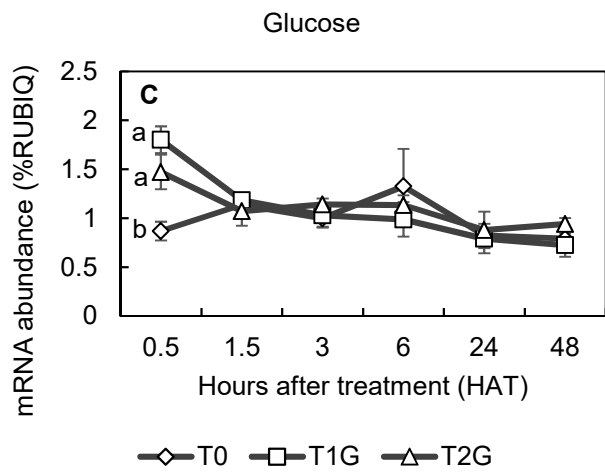
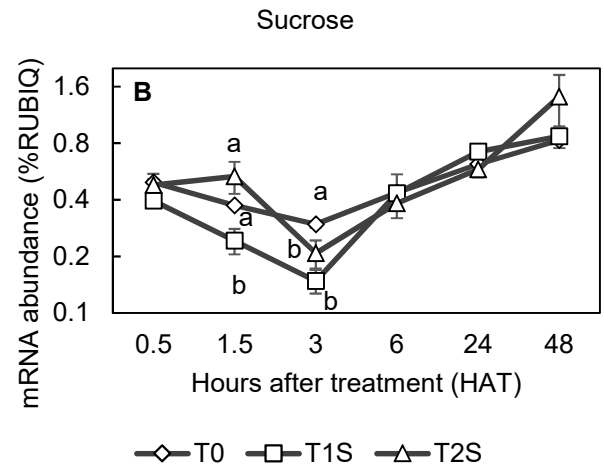


Fig. 3-6 (A-F). Response of *OsINV2* and *OsINV3* to sugars. mRNA abundance was determined in seedlings treated to (A and B) sucrose, (C and D) glucose and (E and F) mannitol at T0 (0%), T1 (0.1%) and T2 (3%) concentrations at 0.5, 1.5, 3, 6, 24 and 48 hours after treatment for (A, C and E) *OsINV2* and (B, D and F) *OsINV3*. Data represent the mean \pm SE (n=3). Same letters indicate insignificant differences between the lines. X-axis is indicative of respective stage, not scaled to the number of hours after treatment.

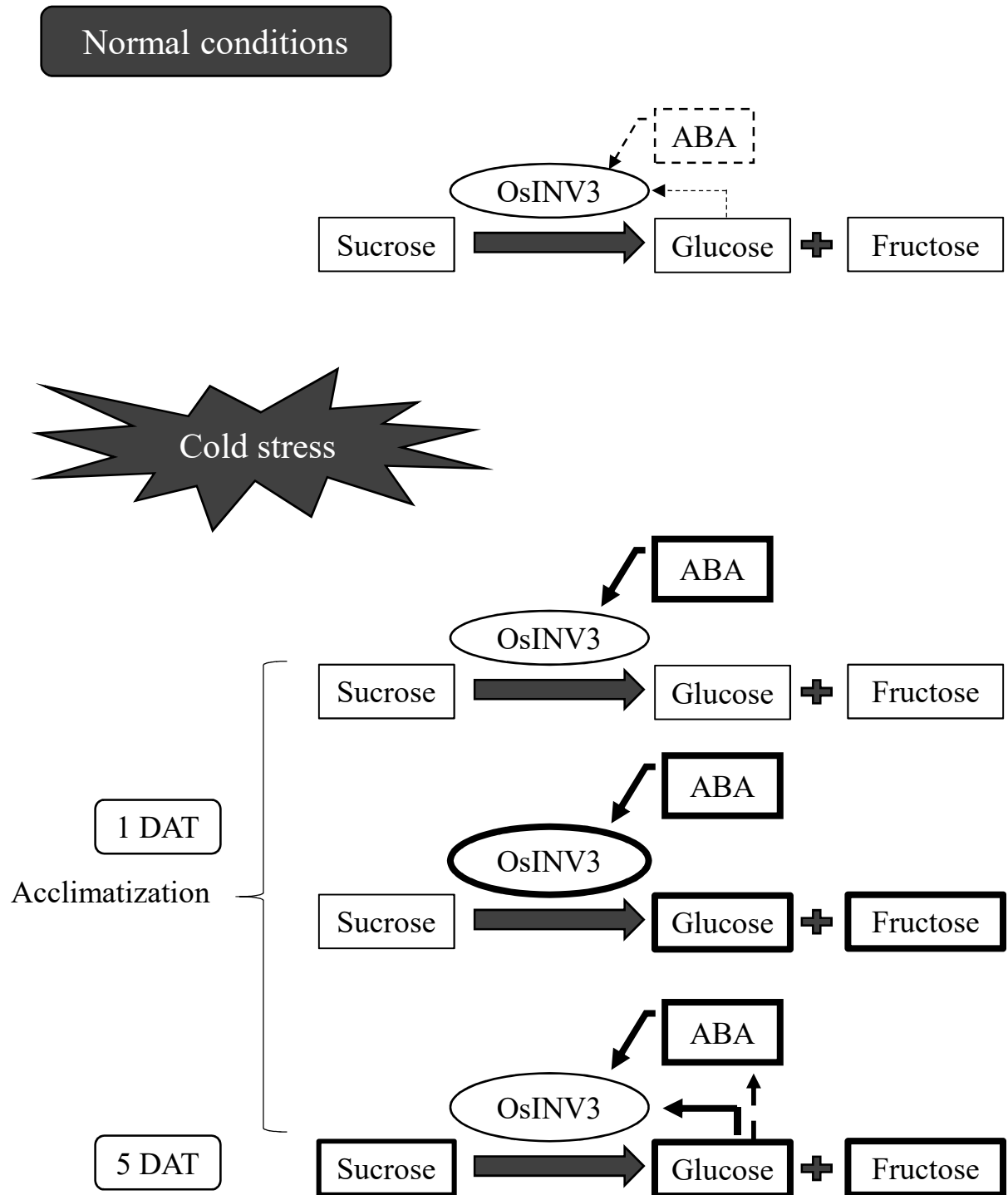


Fig. 3-7. Schematic representation of the mechanism of acclimatization with regulation of *OsINV3* by ABA and glucose. Dotted lines indicate normal regulation pattern, thick dotted lines indicate possible regulation, and thick outline represents an increase in the concentration of glucose, fructose, sucrose and ABA and an increase in transcript levels of *OsINV3*.

CHAPTER 4

ROLES OF VACUOLAR INVERTASE GENES, *SbINV1* AND *SbINV2* IN SUGAR ACCUMULATION IN SORGHUM STEMS

4-1 Introduction

Sorghum (*Sorghum bicolor* (L.) Moench) is a self-pollinating C4 grass belonging to family Poaceae. It is the 5th most important cereal crop in the world (Paterson, 2008) and serves as a staple food in many countries of Asia and Africa (Mace et al., 2013). They can be classified into 4 types based on morphological traits and usage, namely, grain sorghum, sweet sorghum, forage sorghum and energy sorghum (Mathur et al., 2017). While grain sorghums are cultivated for their grain, forage sorghums are mainly used as animal feed and silage (Shoemaker and Bransby, 2010). Sweet sorghums are found to accumulate sugars in their stalk, however, with lower grain yield when compared to the grain sorghum genotypes, while energy sorghums are genotypes that are bred mainly for bioenergy purposes due to their high lignocellulosic biomass. Various factors such as high resilience to harsher climates, ease of extraction, high energy use efficiency and high sugar accumulating capacity have driven attention to the sweet sorghum, as a competitive bioenergy crop.

Being well adapted to the semi-arid regions, sweet sorghum accumulates sugars in its stem during the rainy season, but fails to do so at the same level during post-rainy season. Environmental factors, such as light and water availability, and temperature, influence the sugar accumulating potential of sorghum (Qazi et al., 2012, Rutto et al., 2013). Thus, selection of high sugar yielding varieties suitable for bioethanol production is determined by its performance under the local environmental conditions.

Further, our previous study on comparative transcriptome analysis of genes related to sugar metabolism, between a grain sorghum and sweet sorghum variety, revealed a marked role of a vacuolar invertase, *SbINV2* in sugar accumulation in sweet sorghum (Kurai, 2014, personal communication). This is in concert with previously published data that shed light on the putative roles of VINs in estimation of stem sugar content in sweet sorghums (Qazi et al., 2012, Yang et al., 2013).

In addition to sweet sorghum, sugar accumulation in other grass stems, such as that in sugarcane (*Saccharum* spp.) has been studied. Roles for sucrose phosphate synthase (Zhu et al., 1997; Botha and Black, 2000; Grof et al., 2007; Qazi et al., 2012; Yang et al., 2013), VIN (Zhu et al., 1997; Qazi et al., 2012; Yang et al., 2013; Liu et al, 2014; McKinley et al., 2016), sucrose synthase (Qazi et al., 2012; McKinley et al., 2016), Tonoplast-sugar transporter (TST) (Bihmidine et al., 2016) and sucrose transporter (SUT) (Qazi et al., 2012) in sugar accumulation have been identified. However, an inconsistency in the involvement of the enzymes in sugar accumulation in sorghum is observed, mainly due to the difference in genotypes used, and the influence of external factors on gene expression.

The dependency of stem sugar content on environmental factors and the possible role of VIN on its estimation forms the basis for study elaborated in the current chapter. Relationship between VIN transcript levels and the stem sugar content, in addition to theoretical sugar and bio-ethanol yielding capacity of each of the varieties, with correlation studies between the morphological characters and the stem sucrose content has been described.

4-2 Materials and Methods

4-2.1 Plant materials, growth conditions and sampling time

Nine sorghum varieties, inclusive of four locally available commercial sorghum varieties (Mini sorghum, Meter sorghum, TDN and Supersugar) along with five other global sweet sorghum varieties (Keller, Cowley, Rio, Roma and Wray) were analyzed in 2015 (Fig. 4-1A and B). In addition to these varieties, eight local (Toumitsu, Big sugar, DH, Kanmi, High grain, Hachimitsu, GS-2 and BMR sweet) and 3 global varieties (M81-E, Bromo and Arjuna), leading to a total of 20 varieties were assessed in 2016 (Fig. 4-1C-E). They were grown in an experimental field at the Institute for Sustainable Agro-ecosystem Services (ISAS), The University of Tokyo (35.73°N, 139.53°E, 58m above sea level), in Tokyo, Japan. Fertilizers were applied at 12 g N m⁻², 12 g P₂O₅ m⁻² and 12 g K₂O m⁻² as basal dressing. Cultivation was carried out between months of June and November, with sowing on June 17th, 2015 and June 1st, 2016 under rainfed conditions. The experiments were arranged as completely randomised block designs with three replications. A row spacing of 70 cm and plant-to-plant spacing of 20 cm was maintained resulting in an average planting density of 6.3 plants m⁻².

Sampling for RNA, juice weight estimation and determination of the morphological characteristics was performed at the late soft dough stage of each variety, that was around 30 DAF for most varieties. The early heading varieties however, reached this stage around 25 DAF.

4-2.2 Measurement of morphological characteristics

Plant height, number of leaves, number of tillers, stem girth, panicle length and days to flowering were determined for all the varieties. Plant height was measured from the base to the tip of the panicle, and panicle length was measured from the base of the peduncle to the tip of the panicle. Stem girth was determined by measuring the length of a thin rope that could snugly be wrapped around the base of the stem. Days to flowering was determined as the number of days from the day of sowing to the day of 30% flowering.

4-2.3 Determination of stem juice content, stem juiciness and maximum theoretical ethanol yield (MTEY)

Stem juice content (g cm^{-1}) was determined as the difference in weights of a fixed length of the lower stem before and after drying at 80°C for a minimum of 10 days. This value of stem juice content was divided by the fresh weight of the sample to obtain stem juiciness (g gFW^{-1}). The total juice weight per plant (g) was estimated as a product of the stem juice content (g cm^{-1}) and the harvestable stalk length (cm).

Juice yield (L ha^{-1}) was estimated by the following equation,

Juice yield (L ha^{-1}) = Total juice weight per plant (L) \times Planting density (ha^{-1}), where total juice weight per plant was obtained in litres (L), considering the density of juice as 1.0 for ease of calculation.

MTEY was estimated as the following equation,

MTEY (L ha^{-1}) = juice yield (L ha^{-1}) \times Brix(%)/100 \times (0.85/1.76) (Almodares et.al., 2009).

4-2.4 Determination of brix, and starch and soluble sugar contents

Brix was measured for each internode, using ~ 1 ml juice obtained by squeezing ~ 1 cm of the mid-internode using a hand-held refractometer (PAL-1, ATAGO, Tokyo, Japan). Whole stem brix was estimated as an average of individual brix values obtained for corresponding internodes of the stem. NSC (Starch, sucrose, glucose and fructose) contents for the lowermost internode were determined similar to the methods previously described (Chapter 2, 2-2.11). The choice of lowermost internodes for NSC and transcript level studies, despite maximum sugar accumulation in the intermediate to upper internodes was solely for ease of sampling and maintaining consistency among differently heighted varieties.

4-2.5 Quantitative Real-time PCR

The lowermost internodes from all varieties were sampled in liquid nitrogen and pulverized cryogenically using a Multi-beads shocker (Yasui Kikai, Osaka, Japan) at 2500 rpm for 15 seconds, twice. RNA isolation, cDNA synthesis and real-time PCR were performed similar to the methods previously described (Chapter

2, 2-2.9), with an annealing temperature of 55°C for real-time PCR. Primers specific to *SbINV1*, *SbINV2* and *EF1-a* (*Elongation factor 1-alpha*) are listed in Table 4-1.

4-2.6 Statistical analyses

All statistical analyses were performed in Microsoft Excel 2016. The Pearson's coefficient of correlation was used for correlation studies described in the chapter.

4-3 Results

4-3.1 Non-structural carbohydrates in the lowermost internodes

Total soluble sugar content was determined in both years, in addition to starch content assessed for varieties grown in 2016 (Fig. 4-2). Cowley and Roma consistently fared as the high sucrose yielding cultivars in both 2015 and 2016. While Supersugar performed better under early planting conditions in 2016 than in 2015, TDN failed to accumulate sugars under these conditions (Fig. 4-2B). In 2015, the grain sorghum varieties, Mini and Meter sorghum were grouped into the low sucrose yielding cultivars, along with two sweet sorghum varieties, Keller and Supersugar, which despite having a low sucrose content were comparable to the other sweet sorghum varieties in terms of total soluble sugars (Fig. 4-2A). In 2016, the grain sorghum varieties, Meter, Mini, GS2 and High grain, along with two short-heighted, early flowering sweet sorghum varieties BMR Sweet and TDN failed to accumulate sugars in their stems (Fig. 4-2B). Starch content in all the varieties were considerably lower, and didn't show any comparative trend to the sugar accumulating potential of varieties assessed (Fig. 4-2B)

4-3.2 Relationship between morphological characteristics and sugars in the stem

Plant height, number of leaves, number of tillers, stem girth, panicle length and days to flowering were recorded (Tables 4-2.1 and 4-2.2), and scored for correlation with sucrose and total sugar content in varieties assessed in 2015 and 2016 (Table 4-2.3). Consistent significance for correlation was obtained for plant height, number of leaves and days to flowering with total sugar content in both years, the correlating morphological traits being inherent with sweet sorghum. Consistent data for relationship of morphological traits with sucrose content could not be obtained, where the number of leaves and days to flowering were found to positively correlate with sucrose content in 2015 (Table 4-2.3 A), and panicle length was found to negatively correlate with sucrose content in 2016 (Table 4-2.3 B).

4-3.3 Pattern of sugar accumulation along various growth stages and in the stem

Brix for varieties grown in 2015 was determined at 0 DAF (flowering), 20 DAF and 30 DAF (Fig. 4-3A). Most varieties showed an upward trend of brix from flowering to 30 DAF, a stage that marked the soft

dough stage of grain development. Brix for each internode was measured to determine the pattern of sugar accumulation along the length of the stem for varieties grown in 2016 (Fig. 4-3B). Maximum sugar accumulation was observed in the intermediate or upper intermediate internodes, with the exception of BMR sweet, an early flowering variety that showed maximum sugar accumulation at the lowermost internode.

4-3.4 Relationship of brix and stem juiciness with sucrose content, and estimation of the maximum theoretical ethanol yield (MTEY).

A strong positive correlation was found between brix and sucrose content in stems of varieties grown in both 2015 and 2016 (Fig. 4-4A and B), while a strong negative correlation was found between stem juiciness and brix (Fig. 4-4D), where the grain sorghum varieties, GS2, Meter, Mini and High grain were found to possess the juiciest stems (Fig. 4-4C). MTEY was estimated and found to be highest for Toumitsu, with Cowley and Big sugar showing next higher comparable values (Fig. 4-4D). Despite higher brix, Roma and Cowley were unable to outperform Toumitsu in MTEY mainly due to their lower stem juiciness and relatively smaller plant height.

4-3.5 Relationship of *SbINV1* and *SbINV2* transcript levels and sucrose content in stems

mRNA abundance of *SbINV1* (Fig. 4-5A and C) and *SbINV2* (Fig. 4-5B and D) for varieties grown in 2015 (Fig. 4-5A and B) and 2016 (Fig. 4-5C and D) was determined and plotted against their corresponding sucrose values as shown (Fig. 4-5A-D). A significant negative correlation between *SbINV2* and sucrose content was observed in varieties grown in 2015 (Fig. 4-5F), while no significance for correlation with sucrose content was isolated for *SbINV1* in both years (Fig. 4-5E and G). The significance observed for *SbINV2* in 2015 could not be replicated in 2016 for all the varieties (Fig. 4-5H). However, when estimated for only the high sugar yielding varieties, *SbINV2* and sucrose content were found to be strongly negatively correlated (Fig. 4-5I).

4-4 Discussion

Role of *SbINV2* in estimation of stem sugar content

One of the key results obtained from this study was the differential expression of *SbINV2* among varieties, with significant negative correlation with sucrose content. This isolates *SbINV2* as a key candidate for generation of high sugar yielding varieties through molecular breeding studies. It also highlights the possibility of occurrence of SNPs, and/or allelic variants of this gene, responsible for an expression divergence, not just between the grain and sweet sorghum varieties, but among the sweet sorghum varieties as well – a proposition that needs to be further explored.

Growth of sweet sorghum in temperate climates

Sweet sorghums are not adapted to temperate conditions, however, lately due to the development of photoperiod-insensitive lines, sorghums have been cultivated in temperate regions as well (Thurber et al., 2013). Sweet sorghums have been previously grown in the colder Northern regions of Japan, for stem biomass, with sowing in early to mid-June as ideal for maximum stem yield (Nakamura et al., 2011, Fujii et al., 2015). The period of growth from sowing to flowering in tropical regions is around 55-70 days, with an extension by 20-30 days in temperate conditions (Mocoeur et al., 2015; Rao et al., 2013), which was observed in the varieties grown in our study as well. Maximum stem sucrose accumulation is observed during the soft dough stage, which was observed around 30 DAF in the varieties used in this study. The physiological maturity was reached at 40-45 DAF in most of the varieties analyzed in both years, with the late flowering varieties, Toumitsu and Big sugar being unable to achieve maturity.

Sucrose accumulation potential - an interplay of multiple factors

Various morphological factors, such as the plant height and number of leaves were found to positively correlate with the total stem sugar content (Table 4-2). Taller stems were deemed favorable for sugar accumulation, and thus, found to possess higher number of leaves. In one of the previously reported studies, the photosynthetic ability of a sweet sorghum variety, Wray, was found to be higher than that of a grain sorghum variety, Macia (Bihmidine et al., 2015). The panicle length was negatively correlated while the

flowering date was positively correlated to the total stem sugar content. A longer vegetative stage pointed towards taller plants with a higher ability of stems to accumulate sugar, although recent studies indicate generation of shorter inbred sugar accumulating varieties (Shukla et al., 2017). Taller stems, higher number of leaves, shorter panicles and delayed flowering are traits that are typical to sweet sorghum and were found to correlate consistently with the total stem sugar content among all varieties.

Further, a previous study focused on QTL analysis for sugar related agronomic traits between a grain and a sweet sorghum variety, identified one of the QTLs for plant height, flowering date, panicle weight and brix to be located on chromosome 4 (Shiringani et al., 2010), the chromosome bearing *SbINV2*, a vacuolar invertase isoform found to strongly negatively correlate among the sweet sorghum varieties tested in this chapter (Fig. 4-5B and E). Another study, performed RNA sequencing study of a sweet sorghum variety SIL-05 based on this data and demonstrated almost negligible amounts of *SbINV2* in its stems, but instead found a strong upregulation in the panicles following anthesis (Mizuno et al., 2016). Although, further study for isolation of genes that interlink the sugar-related morphological traits is deemed necessary to make a concrete conclusion, it could be said that *SbINV2* does stand as a key candidate for generation of a molecular marker for breeding studies.

Testing efficacy of varieties based on ethanol yield potential

MTEY, a function of brix and juice yield was found to be the closest determinant for testing efficacy of varieties for bioethanol production. Brix was found to strongly positively correlate with the sucrose content (Fig. 4-4A and B), thus enabling possibility of high throughput screening of varieties for high stem sugar content. A strong negative correlation was found between the stem juiciness and brix (Fig. 4-4D), simply implying that the varieties with lower brix content had juicier stems. Juice yield is a function of stem juiciness and stalk length, thus the taller varieties with moderate stem juiciness were found to have a higher juice yield. This suggested that while the varieties with higher brix values, did fairly well in terms of MTEY, the varieties that maintained a balance with juice yield and brix, i.e. possessing moderate juice yield and moderate-to-high brix values performed extremely well in terms of MTEY, as observed in this study (Figs. 4-2B and 4-4C, E).

Thus, in terms of evaluating varieties for their performance in sugar accumulating potential in terms of bioethanol production, MTEY rather than brix values serves as a key determinant.

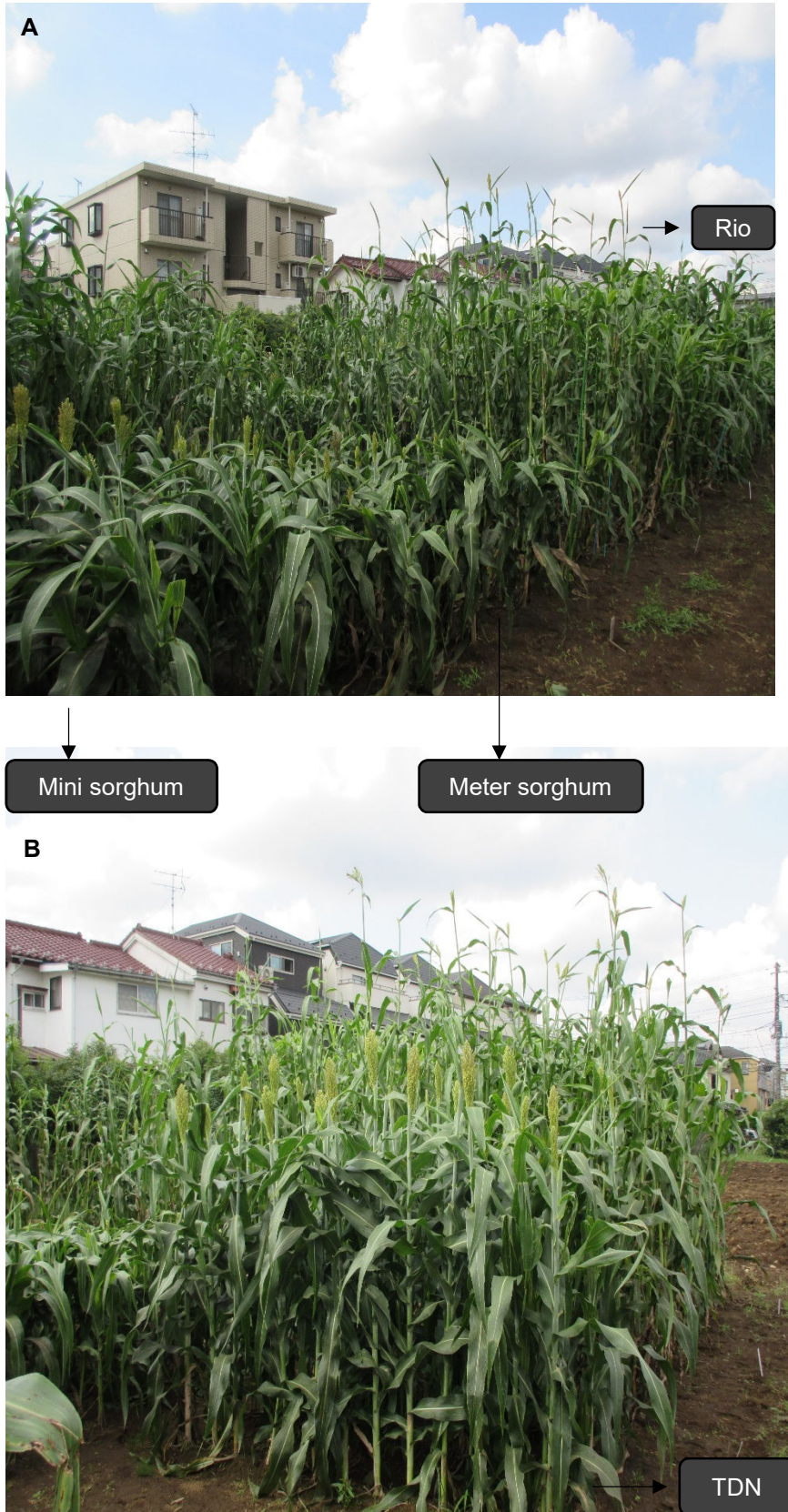


Fig. 4-1 (A-B) Field in 2015 showing (A) Mini sorghum, Meter sorghum, Rio, and (B) TDN.



Fig. 4-1 (C-E) Field in 2016 showing (A) Toumitsu, Big sugar, Kanmi, DH, TDN, (B) Supersugar, Bromo, Wray and Roma, and (C) relative height of the tallest variety Toumitsu (450 cm) grown in 2016.

Primers		Sequence (5'-3')
SbINV1	FW	GCCGTGTA CTTCTACCTGGTCAAGG
	RV	ACGATGGAGTGGTCAACCAGTATTC
SbINV2	FW	CTACCCACCGAGGCCATCTACGC
	RV	TGGGTTGGATGGACGATCGACGGA
EF-1a	FW	CATGGTGGTGGAGACCTTCT
	RV	TCCTTCTTCTCCACGCTCTT

Table 4-1. Primer sequences. EF-1a primer sequences as listed in Milne et al., 2013.

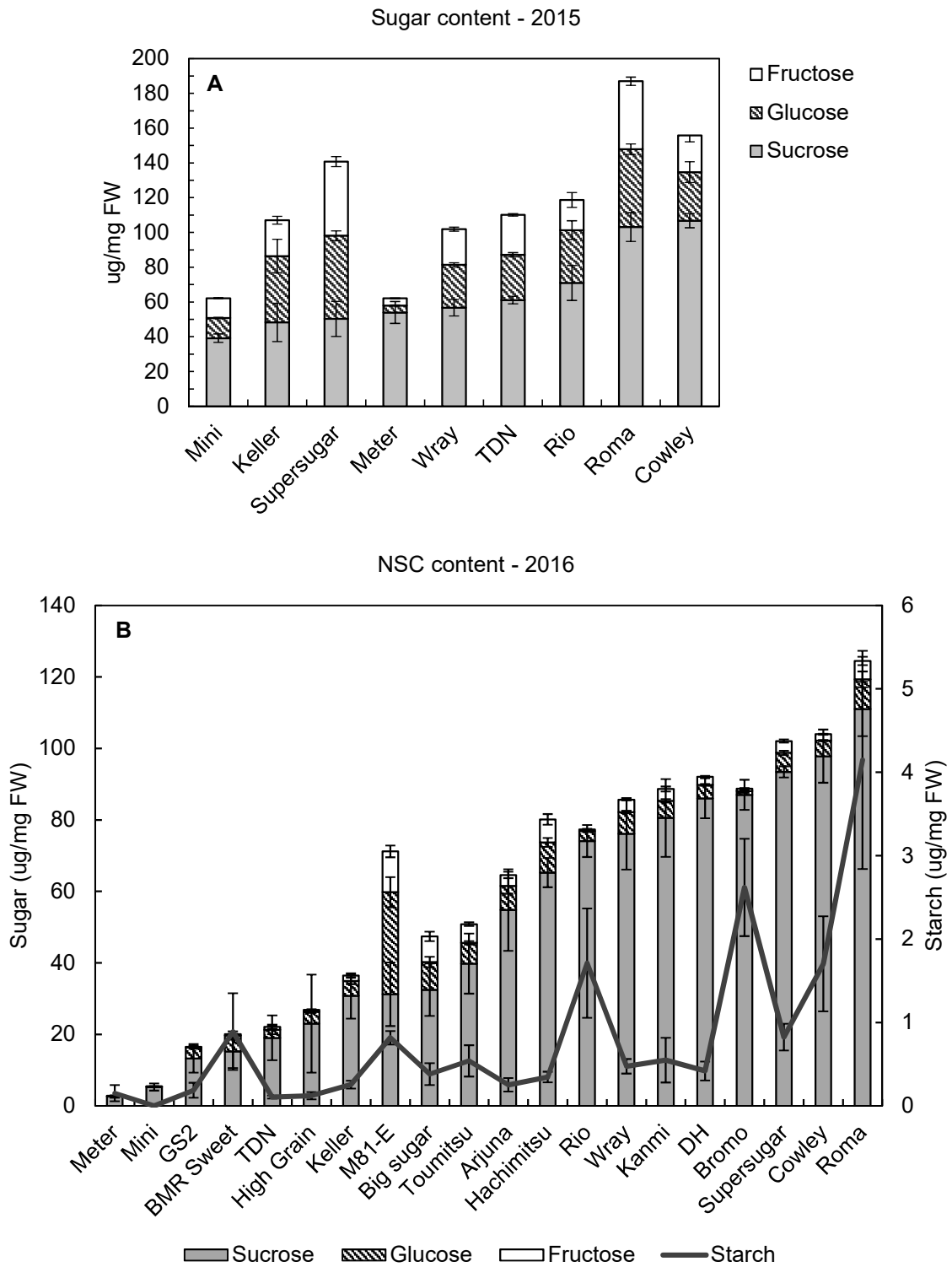


Fig. 4-2. NSC content in the lowermost internodes of sorghum stems, showing (A) Total soluble sugar content for 9 varieties in 2015, and (B) Total NSC content for 20 varieties in 2016. Data represent the mean \pm SE (n=3-4). Varieties sorted on the basis of increasing sucrose content.

2015	Plant height (cm)	Num of leaves	Tillers	Stem girth (cm)	Panicle length (cm)	Days to flowering	Sucrose ($\mu\text{g}/\text{mg}$ FW)	Total sugars ($\mu\text{g}/\text{mg}$ FW)
TDN	183.62 \pm 3.02	16.67 \pm 0.42	0	11.07 \pm 0.32	31.47 \pm 0.83	91	61.10 \pm 4.40	110.08 \pm 13.90
Keller	303.10 \pm 9.09	16.67 \pm 0.80	0.50 \pm 0.50	8.63 \pm 0.59	16.68 \pm 0.94	103	48.30 \pm 22.10	107.05 \pm 6.40
Super sugar	331.38 \pm 9.68	19.50 \pm 0.34	0.67 \pm 0.42	9.40 \pm 0.30	25.33 \pm 1.00	103	50.30 \pm 20.20	140.70 \pm 8.20
Cowlay	285.15 \pm 6.67	20.17 \pm 0.48	2.17 \pm 0.70	8.35 \pm 0.23	15.17 \pm 0.22	112.30 \pm 1.10	106.70 \pm 8.10	155.75 \pm 45.90
Rio	315.23 \pm 5.70	18.00 \pm 0.68	0	8.62 \pm 0.35	24.33 \pm 1.18	93.30 \pm 1.50	70.96 \pm 20.20	118.65 \pm 31.50
Meter	107.85 \pm 1.44	17.50 \pm 0.22	0	9.72 \pm 0.19	29.68 \pm 0.44	91	53.96 \pm 12.60	62.05 \pm 27.30
Mini	131.15 \pm 4.36	17.17 \pm 0.60	0	10.57 \pm 0.64	26.45 \pm 0.68	91	39.20 \pm 4.90	62.17 \pm 39.60
Roma	314.22 \pm 4.59	21.00 \pm 0.26	0	10.00 \pm 0.20	16.70 \pm 0.24	111	103.10 \pm 16.50	186.96 \pm 27.20
Wray	315.27 \pm 7.93	17.17 \pm 0.31	0	9.60 \pm 0.37	16.03 \pm 0.88	91	56.70 \pm 9.40	101.90 \pm 14.30
Bromo	345.63 \pm 5.70	17.67 \pm 0.49	0	9.08 \pm 0.33	23.22 \pm 0.93	102	106.21 \pm 6.50	129.94 \pm 13.70
Arjuna	296.12 \pm 9.81	17.50 \pm 0.85	0	7.25 \pm 0.41	20.60 \pm 1.81	117	84.75 \pm 3.70	197.86 \pm 11.40
M81-E	247.95 \pm 12.74	17.33 \pm 0.84	0.50 \pm 0.50	6.80 \pm 0.46	22.37 \pm 1.30	121.70 \pm 2.50	67.31 \pm 5.90	221.87 \pm 13.80

Table 4-2.1. Morphological characteristics with sucrose content and total sugars for varieties grown in 2015. Data represent the average values \pm SE (n=6).

2016	Plant height (cm)	Num of leaves	Tillers	Stem girth (cm)	Panicle length (cm)	Days to flowering	Sucrose ($\mu\text{g}/\text{mg}$ FW)	Total sugars ($\mu\text{g}/\text{mg}$ FW)
Super sugar	292.88 \pm 6.06	10.83 \pm 0.31	0.33 \pm 0.21	6.48 \pm 0.2	31.65 \pm 0.68	107.5 \pm 0.34	93.44 \pm 1.56	102.05 \pm 2.63
Bromo	279.53 \pm 8.8	10.83 \pm 0.4	0.17 \pm 0.17	7.27 \pm 0.29	30.02 \pm 1.59	94.5 \pm 1.02	87 \pm 4.21	88.70 \pm 4.9
Wray	252.53 \pm 8.55	9.67 \pm 0.49	0	6.48 \pm 0.29	20.38 \pm 0.6	90.83 \pm 0.65	76.1 \pm 9.99	85.61 \pm 10.6
Roma	297.75 \pm 5.87	12.83 \pm 0.6	1.17 \pm 0.17	6.62 \pm 0.58	18.38 \pm 0.63	113 \pm 1.91	111.02 \pm 7.58	124.4 \pm 10.97
Keller	256.43 \pm 8.63	8.5 \pm 0.56	0	5.45 \pm 0.24	28.73 \pm 0.98	84.67 \pm 1.2	30.75 \pm 6.33	36.42 \pm 7.61
Rio	221.69 \pm 8.58	8.33 \pm 0.33	0.33 \pm 0.21	4.03 \pm 0.21	31.07 \pm 1.45	90.83 \pm 1.14	74.09 \pm 4.49	77.32 \pm 4.93
Arjuna	283.83 \pm 8.06	9.5 \pm 0.43	0	6.83 \pm 0.18	21.6 \pm 0.75	95.17 \pm 1.35	54.77 \pm 11.4	64.58 \pm 14.47
Cowley	331.53 \pm 6.59	15.67 \pm 0.71	1.17 \pm 0.4	8 \pm 0.24	19.8 \pm 0.9	114.67 \pm 1.84	97.83 \pm 7.44	103.97 \pm 7.76
M81-E	339.78 \pm 10.45	13 \pm 0.37	1.17 \pm 0.4	7.18 \pm 0.42	28.17 \pm 1.57	120.17 \pm 1.66	31.21 \pm 8.89	71.17 \pm 14.75
Toumitsu	453.57 \pm 5.99	15 \pm 1.1	0.83 \pm 0.31	10.05 \pm 0.74	26.93 \pm 0.57	133.5 \pm 0.72	39.77 \pm 8.39	50.80 \pm 9.43
Hachimitsu	295.47 \pm 9.55	11.5 \pm 0.34	0	6.73 \pm 0.48	28.83 \pm 1.42	103.67 \pm 1.69	65.25 \pm 4.1	80.15 \pm 6.83
Big sugar	445.28 \pm 5.31	16.67 \pm 0.71	0.33 \pm 0.21	9.82 \pm 0.53	28.53 \pm 0.58	133 \pm 0.37	32.48 \pm 7.35	47.4 \pm 10.13
BMR Sweet	159.83 \pm 7.1	5	0.83 \pm 0.31	3.73 \pm 0.49	31 \pm 1.87	70.67 \pm 0.56	15.24 \pm 4.69	20.02 \pm 5.96
Kanmi	293.15 \pm 10.37	12 \pm 0.37	0.67 \pm 0.42	7.8 \pm 0.44	31.9 \pm 1.27	103.5 \pm 2.2	80.55 \pm 10.87	88.63 \pm 12.05
DH	312.63 \pm 8.42	12.17 \pm 0.48	0.17 \pm 0.17	7.27 \pm 0.13	31.55 \pm 0.52	104.83 \pm 1.89	86.04 \pm 5.61	92.07 \pm 6.11
TDN	172.58 \pm 4.2	8.83 \pm 0.31	0	5.58 \pm 0.48	36.28 \pm 1.36	83.5 \pm 0.5	19.01 \pm 6.27	22.12 \pm 8.06
High Grain	196.18 \pm 7.46	12.17 \pm 0.65	0	6.62 \pm 0.3	27.83 \pm 0.92	107.33 \pm 2.94	22.98 \pm 13.7	26.88 \pm 14.22
GS2	219.65 \pm 5.19	8.67 \pm 0.21	5.33 \pm 1.41	4.87 \pm 0.15	33.67 \pm 1.33	84.33 \pm 0.56	13.28 \pm 3.98	16.52 \pm 4.46
Mini	132.23 \pm 3.47	7.67 \pm 0.33	0	4.68 \pm 0.19	29.05 \pm 1.51	83.5 \pm 0.92	5.25 \pm 0.99	5.46 \pm 1.07
Meter	127.72 \pm 2.47	8.67 \pm 0.21	0	5.72 \pm 0.29	35.83 \pm 1.4	84.67 \pm 1.74	2.6 \pm 0.33	2.81 \pm 0.4

Table 4-2.2. Morphological characteristics with sucrose content and total sugars for varieties grown in 2016. Data represent the average values (n=6).

A

R (2015)	Height	Num of leaves	Tillers	Stem girth	Panicle length	Days to flowering
Sucrose	0.388	0.787	0.509	-0.314	-0.512	0.729
Total sugars	0.737	0.834	0.415	-0.290	-0.549	0.839
Sucrose	n.s.	*	n.s.	n.s.	n.s.	*
Total sugars	*	**	n.s.	n.s.	n.s.	**

B

R (2016)	Height	Num of leaves	Tillers	Stem girth	Panicle length	Days to flowering
Sucrose	0.426	0.399	-0.132	0.305	-0.503	0.344
Total sugars	0.533	0.485	-0.113	0.381	-0.544	0.462
Sucrose	n.s.	n.s.	n.s.	n.s.	*	n.s.
Total sugars	*	*	n.s.	n.s.	*	*

Table 4-2.3. Correlation coefficients (R) for relationship of morphological characteristics with sucrose content and total sugars for varieties grown in (A) 2015, and (B) 2016. Data represent the correlation coefficient for data obtained as average (n=3-4). Asterisks indicate statistical significance of difference using Student's T-statistic with *-p<0.05 and **-p<0.01; and n.s. – not significant.

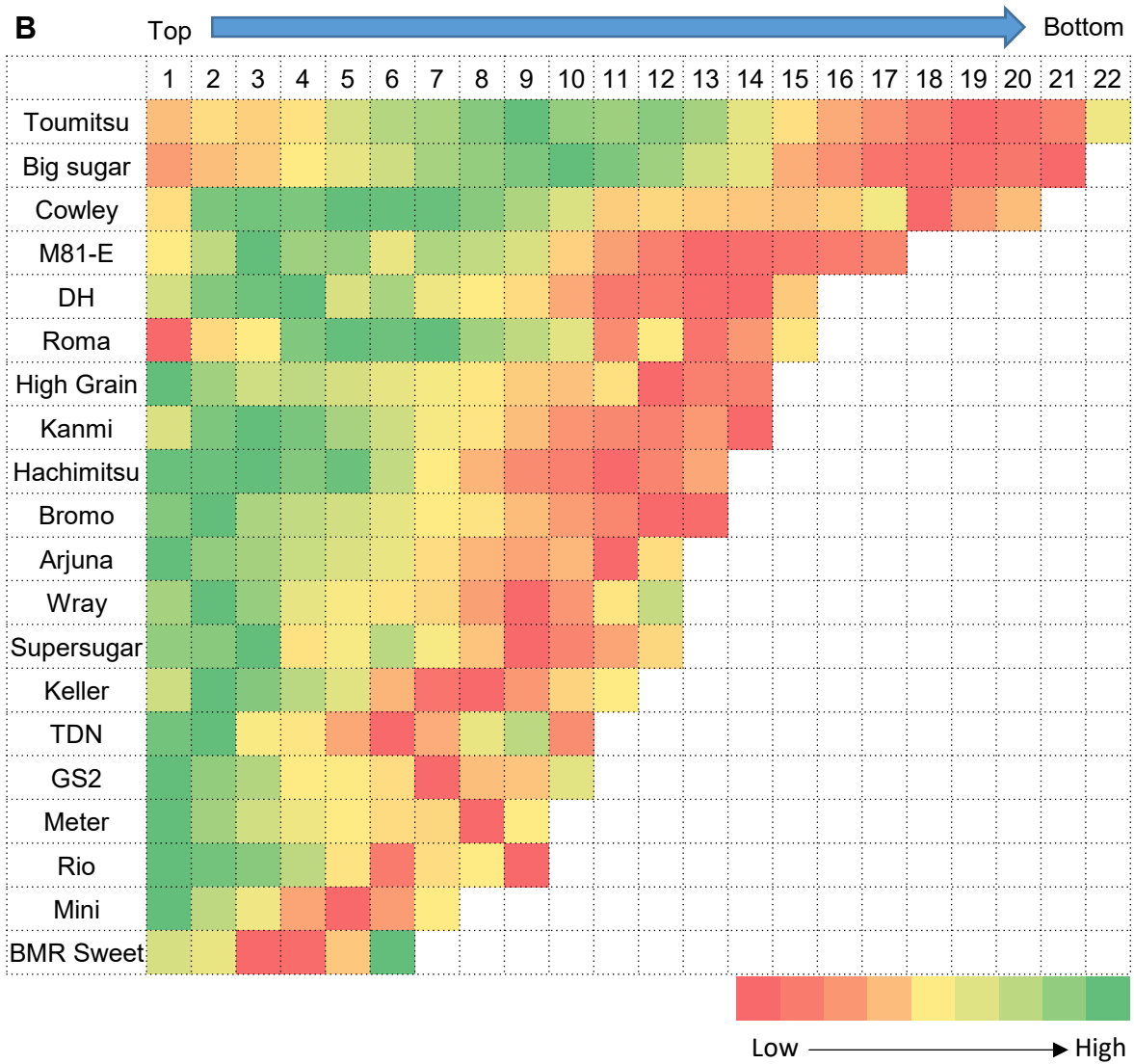
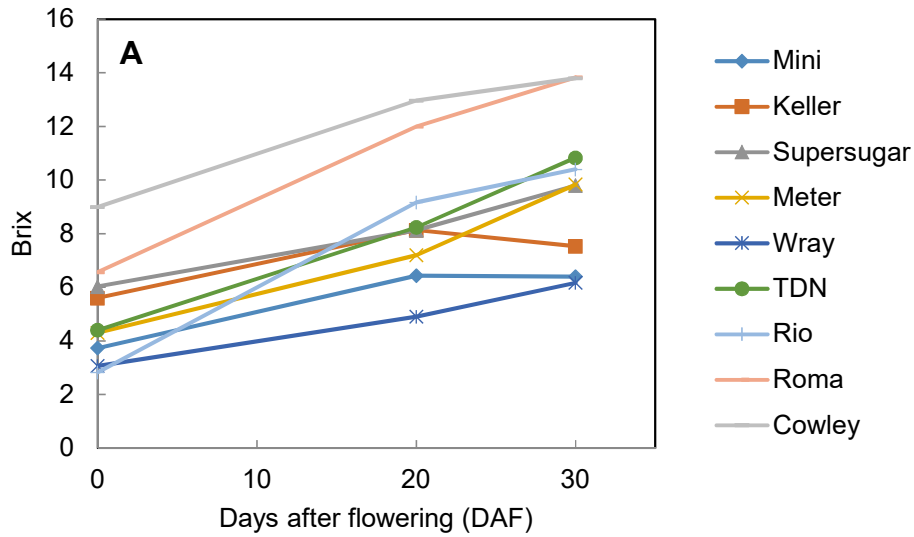


Fig. 4-3. Pattern of sugar accumulation expressed in terms of brix (A) along various growth stages after flowering until 30 DAF for varieties grown in 2015, and (B) for each internode along the whole length of the stem, for varieties grown in 2016. Data represented in terms of average (n=3). The color legend is not numerically universally applicable, but indicative of the high-low pattern of brix for each variety.

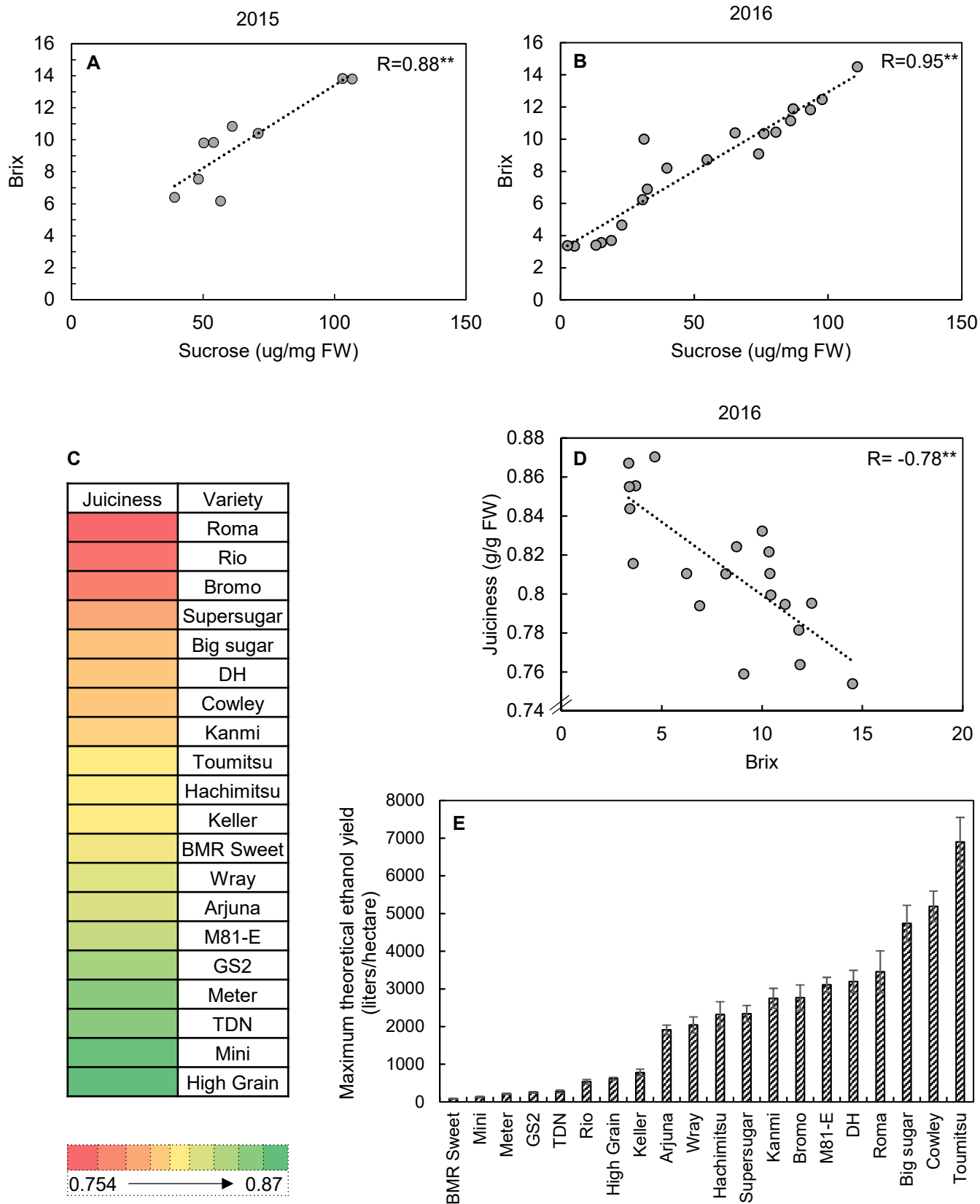
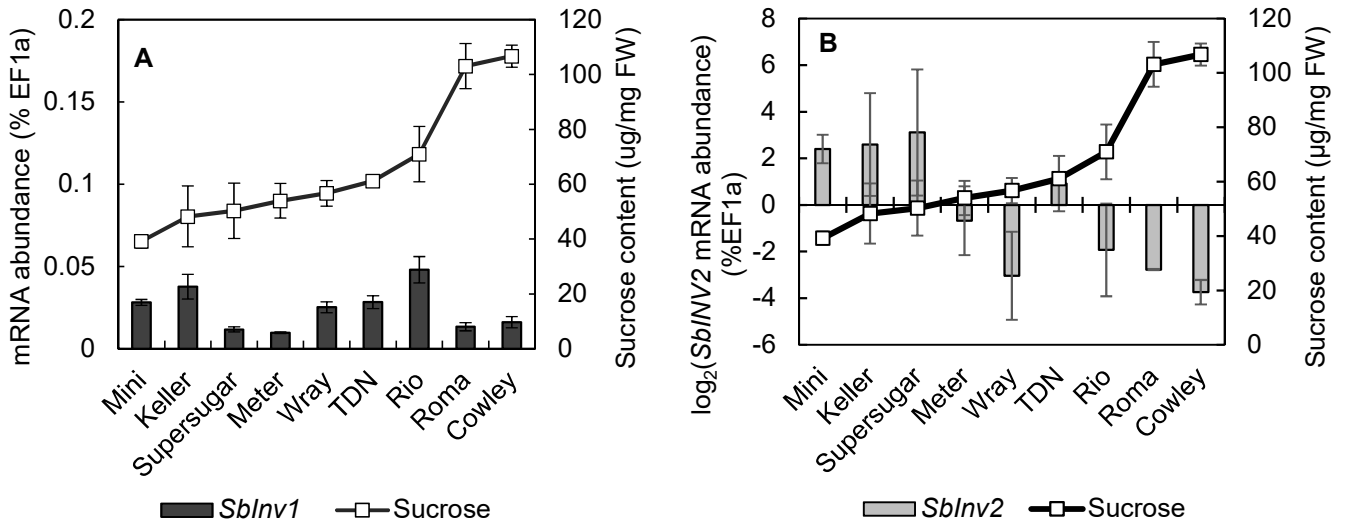


Fig. 4-4. Correlation of brix with sucrose content for varieties grown in (A) 2015, and (B) 2016. (C) Varieties sorted in terms of juiciness of the stems, (D) Correlation of juiciness with brix, and the maximum theoretical ethanol yield for varieties grown in 2016. Data represent the mean \pm SE (n=4-6). Asterisks indicate statistical significance of difference using Student's T-statistic with ** - $p < 0.01$.

2015



2016

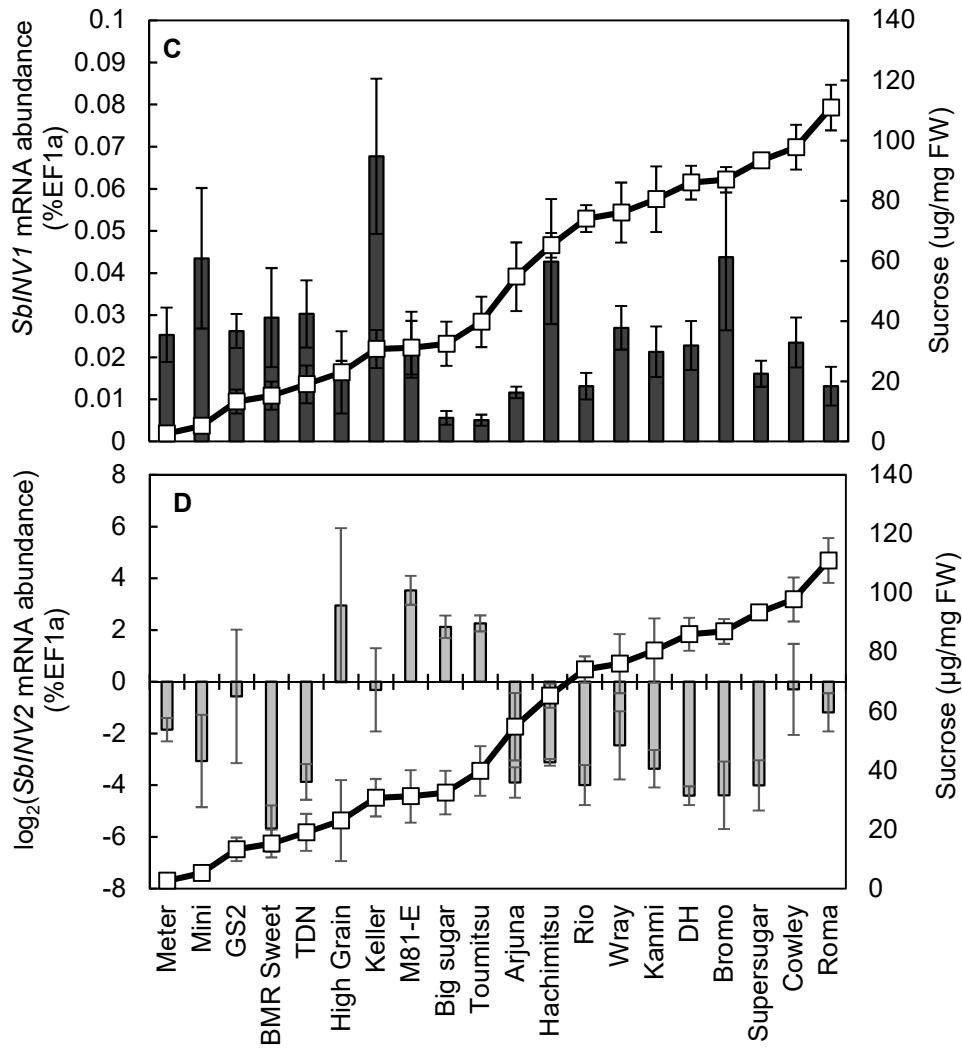
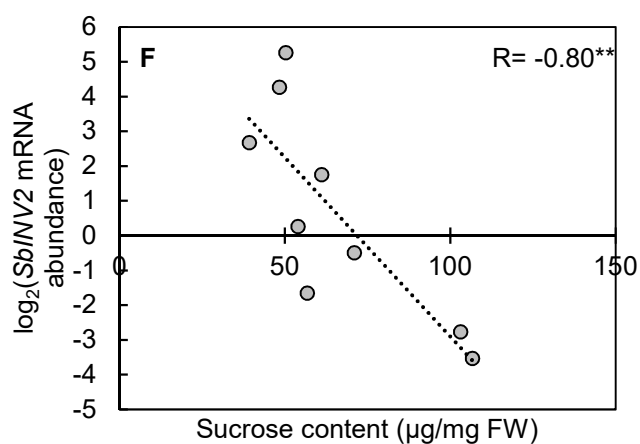
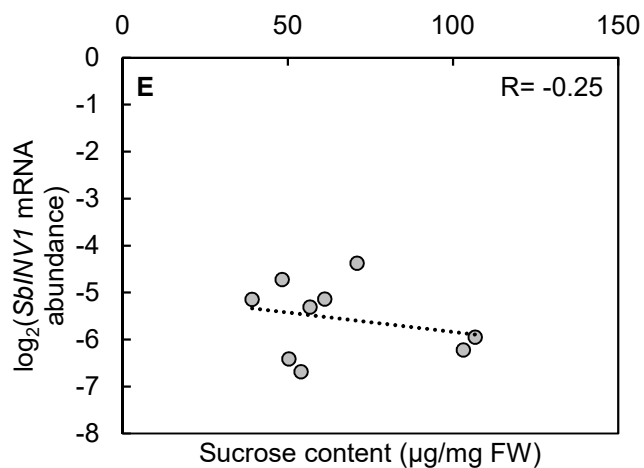
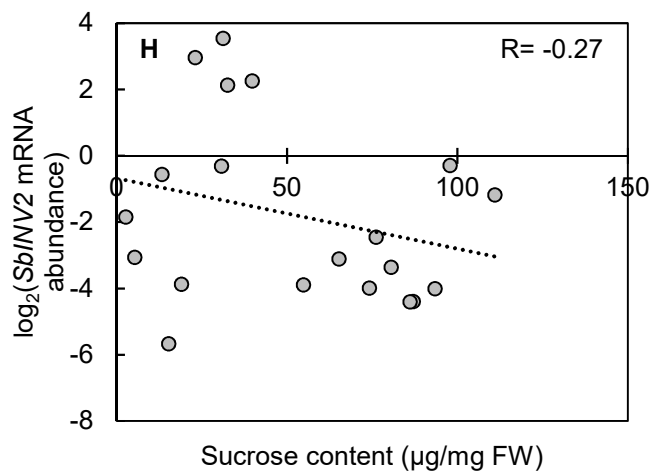
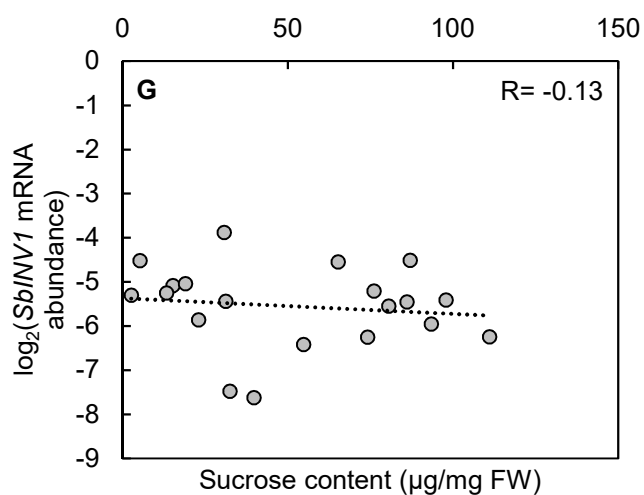


Fig. 4-5 (A-D). mRNA abundance of *SbINV1* (A) and (C), and *SbINV2* (B) and (D), expressed as %EF1a, and corresponding sucrose content for varieties grown in 2015 (A) and (B), and 2016 (C) and (D) in their lowermost internodes. Data represent the mean \pm SE (n=3-4). Varieties sorted on the basis of increasing sucrose content.

2015



2016



For high sugar yielding varieties

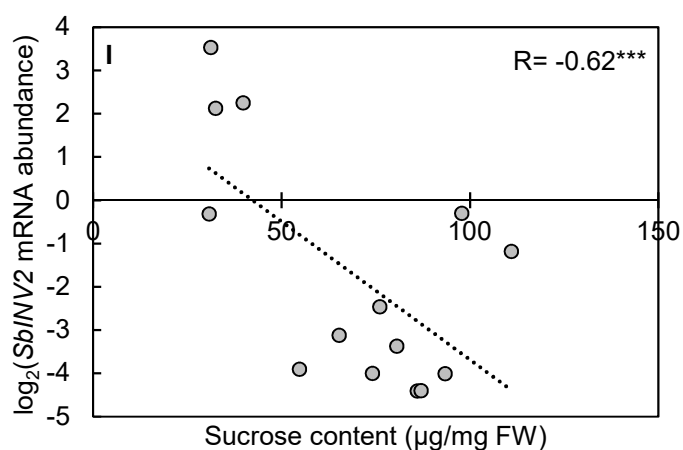


Fig. 4-5 (E-I). Correlation of sucrose content with *SbINV1* (E) and (G), and *SbINV2* (F) and (H) for varieties grown in 2015 (E) and (F), and 2016 (G) and (H). (I) shows the correlation of sucrose content with *SbINV2* for high sugar yielding varieties. Data represent the correlation coefficient for data obtained as average ($n=3$ or 4). Asterisks indicate statistical significance with ** - $p < 0.01$ and *** - $p < 0.001$.

CHAPTER 5

GENERAL DISCUSSION

In plants, VINs are proposed to play a role in sugar storage, osmoregulation and response to cold stress (Sturm, 1999). In relation to crops, namely rice and sorghum, the current study has isolated roles for vacuolar invertase in sugar storage in stems of sweet sorghum, regulation of cell expansion and assimilate partitioning in rice sinks, and acclimatization and recovery from cold stress. An elaborate application of the results from the study, and its significance with crop physiological and agronomical perspectives have also been discussed.

5.1 Roles of VIN in rice

5.1.1 OsINV3 as a key functional isoform of VIN in rice

Mutant studies conducted for *OsINV2* and *OsINV3* revealed a critical role for *OsINV3* in regulation of spikelet size and assimilate partitioning to grain, thus affecting the final grain yield. A role in regulation of hexose-to-sucrose ratios, further influencing assimilate transport was discussed (Chapter 2). An absence for substitution of this physiological role of *OsINV3* was observed, and was suggested to possibly be due to the regulatory differences between the isoforms, which was confirmed in chapter 3, where only *OsINV3* was found to be osmotically-responsive co-incident to its initial response to higher glucose concentration. Thus, the response of *OsINV3* to higher hexose concentrations during the critical pre-grain filling stages could not be mimicked by *OsINV2*, a stage where *OsINV2* was originally not expressed, as confirmed by promoter *GUS::OsINV2* studies. Although, differences in sugar and ABA regulation of the two isoforms was observed, this solely is insufficient to explain the inability of *OsINV2* to fulfil the physiological roles of *OsINV3* despite its high transcript levels, as observed in the key panicle initiation stage. Thus, regulation of VIN isoforms by invertase inhibitor proteins remains a prime domain yet to be explored that could shed more light on the functional validity of *OsINV2*.

5.1.2 Vacuolar invertase and its role in cold tolerance

5.1.2.1 OsINV3 as a molecular marker for cold-tolerant rice

A key role for *OsINV3* in recovery from cold stress and a role in acclimatization in the 3-leaf stage of rice seedlings was also isolated (Chapter 3). With a broad perspective, *OsINV3* could be termed as a sink determinant, mainly due to its ability of remobilizing the assimilate supply to the cold-stressed seedlings, mainly roots and young leaves, which could be considered as the major sinks. This is in line with our mutant study of *OsINV3* (Chapter 2), where *OsINV3* was discussed to be a molecular sink strength determinant, owing to its regulation of sink size and dry matter partitioning differences. However, further study on the possible role of *OsINV3* in stabilizing the photosynthetic ability of the cold-stressed leaves, would be vital to reach a conclusion on the influence of *OsINV3* on the source-sink dynamic in cold-stressed seedlings.

An increase in various metabolites such as sugars, cold-related amino acids and antioxidants has been reported in rice plants under cold stress. Although, these could be utilized as indicators of cold-stress response in rice and the extent of cold tolerance exhibited, isolation of genes involved in increase in the level of these metabolites would prove as a powerful tool for breeding (Zhang et al., 2014). In our study, an up-regulation of *OsINV3* in the shoots during acclimatization was observed that co-occurred with increased sucrose and hexose levels, imparting an ability to recover following exposure to cold stress. Thus, this up-regulation of the *OsINV3* transcript level could be considered as a key signal towards acclimatization during the seedling stage, with a potential of development of *OsINV3* as a molecular marker for development of cold-tolerant rice varieties.

5.1.2.2 Evolutionary relationship of VINs and fructan-biosynthesis enzymes

Fructans, one of the storage forms of carbohydrates impart cold and drought tolerance to crops such as wheat and barley. The fructan-biosynthesis enzymes (FBE) which are fructosyltransferases, belong to the same clade as the VINs in the phylogenetic tree (Fig. 1-1), and are believed to have evolved from VINs. The sub-clade consisting of *SbINV2* and *OsINV3*, which were isolated as key VIN isoforms in sorghum and rice respectively, is the closest in distance to the fructosyltransferases capable of producing fructans (Fig. 1-1). Although FBE enzymes are absent in rice, there are conserved motifs in the N-terminal domain of VINs in rice and the fructan fructosyltransferases of monocots, revealing a possibility of conserved mode of regulation in response to cold and drought stresses (Ji et al., 2007). The response of *OsINV3* to cold treatment could be attributed to this finding (Fig. 3-4A and B). Induction of maize vacuolar invertase *ZmVAC2*, an ortholog of *OsINV3*, by water stress (Kim et al., 2000) could also point to the possibility of a

conservation of the responsiveness of vacuolar invertases and the fructan fructosyltransferases to cold and drought stresses.

5.2 Role of VIN in sweet sorghum

Sweet sorghums accumulate high amounts of soluble sugars in their stems, especially after anthesis, a phenotype that has been targeted for molecular breeding (Shukla et al., 2017). Thus, the stems of sweet sorghums are considered the major sinks, where they tend to store majority of carbohydrates (McBee and Miller, 1982). Roles of VIN in sorghum was found to be contrasting to its roles in rice, wherein, an absence of *OsINV3* reduced the sink strength in rice (Chapter 2), lower transcript levels of *SbINV2*, the ortholog of *OsINV3*, correlated to its higher sink strength in the form of higher sucrose content in its stems. An expression divergence of *SbINV2* between sweet and grain was also isolated to be one of the key reasons for the ability of sweet sorghums to accumulate sugars in its stems. This was in line with a previous study, that assessed the origin of sweet sorghum by studying the genetic differentiation between 75 sweet sorghum cultivars and 660 diverse landraces, and found *SbINV2* as a sole candidate within the top 1% haplotype diversity interval (Burks, Ph.D. dissertation, 2015). *SbINV1*, an ortholog of *OsINV2* was not key in affecting the sugar content in the stems, outlining *SbINV2* as the key functional vacuolar invertase in sorghum, however needing further conclusive evidence.

Sweet sorghums are not capable of accumulating sugars in their stems during the post-rainy season at the same level as in the rainy season, in the semi-arid regions (Kurai et al., 2015). The post-rainy season is characterized by shorter day-length, lower temperature and little/no precipitation. Studies on sweet sorghum under irrigated conditions in the post rainy season, also yielded lower stem sugar content, highlighting towards the key effects of light and temperature on sugar accumulation (Kurai et al., 2015). Our study revealed a strong up-regulation of *OsINV3* to chilling temperatures and the stress hormone, ABA (Chapter 3). Thus, a similar regulatory response of *SbINV2*, a homolog of *OsINV3* could be proposed, an up-regulation of which, under colder post-rainy climates would directly decrease the stem sucrose content in the internodes. Although highly plausible, this is a proposition that needs to be further investigated. In addition to this possibility, a recent study proposed the involvement of *SbINV1* in cold tolerance mechanism of sorghum seedlings, where *SbINV1* was found to be up-regulated in the cold tolerant lines (Chopra et al.,

2017), thus suggesting an up-regulation of *SbINV1* as a complementary or sole cause for lack of sucrose accumulation in the post-rainy season.

5.3 Vacuolar invertase as a molecular marker in breeding studies

VINs in grasses have been found to play a role in sugar accumulation in sugarcane internodes (Zhu et al., 1997), early caryopsis development in barley (Weschke et al., 2003) and strongly induced by water stress in maize (Kim et al., 2000). However, its extensive roles in terms of influence on sink strength has not been previously demonstrated.

In an agronomic point of view, our study highlights on the role of vacuolar invertase as a grain yield determinant. For decades, higher grain yield has been a favoured target for rice breeding studies. The influence of *OsINV3* on yield, could be extended to molecular breeding studies for development of elite varieties bearing grains with bigger size and weight. A differentiation study of *OsINV3* to study polymorphisms, between the varieties bearing grains of varied sizes, could draw more attention to the diversity of *OsINV3* if any, among rice varieties.

It has been long believed that sweet sorghums store most of their carbohydrates as sugars in their stem, while, grain sorghums store most of their carbohydrates in grain (McBee and Miller, 1982). Thus, it is expected that the grain quality in sweet sorghums is lower than that of grain sorghum, mainly due to a limited availability of carbohydrates for grain (Shukla et al., 2017). However, sweet sorghum genotypes with a higher or comparable grain yield to grain sorghums have been reported (Channappagoudar et al., 2007; Ganesh Kumar et al., 2010). Breeding studies to produce sweet sorghum varieties with higher grain yield and higher stem-sucrose content in the stems have been a focus in recent times (Mathur et al., 2017; Shukla et al., 2017). Studies in the past have revealed the independent existence of stem internodes and the panicles as storage sinks in sweet sorghum genotypes (Murray et al., 2008; Rao et al., 2013). Absence of changes in the stem sugar content under elimination of one of the sinks, achieved through pruning or cytoplasmic male-sterile lines supports the prevalence of independent physiological pathways in the stems and panicles (Gutjahr et al., 2013). Thus, the elimination of trade-off between grain yield and stem sugar yield in sweet sorghums can be achieved. The presence of independent physiological pathway in sweet sorghum stems paves way to the utilization of *SbINV2* as a molecular marker for breeding varieties with

high sucrose content in their stems. Further, full length DNA-sequencing of *SbINV2* in the varieties analysed to isolate any polymorphisms could isolate the specific diversity in terms of divergence observed between the sweet sorghum and grain sorghum varieties.

In conclusion, through this study VINs have been demonstrated to play a major role in

1. Sink size by regulating sink expansion in rice, owing to its response to osmotic potential differences and regulation by glucose.
2. Assimilate partitioning into the sinks in rice, by modulating the hexose-to-sucrose ratio and maintaining the sucrose gradient for translocation through the phloem into the sinks.
3. Acclimatization and recovery from cold stress in rice seedlings, owing to their regulation by ABA and glucose.
4. Determination of the sucrose accumulating potential in sweet sorghum, owing to their sucrose-correlating differential expression among various sweet sorghum varieties.

CHAPTER 6

SUMMARY

The current study focusses on isolating key physiological and functional roles of VINs in two major crops, rice and sorghum. This study was undertaken in view of clarifying the contribution of VINs in sugar metabolism in these crop species, mainly with a broader goal of achieving higher sink strength, in terms of grain yield and stem-sugar yield in rice and sorghum respectively.

1. Mutant analysis of two vacuolar invertase genes, *OsINV2* and *OsINV3* in rice

Two rice vacuolar invertases, *OsINV2* and *OsINV3*, were assessed for various physiological and agronomic traits using *Tos-17* retrotransposon mutants. In the seedling stage, *OsINV3* was found to regulate the dry matter production, wherein the mutant seedlings possessed lower shoot and root dry weights, with observed recovery in the complementation lines. In the reproductive stage, *OsINV3* mutants showed shorter panicles with lighter and smaller grains, owing to a smaller cell size on the outer and inner surfaces of the palea and lemma as observed by scanning electron microscopy. Further, a strong *promoter::GUS* expression was observed in the palea, lemma and the rachis branches in the young elongating panicles, which supported the role of *OsINV3* in cell expansion and thus, in spikelet size and panicle length determination. Assessment of field grown mutants not only revealed a drastic reduction in the percentage of ripened grain, 1000-grain weight and final yield, but also a significant reduction in partitioning of assimilates to the panicles, whereby the total dry weight remained unaffected. Determination of the non-structural carbohydrate contents revealed a lower hexose-to-sucrose ratio in the panicles of the mutants from panicle initiation to 10 days after heading, a stage that identifies as the critical pre-storage phase of grain filling, whereas the starch contents were not found to be affected. In addition, a strong *promoter::GUS* expression was observed in the dorsal end of ovary during the pre-storage phase until 6 days after flowering, highlighting a function for *OsINV3* in monitoring the initial grain filling stage. Thus, *OsINV3* was found to be a sink strength determinant in rice, mainly by its role in cell expansion, thus, regulating the spikelet size, and driving the movement

of assimilates for grain filling by modulating the hexose-to-sucrose ratio, contributing in grain weight determination and thus, the grain yield.

Field grown *OsINV2* mutants showed a higher total sugar content in the leaves, stem and culm at harvest, a phenotype that couldn't be confirmed by complementation, further supported by its lack of expression at this stage in the *promoter::GUS* lines. However, studies with hetero lines of *OsINV2* could shed more light on its role in regulating the stem sugar levels in the field conditions. *OsINV2* and *OsINV3* were found to have contrasting patterns of *promoter::GUS* expression in the development of panicles, with *OsINV2* being expressed in the early initiation stages, and *OsINV3* being expressed in the critical grain filling stage and the stages before heading.

Thus, we isolate *OsINV3* as a key functional VIN in rice, with critical physiological roles that leads to a compromise in grain yield upon its failure.

2. Role of *OsINV3* in cold stress recovery during the seedling stage in rice

The *OsINV3* WT, KO and the complement lines were tested for cold recovery following exposure to 4°C, and the WT seedlings showed a higher survival rate when compared to the KO, with an observed recovery in the complement lines. This isolated a key role for *OsINV3* in cold stress recovery in rice seedlings at the 3-leaf stage. Further, acclimatization studies were carried out to establish contrasting survival rates between the WT and KO post-cold stress following acclimatization. The WT showed greater signs of recovery in comparison to the KO. Estimation of *OsINV2* and *OsINV3* transcript levels revealed a higher transcript level of *OsINV3* during acclimatization, as were the levels of sucrose and hexoses.

The upregulation of *OsINV3* in cold stressed seedlings outlined a possible regulation by ABA, a stress hormone, and sugars that were found to be accumulated in the cold stressed seedlings. A strong response of *OsINV3* to ABA and glucose was attributed to be a key finding in demonstrating a mechanism for *OsINV3* induced cold acclimatization, and thus cold tolerance.

3. Role of vacuolar invertase genes, *SbINV1* and *SbINV2* in sugar accumulation in sorghum stems.

The sugar accumulating potential of global and local sweet and grain sorghum varieties were tested under local conditions. The basis for this study was the dependency of sugar accumulation on temperature and photoperiod, thus creating a necessity to test the performance of the cultivars under local conditions to assess its sugar accumulating potential, thus its efficacy as a bioenergy source.

A strong correlation of sucrose content with brix was observed, enabling the large-scale screening of varieties for high sucrose content. There was no major trend observed in terms of starch content in the varieties with respect to their sugar accumulating potential. The morphological characteristics inherent to sweet sorghum, such as, tall stems, greater number of leaves and a longer vegetative period were found to correlate with the stem sucrose content. Assessment of sugars along the stem revealed, maximum sugar accumulation in the intermediate to upper internodes in most of the varieties tested. The MTEY, which was a function of brix and juice volume was isolated as a better indicator of testing the performance of a variety as a potential source of bioethanol, mainly due to a negative correlation of stem juiciness with sucrose content in the varieties tested. Further, the relative expression of *SbINV1* and *SbINV2* revealed a strong negative correlation of *SbINV2* to stem sucrose content, thus isolating it as a key candidate for molecular breeding studies.

In conclusion, we isolated key physiological roles for VINs in rice, in regulation of

- Sink size, due to role of *OsINV3* in cell expansion in the spikelet, mainly driven by its osmotic dependence and regulation by glucose.
- Assimilate partitioning to sinks, by *OsINV3* regulation of hexose-to-sucrose ratio during the critical pre-storage phase.
- Cold acclimatization and recovery, owing to *OsINV3* regulation by ABA and sugars;

and, in determination of the sucrose accumulating potential in sweet sorghum, owing to differential expression of *SbINV2*, demonstrating a strong negative correlation with sucrose content, among various sweet sorghum varieties.

ACKNOWLEDGEMENTS

For accepting me into the Ph.D. program and providing me a platform to put my ideas to work, I thank my first supervisor, Dr. Ryu Ohsugi. My heartfelt thanks to Dr. Junko Yamagishi, my current supervisor, for her kind support during the final stages of my study. I'm extremely grateful to Dr. Naohiro Aoki, my mentor and teacher, for believing in my research instincts and offering support and motivation to keep going, and for not losing his sense of humor, even when I lost mine. The immensely engaging discussions with Dr. Tomohiro Kurai, my first informal teacher and friend, gave me direction and perspective during the beginning of my doctoral study, for which I'm eternally grateful. My heartfelt thanks to Dr. Tatsuro Hirose and Dr. Masaki Okamura for having provided me insight and clarity in many of the concepts, and to Dr. Yoichi Hashida, for playing an immense role in teaching me, through his support with the protocols, research methodologies, and the invaluable discussion sessions. I'm also grateful to Dr. Yoshida for teaching me western blot and letting me use her research facilities, and Dr. Fumiko Ishizuna for her assistance with Scanning Electron Microscopy (SEM) image acquisition. I'd also like to extend my sincere thanks to Mr. Akira Murakami for his preliminary analysis of the rice VIN mutants, and Dr. Satoshi Nakamura, Miyagi University and Dr. Tadashi Takamizo, NARO Livestock and Grassland Science, for their kind contribution of sorghum seeds. Heartfelt thanks to the technical staff of Institute for Sustainable Agro-ecosystem services (ISAS) for their cultivation management of rice and Sorghum and to all my supporting lab mates, with special mention to Rei Tanimoto; for their tireless efforts with the field samplings and for constantly cheering me on.

I cannot thank my friends and family enough, for uplifting my spirits and helping me regain confidence and faith in myself during the times of self-doubt. I'd especially like to thank my parents, Hemaprabha G. Rao and Ganesh Rao Morey, my sister, Swarup for their immense love and support; and my friends, Komal, Maggi, PK, Kirti, Kamakshi, Sleaters, Sonali, Shwetha, Sarthak, Kamo-chan, Kiran, Dee, Ruta and Runit for their endless motivation and encouragement during the course of my study. I'd also like to extend special thanks to my partner Ryu for his constant support during the final stages of my Ph.D.

REFERENCES

- Agrawal GK, Abe K, Yamazaki M, Miyao A, Hirochika H (2005) Conservation of the E-function for floral organ identity in rice revealed by the analysis of tissue culture-induced loss-of-function mutants of the OsMADS1 gene. *Plant Molecular Biology* 59: 125-135
- Aoki N, Hirose T, Furbank RT (2012) Sucrose transport in higher plants: From source to sink. *In* JJ Eaton-Rye, BC Tripathy, TD Sharkey, eds, *Photosynthesis: Plastid Biology, Energy Conversion and Carbon Assimilation, Advances in Photosynthesis and Respiration, Vol 34*, pp 703-729
- Bhaskar PB, Wu L, Busse JS, Whitty BR, Hamernik aJ, Jansky SH, Buell CR, Bethke PC, Jiang J (2010) Suppression of the Vacuolar Invertase Gene Prevents Cold-Induced Sweetening in Potato. *Plant Physiology* 154: 939-948
- Bihmidine S, Hunter CT, Johns CE, Koch KE, Braun DM (2013) Regulation of assimilate import into sink organs: update on molecular drivers of sink strength. *Frontiers in Plant Science* 4: 1-15
- Bihmidine S, Baker RF, Hoffner C, Braun DM (2015) Sucrose accumulation in sweet sorghum stems occurs by apoplasmic phloem unloading and does not involve differential Sucrose transporter expression. *BMC Plant Biology* 15: 186-186
- Bihmidine S, Julius BT, Dweikat I, Braun DM (2016) Tonoplast sugar transporters (SbTSTs) putatively control sucrose accumulation in sweet sorghum stems. *Plant Signaling and Behavior* 11: 1-7
- Botha FC, Black KG (2000) Sucrose phosphate synthase and sucrose synthase activity during maturation of internodal tissue in sugarcane Frederik. *Australian Journal of Plant Physiology* 27: 81-85
- Brummell Da, Chen RKY, Harris JC, Zhang H, Hamiaux C, Kralicek AV, McKenzie MJ (2011) Induction of vacuolar invertase inhibitor mRNA in potato tubers contributes to cold-induced sweetening resistance and includes spliced hybrid mRNA variants. *Journal of Experimental Botany* 62: 3519-3534
- Burch LR, Davies HV, Cuthbert EM, Machray EC, Hedley P, Waugh R (1992) Purification of soluble invertase from potato. *Phytochemistry* 31: 1901-1904
- Burks PS (2015) Sweet Sorghum Diversity, Genetics and Breeding. Ph.D. dissertation
- Channappagoudar BB, Biradar NR, Patil JB, Hiremath SM (2007) Study on Morpho-Physiological, Biophysical

- Characters and Alcohol Production in Sweet Sorghum Genotypes. *Karnataka Journal of Agricultural Sciences* 20: 234-237
- Cheng W, Taliencio E, Chourey P (1996) The Miniature1 Seed Locus of Maize Encodes a Cell Wall Invertase Required for Normal Development of Endosperm and Maternal Cells in the Pedicel. *The Plant Cell* 8: 971-983
- Chopra R, Burow G, Burke JJ, Gladman N, Xin Z (2017) Genome-wide association analysis of seedling traits in diverse Sorghum germplasm under thermal stress. *BMC Plant Biology* 17: 12-12
- French S, Abu-Zaitoon Y, Uddin M, Bennett K, Nonhebel H (2014) Auxin and Cell Wall Invertase Related Signaling during Rice Grain Development. *Plants* 3: 95-112
- Fujii A, Nakamura S, Nabeya K, Nakajima T, Goto Y (2016) Relation between seeding times and stem yield of sorghum in cold region in Japan. *Plant Production Science* 19: 73-80
- Ganesh Kumar C, Fatima A, Srinivasa Rao P, Reddy BVS, Rathore A, Nageswar Rao R, Khalid S, Ashok Kumar a, Kamal A (2010) Characterization of Improved Sweet Sorghum Genotypes for Biochemical Parameters, Sugar Yield and Its Attributes at Different Phenological Stages. *Sugar Tech* 12: 322-328
- Goetz M, Guivar ch A, Hirsche J, Bauerfeind MA, Gonz lez M-C, Hyun TK, Eom SH, Chriqui D, Engelke T, Grobkinsky DK, Roitsch T (2017) Metabolic Control of Tobacco Pollination by Sugars and Invertases. *Plant Physiology* 173: 984-997
- Gonz lez MC, Roitsch T, Cejudo FJ (2005) Circadian and developmental regulation of vacuolar invertase expression in petioles of sugar beet plants. *Planta* 222: 386-395
- Greiner S, Rausch T, Sonnewald U, Herbers K (1999) Ectopic expression of a tobacco invertase inhibitor homolog prevents cold-induced sweetening of potato tubers. *Nature Biotechnology* 17: 708-711
- Grof CPL, Albertson PL, Bursle J, Perroux JM, Bonnett GD, Manners JM (2007) Sucrose-phosphate synthase, a biochemical marker of high sucrose accumulation in sugarcane. *Crop Science* 47: 1530-1539
- Gutjahr S, Cl ment-Vidal A, Soutiras A, Sonderegger N, Braconnier S, Dingkuhn M, Luquet D (2013) Grain, sugar and biomass accumulation in photoperiod-sensitive sorghums. II. Biochemical processes at internode level and interaction with phenology. *Functional Plant Biology* 40: 355-368
- Guy C, Kaplan F, Kopka J, Selbig J, Hinch DK (2008) Metabolomics of temperature stress. *Physiologia Plantarum* 132: 220-235

- Hasilik A, Tanner W (1978) Carbohydrate Moiety of Carboxypeptidase Y and Perturbation of Its Biosynthesis. *European Journal of Biochemistry* 91: 567-575
- Herbers K, Sonnewald U (1998) Molecular determinants of sink strength. *Current Opinion in Plant Biology* 1: 207-216
- Hirose T, Aoki N, Harada Y, Okamura M, Hashida Y, Ohsugi R, Akio M, Hirochika H, Terao T (2013) Disruption of a rice gene for α -glucan water dikinase, OsGWD1, leads to hyperaccumulation of starch in leaves but exhibits limited effects on growth. *Frontiers in Plant Science* 4: 1-9
- Hirose T, Hashida Y, Aoki N, Okamura M, Yonekura M, Ohto C, Terao T, Ohsugi R (2014) Analysis of gene-disruption mutants of a sucrose phosphate synthase gene in rice, OsSPS1, shows the importance of sucrose synthesis in pollen germination. *Plant Science* 225: 102-106
- Hirose T, Takano M, Terao T (2002) Cell wall invertase in developing rice caryopsis: molecular cloning of OsCIN1 and analysis of its expression in relation to its role in grain filling. *Plant & cell physiology* 43: 452-459
- Ho LC (1988) Metabolism and Compartmentation of Imported Sugars in Sink Organs in Relation to Sink Strength. *Annual Review of Plant Physiology and Plant Molecular Biology* 39: 355-378
- Hothorn M, Wolf S, Aloy P, Greiner S, Scheffzek K (2004) Structural insights into the target specificity of plant invertase and pectin methylesterase inhibitory proteins. *Plant Cell* 16: 3437-3447
- Huang LF (2006) Molecular Analysis of an Acid Invertase gene family in Arabidopsis, Ph.D. dissertation.
- Ishimaru T, Hirose T, Matsuda T, Goto A, Takahashi K, Sasaki H, Terao T, Ishii RI, Ohsugi R, Yamagishi T (2005) Expression patterns of genes encoding carbohydrate-metabolizing enzymes and their relationship to grain filling in rice (*Oryza sativa* L.): Comparison of caryopses located at different positions in a panicle. *Plant and Cell Physiology* 46: 620-628
- Ji X, Van Den Ende W, Schroeven L, Clerens S, Geuten K, Cheng S, Bennett J (2007) The rice genome encodes two vacuolar invertases with fructan exohydrolase activity but lacks the related fructan biosynthesis genes of the Pooideae. *New Phytologist* 173: 50-62
- Ji X, Van Den Ende W, Van Laere A, Cheng S, Bennett J (2005) Structure, evolution, and expression of the two invertase gene families of rice. *Journal of Molecular Evolution* 60: 615-634
- Jin Y, Ni Da, Ruan YL (2009) Posttranslational Elevation of Cell Wall Invertase Activity by Silencing Its Inhibitor in Tomato Delays Leaf Senescence and Increases Seed Weight and Fruit Hexose Level. *the Plant Cell*

Online 21: 2072-2089

- Kim J-Y, Mahé A, Brangeon J, Prioul J-L (2000) A Maize Vacuolar Invertase, *IVR2*, Is Induced by Water Stress. Organ/Tissue Specificity and Diurnal Modulation of Expression. *Plant Physiology* 124: 71-84
- Klann EM, Hall B, Bennett aB (1996) Antisense acid invertase (TIV1) gene alters soluble sugar composition and size in transgenic tomato fruit. *Plant Physiol* 112: 1321-1330
- Klemens PaW, Patzke K, Trentmann O, Poschet G, Buttner M, Schulz A, Marten I, Hedrich R, Neuhaus HE (2014) Overexpression of a proton-coupled vacuolar glucose exporter impairs freezing tolerance and seed germination. *New Phytologist* 202: 188-197
- Klionsky DJ, Banta LM, Emr SD (1988) Intracellular sorting and processing of a yeast vacuolar hydrolase: proteinase A propeptide contains vacuolar targeting information. *Molecular and cellular biology* 8: 2105-2116
- Koch K (2004) Sucrose metabolism: Regulatory mechanisms and pivotal roles in sugar sensing and plant development. *Current Opinion in Plant Biology* 7: 235-246
- Kong J, Li Z, Tan YP, Wan CX, Li SQ, Zhu YG (2007) Different gene expression patterns of sucrose-starch metabolism during pollen maturation in cytoplasmic male-sterile and male-fertile lines of rice. *Physiologia Plantarum* 130: 136-147
- Kurai T, Morey SR, Wani SP, Watanabe T (2015) Efficient rates of nitrogenous fertiliser for irrigated sweet sorghum cultivation during the post-rainy season in the semi-arid tropics. *European Journal of Agronomy* 71: 63-72
- Kuroda M, Kimizu M, Mikami C (2010) A Simple Set of Plasmids for the Production of Transgenic Plants. *Bioscience, Biotechnology, and Biochemistry* 74: 2348-2351
- Kuroda M, Isenaga S (2015) Single-tube Hydroponics as a Novel Idea for Small-Scale Production of Crop Seed in a Plant Incubator. *Bioscience, Biotechnology and Biochemistry* 79: 63-67
- Leskow CC, Kamenetzky L, Dominguez PG, Díaz Zirpolo JA, Obata T, Costa H, Martí M, Taboga O, Keurentjes J, Sulpice R, Ishihara H, Stitt M, Fernie AR, Carrari F (2016) Allelic differences in a vacuolar invertase affect *Arabidopsis* growth at early plant development. *Journal of Experimental Botany* 67: 4091-4103
- Li B, Liu H, Zhang Y, Kang T, Zhang L, Tong J, Xiao L, Zhang H (2013) Constitutive expression of cell wall invertase genes increases grain yield and starch content in maize. *Plant Biotechnology Journal* 11: 1080-

- Li Y, Fan C, Xing Y, Jiang Y, Luo L, Sun L, Shao D, Xu C, Li X, Xiao J, He Y, Zhang Q (2011) Natural variation in GS5 plays an important role in regulating grain size and yield in rice. *Nature Genetics* 43: 1266-1269
- Liu Y, Nie YD, Han FX, Zhao XN, Dun BQ, Lu M, Li GY (2014) Allelic variation of a soluble acid invertase gene (SAI-1) and development of a functional marker in sweet sorghum [*Sorghum bicolor* (L.) Moench]. *Molecular Breeding* 33: 721-730
- Mace ES, Tai S, Gilding EK, Li Y, Prentis PJ, Bian L, Campbell BC, Hu W, Innes DJ, Han X, Cruickshank A, Dai C, Frère C, Zhang H, Hunt CH, Wang X, Shatte T, Wang M, Su Z, Li J, Lin X, Godwin ID, Jordan DR, Wang J (2013) Whole-genome sequencing reveals untapped genetic potential in Africa's indigenous cereal crop sorghum. *Nature Communications* 4
- Marcelis LF (1996) Sink strength as a determinant of dry matter partitioning in the whole plant. *Journal of experimental botany* 47: 1281-1291
- Mathur S, Umakanth aV, Tonapi Va, Sharma R, Sharma MK (2017) Sweet sorghum as biofuel feedstock: recent advances and available resources. *Biotechnology for Biofuels* 10: 146-146
- McBee G, Waskom R, Miller F, Creelman R (1983) Effect of senescence and non-senescence on carbohydrates in sorghum during late kernel maturity states. *Crop Science* 23:370-375
- McKinley B, Rooney W, Wilkerson C, Mullet J (2016) Dynamics of biomass partitioning, stem gene expression, cell wall biosynthesis, and sucrose accumulation during development of *Sorghum bicolor*. *Plant Journal* 88: 662-680
- Miller M, Chourey P (1992) The Maize Invertase-Deficient miniature-1 Seed Mutation Is Associated with Aberrant Pedicel and Endosperm Development. *The Plant cell* 4: 297-305
- Miyao A, Tanaka K, Murata K, Sawaki H, Takeda S, Abe K, Shinozuka Y, Onosato K, Hirochika H (2003) Target Site Specificity of the Tos17 Retrotransposon Shows a Preference for Insertion within Genes and against Insertion in Retrotransposon-Rich Regions of the Genome. *The Plant Cell* 15: 1771-1780
- Mizuno H, Kasuga S, Kawahigashi H (2016) The sorghum SWEET gene family: stem sucrose accumulation as revealed through transcriptome profiling. *Biotechnology for Biofuels* 9: 127-127
- Mocoeur A, Zhang YM, Liu ZQ, Shen X, Zhang LM, Rasmussen SK, Jing HC (2015) Stability and genetic control of morphological, biomass and biofuel traits under temperate maritime and continental conditions in sweet

- sorghum (*Sorghum bicolor*). *Theoretical and Applied Genetics* 128: 1685-1701
- Murray SC, Sharma A, Rooney WL, Klein PE, Mullet JE, Mitchell SE, Kresovich S (2008) Genetic improvement of sorghum as a biofuel feedstock: I. QTL for stem sugar and grain nonstructural carbohydrates. *Crop Science* 48: 2165-2179
- Nagao M, Minami A, Arakawa K, Fujikawa S, Takezawa D (2005) Rapid degradation of starch in chloroplasts and concomitant accumulation of soluble sugars associated with ABA-induced freezing tolerance in the moss *Physcomitrella patens*. *Journal of Plant Physiology* 162: 169-180
- Nakamura S, Nakajima N, Nitta Y, Goto Y (2011) Analysis of Successive Internode Growth in Sweet Sorghum Using Leaf Number as a Plant Age Indicator. *Plant production science* 14: 299-306
- Ni DA (2012) Role of vacuolar invertase in regulating *Arabidopsis* stomatal opening. *Acta Physiologiae Plantarum* 34: 2449-2452
- Nägele T, Stutz S, Hörmiller II, Heyer AG (2012) Identification of a metabolic bottleneck for cold acclimation in *Arabidopsis thaliana*. *Plant Journal* 72: 102-114
- Paterson AH (2008) Genomics of Sorghum. *International Journal of Plant Genomics*, 2008: Article ID 362451, 6 pages
- Proels RK, Roitsch T (2009) Extracellular invertase LIN6 of tomato: A pivotal enzyme for integration of metabolic, hormonal, and stress signals is regulated by a diurnal rhythm. *Journal of Experimental Botany* 60: 1555-1567
- Qazi HA, Paranjpe S, Bhargava S (2012) Stem sugar accumulation in sweet sorghum - Activity and expression of sucrose metabolizing enzymes and sucrose transporters. *Journal of Plant Physiology* 169: 605-613
- Qin G, Zhu Z, Wang W, Cai J, Chen Y, Li L, Tian S (2016) A Tomato Vacuolar Invertase Inhibitor Mediates Sucrose Metabolism and Influences Fruit Ripening. *Plant Physiology* 172: 1596-1611
- Rao PS, Kumar CG, Reddy BVS (2013) Sweet sorghum: from theory to practice. In: Rao PS, Kumar CG, editors. *Characterization of improved sweet sorghum cultivars*. Berlin: Springer. 1-15
- Roitsch T, González MC (2004) Function and regulation of plant invertases: Sweet sensations. *Trends in Plant Science* 9: 606-613
- Ruan YL, Jin Y, Yang YJ, Li GJ, Boyer JS (2010) Sugar input, metabolism, and signaling mediated by invertase: Roles in development, yield potential, and response to drought and heat. *Molecular Plant* 3: 942-955

- Rutto LK, Xu Y, Brandt M, Ren S, Kering MK (2013) Juice, Ethanol, and Grain Yield Potential of Five Sweet Sorghum (*Sorghum bicolor* [L.] Moench) Cultivars. *Journal of Sustainable Bioenergy Systems* 3: 113-118
- Sagehashi Y and Sato Y (2015a) Effects of cold acclimation of rice seedlings predicted by a sucrose content which is a candidate of a biomarker. *Proceedings of the Meeting of the Crop Science Society of Japan*. p103
- Sagehashi Y and Sato Y (2015b) Improvement of cold tolerance of rice seedlings by a treatment of cold acclimation. *Proceedings of the Meeting of the Crop Science Society of Japan*. p24
- Saitou N and Nei M (1987) The neighbor-joining method: A new method for reconstructing phylogenetic trees. *Molecular Biology and Evolution* 4:406-425
- Schneider Ca, Rasband WS, Eliceiri KW (2012) NIH Image to ImageJ: 25 years of image analysis. *Nature Methods* 9: 671-675
- Sergeeva LI, Keurentjes JJB, Bentsink L, Vonk J, van der Plas LHW, Koornneef M, Vreugdenhil D (2006) Vacuolar invertase regulates elongation of *Arabidopsis thaliana* roots as revealed by QTL and mutant analysis. *Proceedings of the National Academy of Sciences* 103: 2994-2999
- Shao HB, Guo QJ, Chu LY, Zhao XN, Su ZL, Hu YC, Cheng JF (2007) Understanding molecular mechanism of higher plant plasticity under abiotic stress. *Colloids and Surfaces B: Biointerfaces* 54: 37-45
- Shiringani AL, Frisch M, Friedt W (2010) Genetic mapping of QTLs for sugar-related traits in a RIL population of *Sorghum bicolor* L. Moench. *Theoretical and Applied Genetics* 121: 323-336
- Shoemaker CE, Bransby DI (2010) The Role of Sorghum as a Bioenergy Feedstock. *Sustainable Alternative Fuel Feedstock Opportunities, Challenges and Roadmaps for Six U.S. Regions*: 149-159
- Shukla S, Felderhoff TJ, Saballos A, Vermerris W (2017) The relationship between plant height and sugar accumulation in the stems of sweet sorghum (*Sorghum bicolor* (L.) Moench). *Field Crops Research* 203: 181-191
- Smeekens S (2000) Sugar-induced signal transduction in plants. *Annual Reviews of Plant Physiology and Plant Molecular Biology* 51: 49-81
- Song XJ, Kuroha T, Ayano M, Furuta T, Nagai K, Komeda N, Segami S, Miura K, Ogawa D, Kamura T, Suzuki T, Higashiyama T, Yamasaki M, Mori H, Inukai Y, Wu J, Kitano H, Sakakibara H, Jacobsen SE, Ashikari M (2015) Rare allele of a previously unidentified histone H4 acetyltransferase enhances grain weight, yield, and plant biomass in rice. *Proceedings of the National Academy of Sciences* 112: 76-81

- Stitt M, Hurry V (2002) A plant for all seasons: Alterations in photosynthetic carbon metabolism during cold acclimation in Arabidopsis. *Current Opinion in Plant Biology* 5: 199-206
- Sturm A (1999) Update on Biochemistry Invertases . Primary Structures , Functions , and Roles in Plant Development and Sucrose Partitioning. *Plant physiology* 121: 1-7
- Sturm a, Chrispeels MJ (1990) cDNA cloning of carrot extracellular beta-fructosidase and its expression in response to wounding and bacterial infection. *The Plant cell* 2: 1107-1119
- Sturm A, Šebková V, Lorenz K, Hardegger M, Lienhard S, Unger C (1995) Development- and organ-specific expression of the genes for sucrose synthase and three isoenzymes of acid B-fructofuranosidase in carrot. *Planta* 195: 601-610
- Tamura K, Stecher G, Peterson D, Filipski A, and Kumar S (2013) MEGA6: Molecular Evolutionary Genetics Analysis version 6.0. *Molecular Biology and Evolution* 30: 2725-2729
- Tang GQ (1999) Antisense Repression of Vacuolar and Cell Wall Invertase in Transgenic Carrot Alters Early Plant Development and Sucrose Partitioning. *the Plant Cell Online* 11: 177-190
- Tang X, Su T, Han M, Wei L, Wang W, Yu Z, Xue Y, Wei H, Du Y, Greiner S, Rausch T, Liu L (2016) Suppression of extracellular invertase inhibitor gene expression improves seed weight in soybean (*Glycine max*). *Journal of Experimental Botany* 68: 469-482
- Tarkowski ŁP, Van den Ende W (2015) Cold tolerance triggered by soluble sugars: a multifaceted countermeasure. *Frontiers in Plant Science* 6: 1-7
- Thurber CS, Ma JM, Higgins RH, Brown PJ (2013) Retrospective genomic analysis of sorghum adaptation to temperate-zone grain production. *Genome Biology* 14: 68-68
- Toki S (1997) Rapid and Efficient Agrobacterium-Mediated Transformation in Rice. *In Plant Molecular Biology Reporter*, Vol 15 (1), 16-21
- Trouverie J, Chateau-Joubert S, Thévenot C, Jacquemot MP, Prioul JL (2004) Regulation of vacuolar invertase by abscisic acid or glucose in leaves and roots from maize plantlets. *Planta* 219: 894-905
- Tymowska-Lalanne Z, Kreis M (1998) Expression of the Arabidopsis thaliana invertase gene family. *Planta* 207: 259-265
- Unger C, Hardegger M, Lienhard S, Sturm a (1994) cDNA cloning of carrot (*Daucus carota*) soluble acid b-fructofuranosidases and comparison with the cell wall isoenzyme. *Plant Physiology* 104: 1351-1357

- Wang E, Wang J, Zhu X, Hao W, Wang L, Li Q, Zhang L, He W, Lu B, Lin H, Ma H, Zhang G, He Z (2008) Control of rice grain-filling and yield by a gene with a potential signature of domestication. *Nature Genetics* 40: 1370-1374
- Wang J, Jiang J, Oard JH (2000) Structure, expression and promoter activity of two polyubiquitin genes from rice (*Oryza sativa* L.). *Plant Science* 156: 201-211
- Wang L, Li XR, Lian H, Ni Da, He Yk, Chen XY, Ruan YL (2010) Evidence That High Activity of Vacuolar Invertase Is Required for Cotton Fiber and Arabidopsis Root Elongation through Osmotic Dependent and Independent Pathways, Respectively. *Plant Physiology* 154: 744-756
- Wang L, Ruan Y-L (2016) Critical Roles of Vacuolar Invertase in Floral Organ Development and Male and Female Fertilities Are Revealed through Characterization of *GhVIN1*-RNAi Cotton Plants. *Plant Physiology* 171: 405-423
- Wanner La, Junttila O (1999) Cold-induced freezing tolerance in Arabidopsis. *Plant physiology* 120: 391-400
- Wardlaw IF (2008) The control of carbon partitioning in plants. *New Phytologist*. 116: 341-381
- Weber H (1995) Seed Coat-Associated Invertases of Fava Bean Control Both Unloading and Storage Functions: Cloning of cDNAs and Cell Type-Specific Expression. *the Plant Cell Online* 7: 1835-1846
- Weiszmann J, Fürtauer L, Weckwerth W, Nägele T (2017) Vacuolar invertase activity shapes photosynthetic stress response of Arabidopsis thaliana and stabilizes central energy supply. *bioRxiv*: 1-31
- Weschke W, Panitz R, Gubatz S, Wang Q, Radchuk R, Weber H, Wobus U (2003) The role of invertases and hexose transporters in controlling sugar ratios in maternal and filial tissues of barley caryopses during early development. *Plant Journal* 33: 395-411
- Wiberley-Bradford AE, Busse JS, Jiang J, Bethke PC (2014) Sugar metabolism, chip color, invertase activity, and gene expression during long-term cold storage of potato (*Solanum tuberosum*) tubers from wild-type and vacuolar invertase silencing lines of Katahdin. *BMC research notes* 7: 801-801
- Xiang L, Etxeberria E, Van Den Ende W (2013) Vacuolar protein sorting mechanisms in plants. *FEBS Journal* 280: 979-993
- Xu J, Avigne WT, McCarty DR, Koch KE (1996) A similar dichotomy of sugar modulation and developmental expression affects both paths of sucrose metabolism: Evidence from a maize invertase gene family. *Plant Cell* 8: 1209-1220

- Yang L, Bao-qing D, Mei-qi Z, Ming L, Gui-ying L (2013) Correlation analysis between the key enzyme activities and sugar content in sweet sorghum (*Sorghum bicolor* L. Moench) stems at physiological maturity stage. *Australian Journal of Crop Science* 7:84-92
- Yoshida S, Forno DA, Cock JH, Gomez KA (1976) *Laboratory Manual for Physiological Studies of Rice*, International Rice Research Institute. 3: 61–64
- Zhang Q, Chen Q, Wang S, Hong Y, Wang Z (2014) Rice and cold stress: methods for its evaluation and summary of cold tolerance-related quantitative trait loci. *Rice* 7: 24-24
- Zhu J, Dong CH, Zhu JK (2007) Interplay between cold-responsive gene regulation, metabolism and RNA processing during plant cold acclimation. *Current Opinion in Plant Biology* 10: 290-295
- Zhu YJ, Komor E, Moore PH (1997) Sucrose Accumulation in the Sugarcane Stem Is Regulated by the Difference between the Activities of Soluble Acid Invertase and Sucrose Phosphate Synthase. *Plant physiology* 115: 609-616
- Zrenner R, Schüler K, Sonnewald U (1996) Soluble acid invertase determines the hexose-to-sucrose ratio in cold-stored potato tubers. *Planta* 198: 246-252
- Zuckerkindl E and Pauling L (1965) Evolutionary divergence and convergence in proteins. Edited in *Evolving Genes and Proteins* by V. Bryson and H.J. Vogel, 97-166. Academic Press, New York.